

**IDENTIFICATION OF GENES
INVOLVED IN *IN VIVO* VIRULENCE OF
MYCOBACTERIUM FORTUITUM AS POTENTIAL
DRUG TARGET**

Thesis submitted in fulfillment of the requirements for the Degree of

DOCTOR OF PHILOSOPHY

BY

POONAM



Department of Biotechnology and Bioinformatics

JAYPEE UNIVERSITY OF INFORMATION TECHNOLOGY

WAKNAGHAT, SOLAN, HP-173234, INDIA

DECEMBER 2019

@ Copyright

JAYPEE UNIVERSITY OF INFORMATION TECHNOLOGY, WAKNAGHAT

DECEMBER 2019

ALL RIGHTS RESERVED

TABLE OF CONTENTS

CONTENT	PAGE NO.
TABLE OF CONTENTS	i-iv
DECLARATION BY THE SCHOLAR	v
SUPERVISOR'S CERTIFICATE	vi
ACKNOWLEDGEMENT	vii-viii
ABSTRACT	ix
LIST OF ABBREVIATION	x-xiii
LIST OF FIGURES	xiv-xv
LIST OF TABLES	xvi
CHAPTER 1: INTRODUCTION	1-5
CHAPTER 2: REVIEW OF LITERATURE	6-42
2.1 Genus Mycobacterium	6-17
2.1.1 Cell wall of genus Mycobacteria	6-8
2.1.2 Classification of genus Mycobacteria	8
2.1.2.1 Mycobacterium tuberculosis complex	8-11
2.1.2.2 Non-tuberculous Mycobacteria	11-17
2.2 <i>Mycobacterium fortuitum</i>	17-24
2.2.1 Types of infections caused by <i>M. fortuitum</i>	18-21
2.2.2 Virulence of <i>M. fortuitum</i>	22-23
2.2.3 Models to study <i>M. fortuitum</i> infections	23-24
2.3 Membrane/Secretory proteins as virulent factors	25-29
2.3.1 Host-pathogen interaction	25-27
2.3.2 Role of peptidoglycan in immune signaling and modification	27-28
2.3.3 Role of other components of cell wall in immune signaling and modification	28
2.3.4 Transport of nutrient	28

2.3.5 Protection against osmotic and mechanical stress	29
2.4 Immune response against mycobacterial infections	29-34
2.4.1 Proinflammatory cytokines	30-32
2.4.2 Anti-inflammatory cytokines	33-34
2.5 Genetic strategies for identifying new drug targets	34-40
2.5.1 Bioinformatics tools	34-35
2.5.2 Gene knockout strategies	35-36
2.5.3 Antisense Technology	37
2.5.4 Complementation	37
2.5.5 Transposon mutagenesis	37-38
2.5.6 CRISPR Interference	39
2.5.7 Conditional Mutagenesis	40
2.6 Genes used in reporter fusion and promoter trap strategies	40-42
CHAPTER 3: MATERIALS AND METHODS	43-57
3.1 Material	43-44
3.1.1 Bacterial strains and plasmids	43
3.1.2 Culture media and buffers	43
3.1.3 Chemicals	43
3.1.4 Primers	44
3.2 Methods	44-57
3.2.1 Media and growth conditions	44
3.2.2 Zeihl-Neelson (AFB) staining	44-45
3.2.3 Construction and screening of transposon mutant library	45
3.2.3.1 Electroporation of plasmid into <i>M. fortuitum</i>	45
3.2.3.2 Biochemical assay for screening of the mutant library	45-46
3.2.4 <i>In vivo</i> infection studies	46-48
3.2.4.1 Animals	46
3.2.4.2 Infection	46
3.2.4.3 Bacillary load determination	47
3.2.4.4 Histopathology	47
3.2.4.5 Cytokine profiling	47

3.2.5 Molecular methods used for identification of genes affected by mutation	47-52
3.2.5.1 Genomic analysis of mutants	48-50
3.2.5.2 Cloning of transposon inserted DNA segment	50-52
3.2.5.3 Sequencing	52
3.2.6 Bioinformatics tools used for homology study	52-53
3.2.7 Growth kinetics of mutants under <i>in vitro</i> stress conditions	53-55
3.2.7.1 Acidic stress	53
3.2.7.2 Oxidative stress	54
3.2.7.3 Nutrient starvation	54
3.2.7.4 Detergent stress	54
3.2.7.5 Heat stress	54
3.2.7.6 Hypoxic stress	55
3.2.8 Prediction of transmembrane helix and <i>in silico</i> interaction studies	55
3.2.9 Molecular modeling	55-56
3.2.10 Molecular docking	56-57
CHAPTER 4: RESULTS	58-87
4.1 Identification of mutants defective in <i>in vivo</i> virulence	58-66
4.1.1 Construction of transposon mutant library and shortlisting of mutants	58-60
4.1.2 Mutants MT726, MT725, and MT727 showed virulence attenuation	60-62
4.1.3 The mutants showing virulence attenuation also showed reduced tissue pathology	63-65
4.1.4 Attenuated mutants showed lower levels of IFN- γ and TNF- α	65-66
4.2 Analysis of mutants for identification of potential drug targets	67-81
4.2.1 PCR amplification confirmed the presence of transposon in mutants	67
4.2.2 Genomic analysis led to identification of ORFs mutated in attenuated mutants	67

4.2.2.1 Short-chain dehydrogenase was found to be mutated in mutant MT726	68-69
4.2.2.2 Anthranilate synthase complex was found to be mutated in mutant MT725	69-72
4.2.2.3 Ribosomal maturation factor RimP was found to be mutated in mutant MT727	72-74
4.2.3 Response to different <i>in vitro</i> stress conditions by mutants and wild type <i>M. fortuitum</i> (WTMF)	74
4.2.3.1 Mutants showed growth defect under <i>in vitro</i> acidic stress	74-76
4.2.3.2 Mutants showed no growth defect under oxidative and heat stress	77-78
4.2.3.3 Mutant MT727 showed growth defect under <i>in vitro</i> detergent stress	79
4.2.3.4 Mutant MT726 showed slight deviation in growth under <i>in vitro</i> nutrient starvation	79-80
4.2.3.5 Mutants showed sensitivity to <i>in vitro</i> hypoxic stress	81
4.3 Structure Prediction, interaction and molecular docking studies to identify potential inhibitors	82-87
4.3.1 MfSdr showed the presence of transmembrane helix	82
4.3.2 Short-chain dehydrogenase shows functional interaction with proteins involved in mycolic acid biosynthesis	83-84
4.3.3 Predicted secondary structure of MfSdr	84-85
4.3.4 Potential inhibitors were identified against MfSdr through molecular docking studies	86-87
CHAPTER 5: DISCUSSION	88-97
CONCLUSION AND FUTURE PROSPECTS	98
REFERENCES	99-125
APPENDIX	126-130
LIST OF PUBLICATIONS	131-133

DECLARATION BY THE SCHOLAR

I, **Poonam (Enrollment No. 136553)**, hereby declare that the work reported in the Ph.D. thesis entitled “**Identification of genes involved in *in vivo* virulence of *Mycobacterium fortuitum* as potential drug target**” submitted at the **Jaypee University of Information Technology, Wagnaghat, Solan (HP), India** is an authentic record of my work carried out under the supervision of **Dr. Rahul Shrivastava**. I have not submitted this work elsewhere for any other degree or diploma. I am fully responsible for the contents of my Ph.D. thesis.



Name: Poonam

Date: 31.12.2019

Enrollment No.: 136553

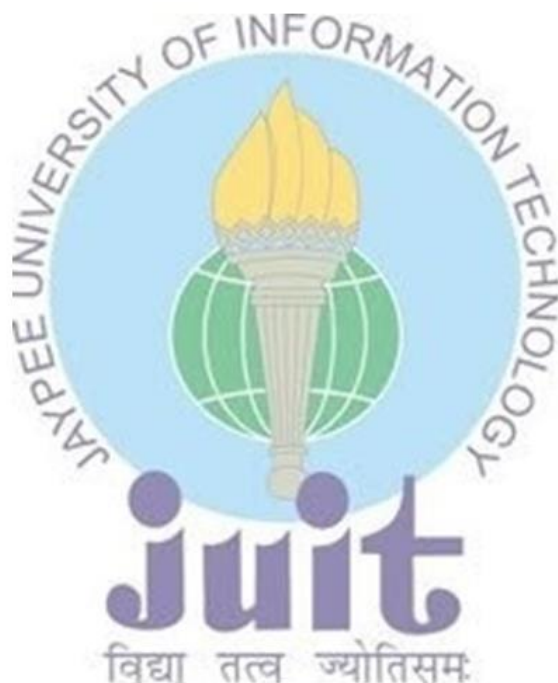
Department of Biotechnology & Bioinformatics

Jaypee University of Information Technology

Wagnaghat, Solan (HP), India

SUPERVISOR'S CERTIFICATE

This is to certify that the work reported in the Ph.D. thesis entitled “**Identification of genes involved in *in vivo* virulence of *Mycobacterium fortuitum* as potential drug target**” submitted by **Ms. Poonam** at **Jaypee University of Information Technology, Wagnaghat, Solan (HP), India** is a bonafide record of her original work carried out under my supervision. This work has not been submitted elsewhere for any other degree or diploma.



Supervisor:

Dr. Rahul Shrivastava

Associate Professor

Department of Biotechnology & Bioinformatics

Jaypee University of Information Technology

Wagnaghat, Solan (HP), India

Date: 31.12.2019

ACKNOWLEDGMENT

Completing the work and submitting Ph.D. thesis is a dream comes true for me. Though it was a very long journey with ups and downs, yet the joy of reaching the finishing line is worth it. I deem it my privilege and honor to place and record my gratitude and indebtedness to the following without whose guidance, support, and concern I would not have been able to complete my Ph.D. thesis.

*First and foremost, I would like to thank the almighty **God** for always showering his blessings upon me. I feel privileged to express my deep sense of reverence and gratitude to my revered mentor, **Dr. Rahul Shrivastava**, for his support, immaculate guidance, constructive criticism, constant encouragement and providing requisite facilities to carry out my research, which otherwise would have remained incomplete. His nurturing and caring concern has been a stimulus, which I will always cherish. He was always there with his vision, encouragement, and advice to proceed through the work and complete it. I also appreciate him for untiring efforts during the entire tenure of my research work and patience during the writing of this thesis. I am indebted to the **Department of Science and Technology, Science and Engineering Research Board (DST-SERB)** for providing financial support in the form of research grant to carry out this research.*

*I gratefully acknowledge the help rendered by **Prof. Dr. Sudhir Kumar** (HoD, Dept. of BT & BI) for his encouragement and cooperation throughout my research work. I owe a sincere thanks to **Dr. Raghothaman M. Yennamalli** for his kind support and help to carry out the Bioinformatics part of the study. Because of his support, I learned about Bioinformatics work, which was completely new for me. I also want to express my gratitude to **Dr. Sudarshan Kumar Sharma** IGMC Shimla, for helping in histopathology study.*

*I express my esteemed thanks to **JUIT administration, Prof. Dr. Vinod Kumar** (Vice-Chancellor JUIT); **Prof. Dr. Samir Dev Gupta**, (Director & Academic Head), **Maj. Gen. (Retd.) Rakesh Bassi** (Registrar & Dean of Student Welfare) for providing financial assistance and all the facilities to pursue the degree and advanced laboratory infrastructure for completion of this work. I also express my sincere thanks to the **Institutional Animal Ethics Committee (IAEC)** for the approval of mice for virulence-related studies.*

*The completion of this document had received its necessary 'diet' in the form of comments and suggestions by my DPMC members **Prof. Karanjeet Singh, Dr. Harish Changotra and***

*Dr. Raj Kumar, and. I am short of words in expressing my thanks to them, for their innovative ideas that shaped this document. I am also grateful to **Dr. Gopal Singh Bisht** and **Dr. Jitendraa Vashistt** for their constant guidance and support at the various stages of this study. I wish to convey my sincere thanks to **all the faculty members** of the Department of BT & BI, for their kind support.*

*I'm also thankful to all the members of the technical and non-technical staff of the department, especially, **Mr. Baleshwar Shukla, Mrs. Mamta Mishra, Mrs. Sonika Gupta, Mrs. Somlata Sharma, Mr. Ismail Siddiqui** and **Mr. Kamlesh** for their assistance and valuable contributions.*

*I am extremely thankful to my seniors **Dr. Shivani Sood, Dr. Swapnil Jain** and **Dr. Jibesh**, and my friends **Deepika Sharma, Nupur, Swati, Dr. Sanjay, Dr. Nutan, Dr. Raman, Dr. Anil, Dr. Manali** and **Dr. Shraddha** for their help, support and always standing by my side in my hard times. I am fortunate to have friends like **Ritika** and **Avni** who have always stood beside me. This acknowledgment would be incomplete without thanking my lab mates **Ayushi Sharma, Anant, Ritu, Monika, Kanika, Shubham Mittal, Arpita, Keenam, Divya, Bishal, Rahul Parmajeet, Vedika** and B-tech students **Poonam, Nitin, Apoorv, Anushruti**, for their support, help, and care. I want to convey my special thanks to **Neha, Sameer and Monika**, for helping me and supporting me. I want to thank **all research scholars** from all departments of JUIT for helping me in numerous ways.*

*Thanks would be a small word for what I owe to my father, **Late Sh. Bhumi Nand** and my mother **Mrs. Shaila Devi**. It was because of their love and blessing that I was able to strongly steer through the rough winds of time. Their unconditional love, guidance, care, support and motivation always inspired me throughout my life. I earnestly want to thank my brother **Sandeep Katoch** for always guiding me in a better way, my sister **Sapna Chandel**, my jiju **Sanjeev Chandel** and my nephew **Uday**. I bow my head to thank my Dadi ji **Smt. Giano Devi** and Dada ji **Late Sh. Hari Ram**. I would like to express my heartfelt gratitude to all those who have contributed directly or indirectly towards the completion of this work. I might have missed many names but I am thankful to all who have contributed and I extend my apologies for forgetting those who are unmentioned.*

Poonam

ABSTRACT

Mycobacterium fortuitum is an important human pathogenic NTM, which resists stress conditions inside macrophages by exploitation of virulence specific genes. TnphoA-based transposon mutagenesis was employed to identify membrane protein-encoding genes responsible for virulence of *M. fortuitum*, as potential drug target. A library of about 5000 mutants was constructed after electroporation of plasmid pRT291 into wild-type *M. fortuitum*. On the basis of blue color development, and alkaline phosphatase assay, six mutants were shortlisted for *in vivo* virulence studies. Three mutants were obtained with virulence attenuation, of which mutant MT726 showed highest attenuation followed by mutant MT725 and MT727. Genomic and bioinformatics analysis of attenuated mutants led to identification of four novel *M. fortuitum* ORFs namely, short-chain dehydrogenase (Mfsdr) in mutant MT726, anthranilate synthase component I (MftrpE) and anthranilate synthase component II (MftrpG) in mutant MT725, and ribosomal maturation factor (MfrimP) in mutant MT727. Growth kinetics analyses of attenuated mutants suggested role of Mfsdr for survival under acidic stress, hypoxic stress, and nutrient starvation conditions; role of anthranilate synthase encoding gene MftrpE and MftrpG under acidic and hypoxic stress; and role of MfrimP under acidic, hypoxic and detergent stress conditions. Structural and functional characterization of most potent ORF Mfsdr was done using *in silico* approaches. MfSdr was predicted to be localized on membrane, using TMpred database. *In silico* functional interaction of short-chain dehydrogenase (SDR) protein, using STRING database predicted its interaction with proteins involved in mycolic acid synthesis pathway, indicating probable role of MfSdr in mycolic acid synthesis. Secondary structure of MfSdr generated using Robetta server showed presence of Rossmann fold which is a characteristic of short chain dehydrogenase/reductase protein family. Virtual screening of MfSdr structure as drug target, using molecular docking tools led to the identification of five potential inhibitors, which can be exploited for *in vitro* and *in vivo* growth inhibition assays against *M. fortuitum* as well as other related mycobacterial species.

LIST OF ABBREVIATIONS

%	Percent
°C	Degree Celsius
µg	Microgram
µl	Microliter
µM	Micromolar
AFB	Acid Fast Bacilli
AIDS	Acquired Immune Deficiency Syndrome
ATCC	American Type Culture Collection
BCG	Bacillus Calmette Guerin
BLAST	Basic Local Alignment Search Tool
bp	Base pair
CDRI	Central Drug Research Institute, Lucknow
CFU	Colony Forming Units
CRI	Central Research Institute
DLG	Docking Log File
DNA	Deoxyribonucleic acid
EDTA	Ethylenediaminetetraacetic acid
ESAT	Early Secretory Antigenic Target
EtBr	Ethidium Bromide
FDA	Food and Drug Administration
g	Grams
gDNA	Genomic DNA
GTE	Glucose Tris EDTA
H ₂ O ₂	Hydrogen Peroxide
HIV	Human Immunodeficiency Virus
IAEC	Institutional Animal Ethics Committee
IDSA	Infectious Disease Society of America
IFN-γ	Interferon-gamma
IL	Interleukin
IMTECH	Institute of Microbial Technology, India
IPTG	Isopropyl β-D-1-thiogalactopyranoside

kg	Kilograms
Km ^r	Kanamycin
LAM	Lipoarabinomannan
LB	Luria Bertani
LBGT	Luria Bertani Glycerol Tween
LJ	Lowenstein-Jensen
log ₁₀	Logarithm to base 10
LTBI	Latent Tuberculosis Infection
MA	Mycolic Acid
ManLAM	Mannose capped lipoarabinomannan
MfAS	<i>M. fortuitum</i> anthranilate synthase
MfrimP	<i>M. fortuitum</i> ribosomal maturation factor gene
MfRimP	<i>M. fortuitum</i> ribosomal maturation factor protein
Mfsdr	<i>M. fortuitum</i> short chain dehydrogenase gene
MfSdr	<i>M. fortuitum</i> short chain dehydrogenase protein
MftrpE	<i>M. fortuitum</i> anthranilate synthase component I gene
MfTrpE	<i>M. fortuitum</i> anthranilate synthase component I protein
MftrpG	<i>M. fortuitum</i> anthranilate synthase component II gene
MfTrpG	<i>M. fortuitum</i> anthranilate synthase component II protein
MTBC	<i>Mycobacterium tuberculosis</i> complex
MB	Middle Brook
MBGT	Middle Brook Glycerol Tween
M-DAP	Meso-diamino pimelic acid
mL	Milliliter
mM	Millimolar
MurNAc	N-acetyl muramic acid
MurNGlyc	N-glycosyl muramic acid
NAD	Nicotinamide Adenine Dinucleotide
NAT	Nutrient Agar Tween
NCBI	National Centre for Biotechnology Information
NIPER	National Institute of Pharmaceutical Education and Research
NK	Natural Killer
nm	nanometer

NO	Nitric Oxide
NRP	Non-Replicating Persistence
NTM	Non-Tuberculous Mycobacteria
OD	Optical Density
ONPG	o-nitrophenyl β -D-galactoside
ORF	Open Reading Frame
PBS	Phosphate Buffered Saline
PCR	Polymerase Chain Reaction
PDIM	Phthiocerol Dimycoserate
PGN	Peptidoglycan
pH	power of hydrogen
phoA	Alkaline phosphatase gene
PhoA	Alkaline phosphatase protein
PIM	Phosphatidyl-myo-inositol mannoside
PILAM	Phosphoinositol capped Lipoarabinomannan
pNPP	para-Nitrophenyl phosphate
psi	per square inch
pUC	plasmid University of California
RGM	Rapidly Growing Mycobacteria
RMSD	Root Mean Square Deviation
RNA	Ribonucleic acid
RNI	Reactive nitrogen intermediate(s)
ROS	Reactive oxygen species
Rpf	Resuscitation promoting factors
SD	Standard Deviation
SDS	Sodium Dodecyl Sulphate
sec	Seconds
SGM	Slow Growing Mycobacteria
sigH	Sigma factor H
STRING	Search Tool for the Retrieval of Interacting Genes/Proteins
TAE	Tris acetate EDTA
TB	Tuberculosis
TCS	Two-component signal transduction system

TE	Tris EDTA
TES	Tris EDTA saline
TGF- β	Transforming growth factor-beta
Tn	Transposon
Tnase	Transposase enzyme
TNF	Tumor Necrosis Factor
TnphoA	Tn5 transposon and alkaline phosphatase fusion cassette
UV	Ultra Violet
WHO	World Health Organization
WTMF	Wild type <i>M. fortuitum</i>
X-gal	5-Bromo-4-chloro-3-indolyl- β -galactopyranoside
XP	5-Bromo-4-chloro-3-indolyl phosphate
ZN	Ziehl-Neelsen

LIST OF FIGURES

Figure No.	Title	Page No.
Figure 1.1	TnphoA-based transposon mutagenesis	4
Figure 2.1	Mycobacterium cell wall	8
Figure 2.2	<i>M. tuberculosis</i> pathogenesis mechanism	11
Figure 2.3	Brief introduction of Non-Tuberculous Mycobacteria (NTM)	12
Figure 2.4	Predominant NTM isolated from different regions of the World	17
Figure 2.5	Infections caused by <i>M. fortuitum</i>	18
Figure 2.6	Pro-inflammatory cytokines in <i>M. tuberculosis</i> infection	33
Figure 2.7	Flow diagram of the mechanism of transposition	38
Figure 3.1	Strategy for identification of the mutated gene	48
Figure 3.2	Flow chart for identification of the mutated gene	49
Figure 4.1	Primary screening of <i>M. fortuitum</i> transposon mutants on selection plates containing XP	59
Figure 4.2	Symptoms in mice infected with wild type <i>M. fortuitum</i> (WTMF) and the mutants	61
Figure 4.3	Bacillary load in kidney tissue of mice infected with WTMF and mutants	62
Figure 4.4	Histopathology of kidney tissue infected with WTMF and attenuated mutants (MT726, MT725, and MT727)	64-65
Figure 4.5	Cytokine profiling of WTMF and attenuated mutants (MT726, MT725, and MT727)	66
Figure 4.6	Amplification of transposon specific PCR product	67
Figure 4.7	Nucleotide sequence (GenBank accession number KY250516) and translated protein sequence of probable <i>M. fortuitum</i> short-chain dehydrogenase (MfSdr)	68
Figure 4.8	Multiple sequence alignment of <i>M. fortuitum</i> short-chain dehydrogenase (MfSdr)	69
Figure 4.9	Complete nucleotide sequence obtained after cloning and sequencing of mutant MT725	69

Figure 4.10	Translated protein sequence of putative <i>M. fortuitum</i> anthranilate synthase component I (MfTrpE) and anthranilate synthase component II (MfTrpG)	70
Figure 4.11	Multiple sequence alignment of <i>M. fortuitum</i> Anthranilate synthase component I (MfTrpE) and <i>M. fortuitum</i> Anthranilate synthase component II (MfTrpG) with <i>M. abscessus</i> and <i>M. tuberculosis</i> TrpE and TrpG	71
Figure 4.12	Overlap of nucleotide sequence between two ORFs coding for <i>M. fortuitum</i> Anthranilate synthase component I (MftrpE) and Anthranilate synthase component II (MftrpG) of tryptophan operon in <i>M. fortuitum</i>	72
Figure 4.13	Nucleotide Sequence (GenBank accession number MH052677) and translated protein sequence of putative ribosomal maturation factor (RimP) of <i>M. fortuitum</i>	73
Figure 4.14	Multiple sequence alignment of <i>M. fortuitum</i> Ribosomal maturation factor (MfRimP) with RimP of <i>M. abscessus</i> and <i>M. tuberculosis</i>	73
Figure 4.15	Growth kinetics of mutants under <i>in vitro</i> acidic stress	76
Figure 4.16	Growth kinetics of the mutants under <i>in vitro</i> oxidative and heat stress conditions	78
Figure 4.17	Growth kinetics of mutants under <i>in vitro</i> detergent stress and nutrient starvation conditions	80
Figure 4.18	Growth kinetics of mutants (MT726, MT727, and MT725) under <i>in vitro</i> hypoxic stress	81
Figure 4.19	Transmembrane helix prediction in the amino acid sequence of <i>M. fortuitum</i> short-chain dehydrogenase (MfSdr)	82
Figure 4.20	Protein-protein interaction studies of <i>M. tuberculosis</i> Rv2509, a homolog of <i>M. fortuitum</i> short-chain dehydrogenase (MfSdr) using STRING	83-84
Figure 4.21	Secondary structure of <i>M. fortuitum</i> short-chain dehydrogenase (MfSdr)	85
Figure 4.22	Visualization of ligand-receptor interactions using MegaMol	87

LIST OF TABLES

Table No.	Title	Page No.
Table 2.1	List of virulent mechanisms of MTBC	9
Table 2.2	Runyon classification of NTM	13
Table 2.3	List of NTM incidences report from India	15-16
Table 2.4	List of surface protein-encoding genes of <i>M. tuberculosis</i> involved in host-pathogen interactions	26-27
Table 2.5	List of databases for identification of genes/proteins involved in virulence	35
Table 2.6	Wet lab strategies used for gene knockout studies	36
Table 2.7	<i>In silico</i> approaches used for gene knockout studies	36
Table 2.8	Reporter genes commonly used in bacterial systems	41
Table 3.1	Bacterial strains used in the current study	43
Table 3.2	Plasmids used in the current study	43
Table 3.3	Primers used in the current study	44
Table 3.4	List of tools used for bioinformatics analysis	53
Table 4.1	Alkaline phosphatase activity of transposon mutants	60
Table 4.2	Genes identified in mutants MT721, MT723, and MT724	74
Table 4.3	List of proteins interacting with <i>M. tuberculosis</i> Rv2509, a homolog of <i>M. fortuitum</i> short-chain dehydrogenase and their reported functions (as taken from Mycobrowser database https://mycobrowser.epfl.ch)	84
Table 4.4	Potential inhibitors of <i>M. fortuitum</i> short-chain dehydrogenase (MfSdr) identified by virtual screening using Autodock version 4.2.6	86
Table 5.1	<i>M. tuberculosis</i> genes involved in survival under stress conditions	89

INTRODUCTION

Genus *Mycobacterium* belongs to family Mycobacteriaceae and is characterized by a thick and hydrophobic cell wall that contains mycolic acids. This genus consists of 188 species [1], broadly categorized based on their pathogenesis into *Mycobacterium tuberculosis* complex (MTBC) and Nontuberculous mycobacteria (NTM). *Mycobacterium tuberculosis* complex consists of *Mycobacterium tuberculosis*, *Mycobacterium africanum*, *Mycobacterium canettii*, *Mycobacterium bovis*, *Mycobacterium microti*, etc., and is responsible for causing tuberculosis (TB) or tuberculosis like symptoms. Nontuberculous mycobacteria do not cause tuberculosis; however, they are responsible for a variety of infections in immunocompromised as well as immunocompetent individuals.

NTM have gained significant interest in recent years due to their increased infection incidences and a wide range of virulence among diverse host including humans [2, 3]. NTM can be categorized into rapid-growers and slow-growers based on their generation time. NTM exhibit variable geographical distribution, species spectra, clinical symptoms, and antibiotic susceptibility profile, which lead to complications in their identification and diagnosis [4]. Infections from NTM can also mislead to treatment against *M. tuberculosis*, hence, American Thoracic Society (ATS) and Infectious Disease Society of America (IDSA) have recommended to follow proper diagnostic criteria for identification of NTM along with *M. tuberculosis* in sputum samples. Currently recommended treatment regimens, resistance patterns towards drugs, and treatment outcomes differ according to the NTM species, leading to lengthy and complicated management of such infections with limited therapeutic options.

Mycobacterium fortuitum is one of the most prevalent rapidly growing pathogenic NTM worldwide, which is responsible for varied infections including skin and soft tissue infections, lung infections, bone infections, and bloodborne infections [5-7]. Misinterpretation of *M. fortuitum* infections in the lungs can lead to treatment against *M. tuberculosis*, which further complicates the condition due to resistance of *M. fortuitum* to anti-tuberculous drugs. *M. fortuitum* infections have been reported in immunocompromised as well as immunocompetent individuals indicating increased virulence of the pathogen [8, 9]. *M. fortuitum* infections can

be fatal in immunocompromised patients, while its treatment in immunocompetent individuals may also require long term drug therapy [10]. In ocular mycobacteriosis, *M. fortuitum* has been reported to cause co-infection along with *M. tuberculosis*, with no results from anti-tuberculous drug therapy, indicating the requirement of multidrug treatment for *M. fortuitum* along with *M. tuberculosis* in such cases [11].

M. fortuitum is an intracellular pathogen and resides inside the macrophages in the same way as *M. tuberculosis*. It can evade the bactericidal effects of the immune system by restricting nitrogen oxide radicals and phagosome-lysosome fusion [12]. Acidic environment prevalent inside macrophages contributes to its bactericidal effect, as excessive protons can damage lipids, proteins, and nucleotides of the invading mycobacteria. In addition, acidic pH inside the macrophage adversely affects the biochemical activities of the residing mycobacteria [13]. Besides acidic stress, other stress conditions including oxidative stress, nutrient starvation, detergent stress, and heat stress are also prevalent inside the macrophage, which act as defense arsenal of the host. *M. fortuitum* has been found to be present in necrotic granuloma in a non-replicating persistence (NRP) form [14]. In this state, the bacilli are likely to experience unfavorable environmental conditions including low oxygen tension, i.e., hypoxic stress inside the host [15]. To combat the drastic effect of stress conditions prevalent inside the host, the pathogen evolves various strategies including change of their metabolic behavior.

Cell membrane proteins are an important part of bacteria, as they help the bacteria to maintain its integrity, acts as a guard for entry of molecules, interact with outside molecules and are involved in inducing signaling pathways. Membrane proteins also help the bacteria in the acquisition of antibiotic resistance and combating unfavorable environment inside the host [16]. Owing to essential functions performed by the bacterial cell membrane, the present study was undertaken to identify membrane proteins of *M. fortuitum* which may play an important role in its virulence and pathogenesis, using transposon mutagenesis.

Transposon mutagenesis used in the present study is a valuable and useful method to identify genes of a specific phenotype. TnphoA is a construct derived from transposon Tn5 which is used to generate mutants and characterize genes coding for membrane/transmembrane or secretory proteins. TnphoA based transposon mutagenesis [17] provides a simple and efficient

way to identify membrane/ transmembrane or secretory protein-encoding genes due to the presence of characteristic *phoA* gene from *Escherichia coli*. The gene *phoA* codes for alkaline phosphatase, which is a periplasmic protein. In *TnphoA*, the *phoA* gene is devoid of N' terminal signal sequence. Active expression of alkaline phosphatase requires export signals in the form of N' terminal signal sequence, which helps in its translocation across the cytoplasmic membrane to the periplasmic space (Figure 1.1 A). Thus, the fusion of the *phoA* gene with an export signal of membrane/transmembrane/secretory protein-encoding genes leads to translocation and active expression of the alkaline phosphatase (Figure 1.1 B). Hence, mutants with *TnphoA* insertion into membrane protein-encoding genes can be identified based on the enzymatic activity of the alkaline phosphatase protein. Transposon mutagenesis has been previously used for the identification of virulence genes of pathogenic mycobacterium including *M. tuberculosis* [18, 19] and *M. marinum* [20]. Employing *TnphoA* based transposon mutagenesis, leucine responsive protein-encoding gene *lrp* was identified to play a role in virulence and persistence of *M. fortuitum* [14].

Although incidence of *M. fortuitum* infections are on rise, very scarce information related to its mechanism of pathogenesis and virulence determinants is available. Hence, exploring the role of *M. fortuitum* genes and proteins playing crucial role in its pathogenesis is warranted for identification of novel drug targets, which would lead to better understanding of the molecular mechanism of *M. fortuitum* pathogenesis and serve as steppingstone for development of new drugs as therapeutics.

The aim of the present study was to identify membrane protein-encoding genes of *M. fortuitum* as a potential drug target. The result of the study can also be extrapolated to identify homologs of the identified drug targets for designing and/or screening of inhibitors against other pathogenic mycobacteria including *M. tuberculosis*.

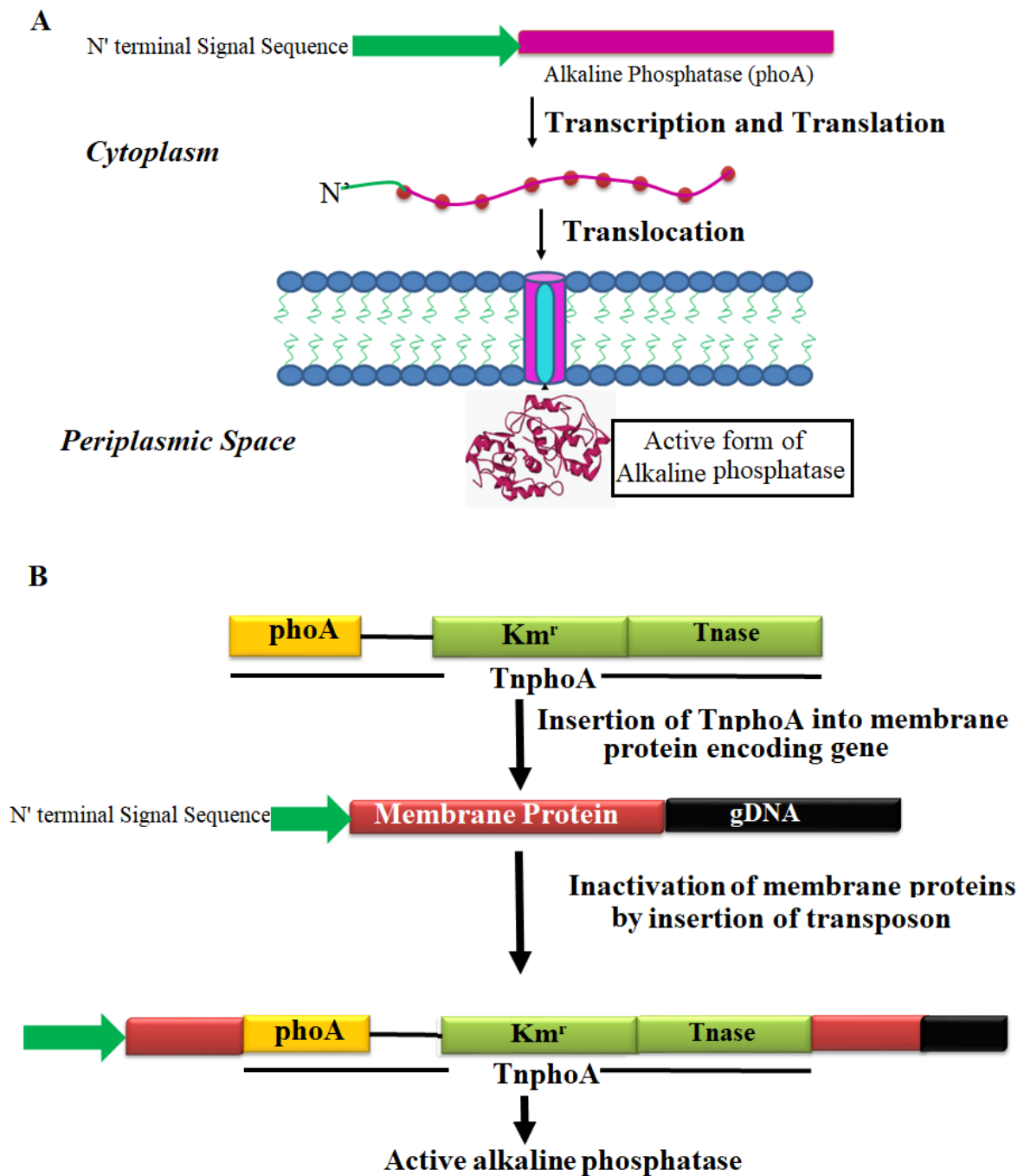


Figure 1.1: TnphoA-based transposon mutagenesis. The figure shows strategy of TnphoA-based transposon mutagenesis for identification of membrane protein-encoding genes. (A) Represents the requirement of the N-terminal signal sequence for translocation of alkaline phosphatase (PhoA) enzyme to the periplasmic space for its active expression. (B) Mechanism of transposon mutagenesis - depicting insertion of TnphoA into genomic DNA (gDNA) of the host for the identification of membrane proteins-encoding genes. TnphoA contains kanamycin resistance gene (Km^r), transposase enzyme (Tnase) and phoA gene which lacks N-terminal sequence, active insertion of TnphoA into N-terminal signal sequence containing membrane protein-encoding genes leads to active expression of alkaline phosphatase that can be determined phenotypically.

The study was designed with the following objectives:

1) Identification of mutants defective in *in vivo* virulence

- a) Construction and screening of transposon mutant library
- b) *In vivo* virulence studies
- c) Histopathology and immuno-profiling

2) Analyses of mutants for the identification of potential drug targets

- a) Genomic and bioinformatics analyses
- b) Growth analyses under *in vitro* stress conditions

3) Structure prediction, interaction and molecular docking studies to identify potential inhibitors

The thesis is divided into the following chapters:

Chapter 1: Introduction to the present study.

Chapter 2: Related Review of Literature.

Chapter 3: Materials and Methods employed in the study.

Chapter 4: The Results obtained in the present study.

Chapter 5: A comprehensive discussion of results obtained in the present study.

Chapter 6: Conclusion and future prospects

REVIEW OF LITERATURE

2.1 Genus *Mycobacterium*

Genus *Mycobacterium* belongs to phylum Actinobacteria and family Mycobacteriaceae. The genus is characterized by its unique, thick, pliable, hydrophobic cell wall containing mycolic acid that provide a special trait of acid-alcohol fastness [21]. In addition to acid-alcohol fastness, the genus also displays a thread-like 'mycelium' growth in liquid culture media. The generation time of genus *mycobacterium* ranges from 2 hours to more than 20 hours [22], requiring an incubation time of a few days to over 8 weeks to produce visible colonies on solid media at optimum temperatures. Based on the incubation period, members of the genus *Mycobacterium* are classified into slow-growing mycobacteria (SGM) and rapidly-growing mycobacteria (RGM). Mycobacterial species generally exhibit whitish or cream-colored colonies; however, species also contain carotene pigment which gives bright yellow or orange color to their colonies [23]. Genus *mycobacterium* consists of 188 species, and with genome sequences of more than 150 members from the genus *Mycobacterium* available in the NCBI genome database [1].

2.1.1 Cell wall of genus *Mycobacteria*

Mycobacterial cell wall functions as an important virulence factor and helps the bacteria to resist antibiotic action and unfavorable stress conditions inside the host [24]. Cell wall of mycobacteria is different from other bacterial species. Its composition also varies between fast-growing and slow-growing mycobacteria. Proteins, lipids, and carbohydrates are major components of the cell wall and make up its inner and outer layer. The structure of a typical mycobacterial cell wall is given in Figure 2.1.

Components of the inner layer of the cell wall include peptidoglycan, arabinogalactan, and mycolic acids. These three components are connected to each other to form an insoluble 'mycolyl-arabinogalactan-peptidoglycan' complex and make a layer over the plasma membrane [25]. Mycobacterial peptidoglycan differs from other bacteria in having N-glycolyl-muramic acid (MurNGlyc) which is a byproduct of N-acetylmuramic acid (MurNAc) oxidation. Cross-linking of meso-diaminopimelic acid (m-DAP) and D-alanine (3→4) produce L-alanyl-D-isoglutaminyl-meso-di aminopimelyl-D-alanine in the side chain

of peptidoglycan. Mycobacteria also have a unique feature to modify peptidoglycan (3→4) cross-linkages to (3→3) cross-linkages for protection against degradation by endopeptidases [21]. Peptidoglycan decreases the susceptibility of mycobacteria to lysozyme and provides a site for hydrogen bonding and arabinogalactan attachment.

Arabinogalactan is a hetero-polysaccharide composed of galactan, and arabinan sugar subunits. Galactan component of arabinogalactan is formed by thirty linearly attached galactose units, while arabinan component is formed by thirty highly branched arabinose residues. Arabinogalactan is connected to mycolic acids in the form of tetramycolyl-pentaarabinofuranosyl clusters. Short α -alkyl and long β -hydroxyl-fatty acids constitute mycolic acids. Mycolic acids are the major and specific lipid components of the mycobacterial cell envelope and are essential for the survival of members of the genus *Mycobacterium* [26].

The presence of lipids such as lipoarabinomannan (LAM), lipomannan, phthiocerol-containing lipids, dimycolyl-trehalose (cord factor), sulfolipids, and phosphatidylinositol mannosides in outer cell wall provides uniqueness to *Mycobacterium*. LAM modifications differentiate between slow-growing and rapidly growing mycobacterium. In slow-growing mycobacterium, β -Ara of LAM is capped with mannose (ManLAM), while in rapidly-growing mycobacterium such as *M. fortuitum* phosphoinositol (PILAM) is present. However, in *Mycobacterium chelonae*, LAM does not contain any capping.

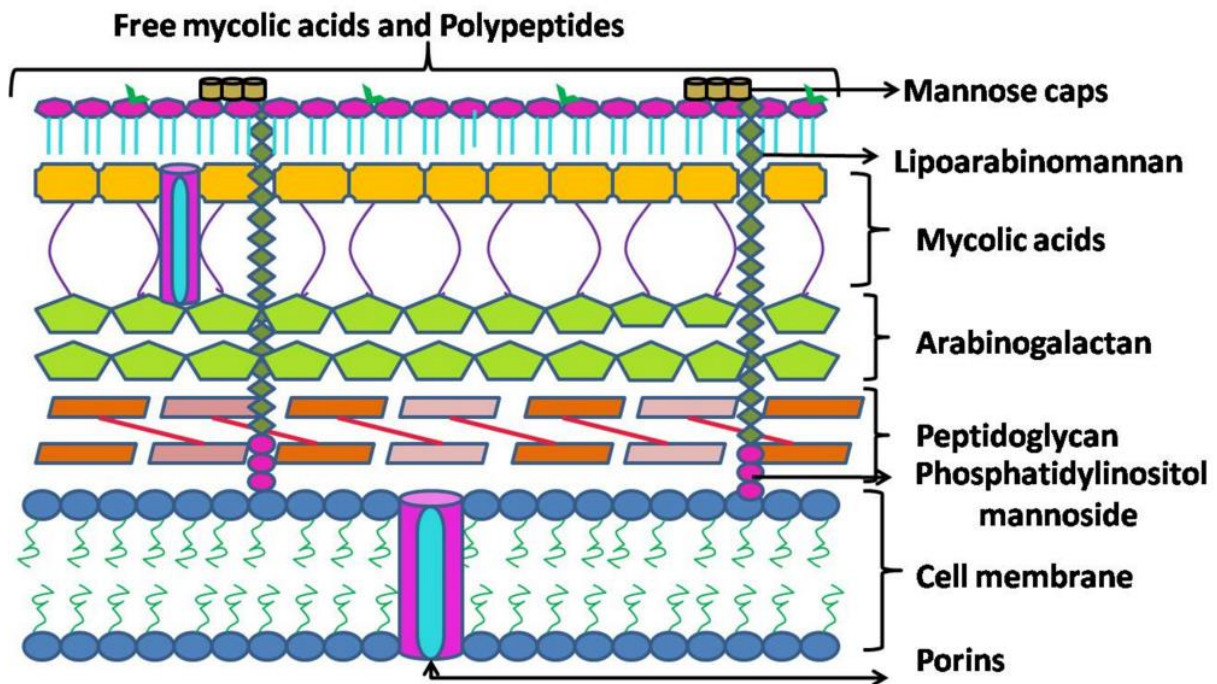


Figure 2.1: Mycobacterium cell wall. The figure shows different components of cell wall of Genus Mycobacteria. (Adapted from Hett and Rubin, 2008 [25]).

2.1.2 Classification of genus Mycobacterium

The genus Mycobacterium is a hub of about 188 species [1], which vary in their pathogenicity. Thus, based on their pathogenicity members of this genus have been broadly divided into two classes: *Mycobacterium tuberculosis* complex (MTBC) and Non-tuberculous mycobacteria (NTM).

2.1.2.1 Mycobacterium tuberculosis complex (MTBC)

Mycobacterium tuberculosis complex (MTBC) is a group of closely related bacterial species, which causes tuberculosis, and infect a huge population including humans and animals. Members of MTBC majorly comprise of *Mycobacterium tuberculosis*, *Mycobacterium bovis*, *Mycobacterium africanum*, *Mycobacterium canettii*, *Mycobacterium microti* etc. [27]. Except *M. tuberculosis*, other members of the MTBC group are genetically related and share about 90% nucleotide similarity [28]. Although MTBC members are genetically related, they differ from one another concerning their pathogenicity and choice of host, e.g. *M. tuberculosis*, and *M. africanum* infect humans, whereas, *M. bovis* and *M. microti* mainly infect animals. The majorly used preventive measure for tuberculosis is BCG (Bacillus Calmette Guerin) vaccine, which is derived from *M. bovis* strain [28].

The presence of a variety of virulent mechanisms in MTBC enables it to cause disease and resisting various unfavorable conditions inside the host. A list of known virulence mechanisms is given below.

Table 2.1: List of virulent mechanisms of MTBC. The table represents various virulence mechanisms used by *M. tuberculosis* complex (MTBC) to resist unfavorable conditions prevalent inside the host. (Adapted from Forrellad et al., 2013 [29]).

S.N.	Mechanism
1	Lipid and fatty acid metabolism inside host which helps the bacteria to use fatty acids of the host during nutrient starvation
2	Cell envelope proteins help the bacteria in initial interaction as well as provide resistance to stress conditions prevalent inside host
3	Proteins neutralizing antimicrobial effectors of the macrophage and help in preventing phagocytosis inside phagocytic cells
4	Protein kinases block intracellular degradation of mycobacteria inside the lysosome
5	Proteases which help in protein secretion, degradation, and virulence
6	Metal-transporter proteins
7	Gene expression regulators, including two-component systems, sigma factors, and other transcriptional regulators
8	Proteins of unknown function, including PE and PE_PGRS families

Mycobacterium bovis

M. bovis is the major cause of tuberculosis in animals, and zoonotic transmission of this pathogen to humans can cause symptoms similar to tuberculosis. *M. bovis* has dysgonic growth behavior i.e. the bacteria show relatively slow and poor growth in comparison to other bacteria. Most strains of *M. bovis* are resistant to commonly used anti-tuberculous drug pyrazinamide [30]. *M. bovis* causes bovine tuberculosis and is also used as a weapon against *M. tuberculosis* in the form of vaccine [31]. The only vaccine currently available against TB is the attenuated *M. bovis* strain BCG. Although the efficacy of BCG vaccine varies among individuals, BCG has been reported to be protective against newborn tuberculosis and can protect children till 10-15 years of age [32].

Mycobacterium tuberculosis

Mycobacterium tuberculosis causes TB, the major cause of mortality in developing countries [33]. TB is one of the top infectious killers globally and affecting about 4000 lives per day. The rate of new cases of TB increased from 6.4 million in 2017 to 7 million in 2018 [34]. The respiratory tract is the main route of infection by *M. tuberculosis*. Inhalation of *M. tuberculosis* contaminated aerosols leads to lodgment of bacilli in terminal air spaces of lungs, where it enters and replicates within alveolar macrophages. Progression of the disease occurs through various phases including, initial replication of the pathogen inside lungs, spread within pulmonary lymph nodes, and dissemination of the bacteria to other parts of the body. Immuno-competent status of host enables control over primary infection by *M. tuberculosis*, and hence prevents the spread of disease to other organs. However, the pathogen has an ability to be present in a latent form, which is characterized by persistence of the pathogen without multiplication in the presence of host immune response. Presence of a latent form of the bacilli is called latent tuberculosis infection (LTBI), which may revert back to its active form in the host during the state of compromised immune response (Figure 2.1). Pathogenesis of this bacilli defines its cleverness to hoax host immune response by hibernating itself inside granuloma. ‘Granuloma’ is a well-defined structure of immune cells, which constricts the spread of the pathogen to other parts of the body, and in process benefits the bacilli in providing a hiding niche to it. Several genes in *M. tuberculosis* have been identified which are involved in safe-guarding the pathogen from the host immune system [29].

M. tuberculosis is the most successful member of MTBC, which has acquired the top position in establishing itself inside unfavorable conditions prevalent in the host-cells. The high incidences of *M. tuberculosis* can be attributed to its ability to combat antimicrobial [35], ability to modify host immune response [36], and ability to adapt various unfavorable stress conditions inside the host [37].

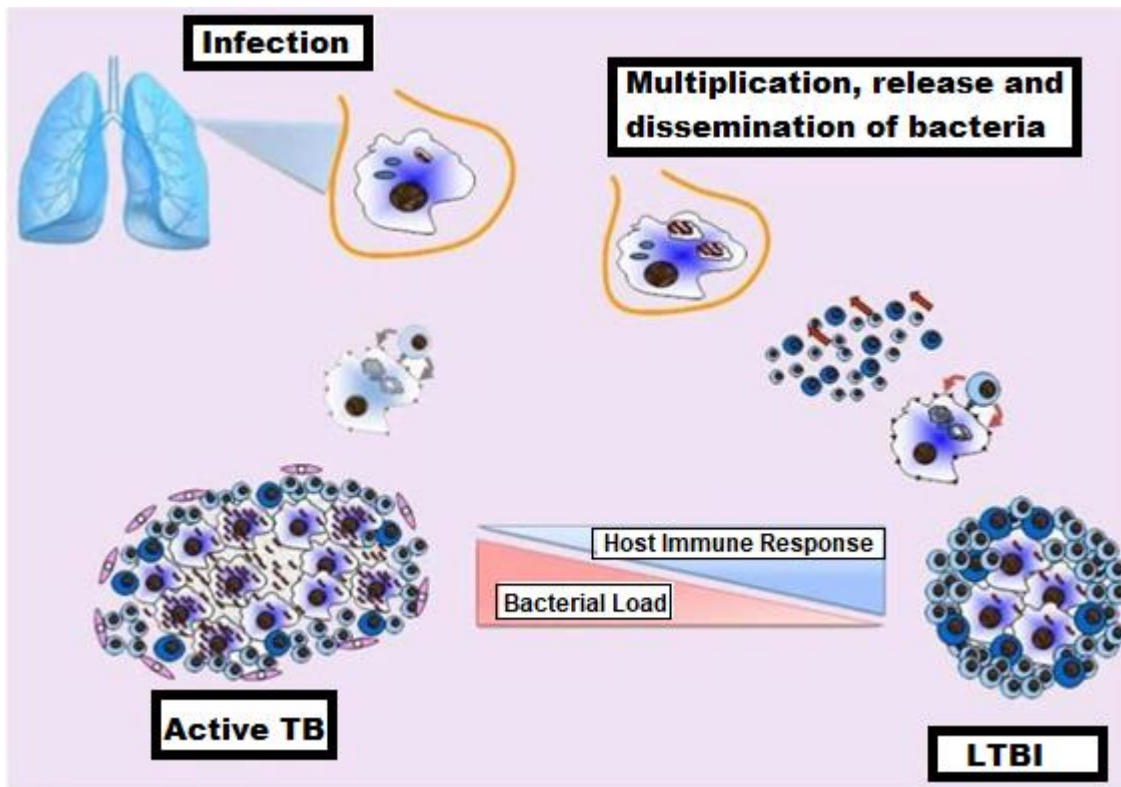


Figure 2.2: *M. tuberculosis* pathogenesis mechanism. The figure represents steps required for pathogenesis of *M. tuberculosis*. After inhalation, *M. tuberculosis* multiplies inside the host-cell followed by release and dissemination to other cells, which results in ‘active tuberculosis (TB)’, whereas in the presence of active immune response *M. tuberculosis* remains in dormant form and cause latent tuberculosis infection (LTBI). (Adapted from Delogu et al., 2013 [38]).

2.1.2.2 Nontuberculous Mycobacteria (NTM)

NTM are ubiquitous, occupying diverse habitats including water, soil, animals, and dairy products. NTM use these range of habitats as their reservoir, which mainly include drinking water distribution systems, household plumbing, and showerheads [39]. The omnipresence of NTMs in the environment enables them to cause infection in broad range of hosts such as mammals, fish, and birds [39]. Inadequacy of available sterilization techniques to decontaminate in hospitals and other health care settings enables NTM to cause nosocomial infections [40]. NTM were not considered as pathogens before 1930, however, due to availability of immunocompromised hosts and the prevalence of AIDS pandemic, NTM have emerged as important pathogen.

The ability of NTM to grow under low oxygen conditions highlights their potential to survive harsh environmental conditions [41]. NTM have an impermeable hydrophobic lipid-rich cell

wall, which helps them to attach to the substrate and make them resistant to environmental stress conditions. Most pathogenic NTM reside inside macrophage, the defense cells of the body, and tolerate the stress conditions generated by macrophages as a defense mechanism [42]. The ability of NTM to remain in a dormant form is also one of the strategies used to adapt stress conditions [42, 43]. Most dormant forms of NTM reside inside the host granuloma meant to contain the bacilli and prevent their further multiplication and transmission [44].

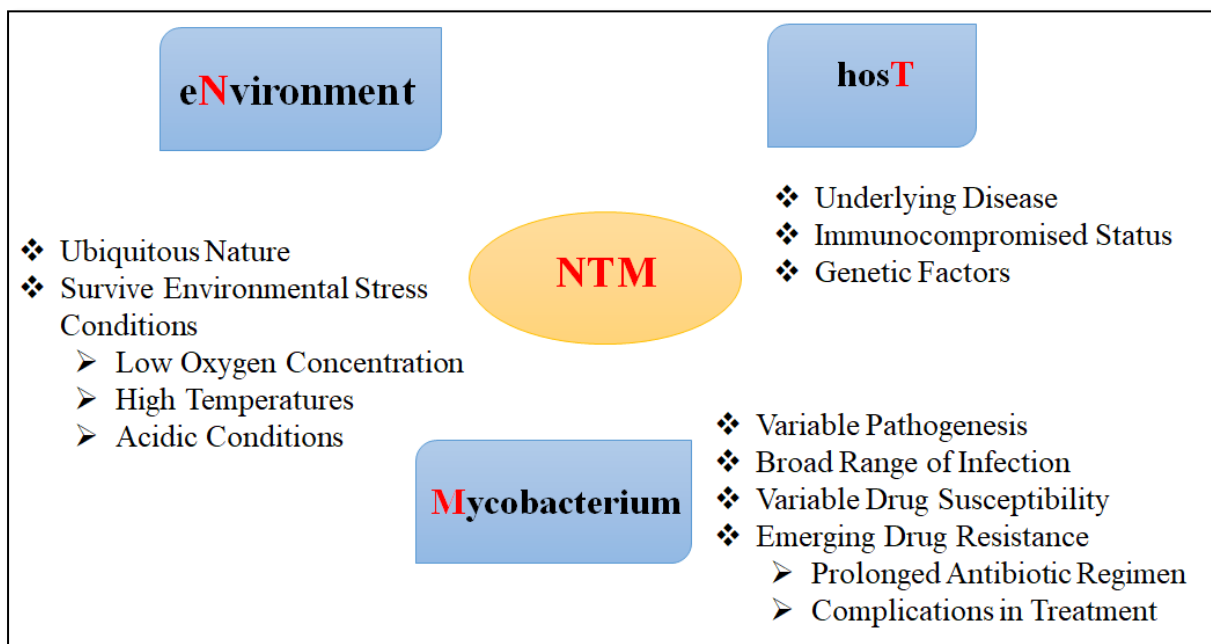


Figure 2.3: Brief introduction of Non-Tuberculous Mycobacteria (NTM). The figure represents characteristics of NTM based on their prevalence in environment, susceptibility of host, and pathogenesis and resistance of NTM group of Genus *Mycobacterium*. (Adapted from Honda et al., 2018) [45]).

NTM are divided into four groups based on growth rate and pigment production according to the Runyon classification [46] (Table 2.2).

Table 2.2: Runyon classification of NTM. The table represents classification of Non-tuberculous Mycobacteria (NTM) along with clinically important pathogenic NTM of each class.

Runyon group	Name of group	Growth/pigment production	Clinically important
I	Photochromogens	Slow growing/ yellow orange pigment production on exposure to light	<i>M. kansasii</i> , <i>M. marinum</i>
II	Scotochromogens	Slow growing/ yellow-orange pigment production with or without light	<i>M. scrofulaceum</i> , <i>M. goodii</i>
III	Nonchromogens	Slow growing/ none	<i>M. avium intracellulare</i> , <i>M. xenopi</i> , <i>M. terrae</i>
IV	Rapid growers	Rapidly growing/ none	<i>M. fortuitum</i> / <i>M. peregrinum</i> , <i>M. chelonae</i>

2.1.2.2.1 Pathogenic NTM

Pathogenic NTM are a global public health concern due to their pervasive presence and ability to cause infection in diverse host range including humans, livestock, and wildlife [47, 48]. NTM can cause a diverse range of infections viz. pulmonary infections, extrapulmonary infections, and disseminated infections [49-51]. Catheter-associated infections and sepsis are the most common hospital associated infections due to NTM in both immunocompromised as well as immunocompetent patients [40]. Association of NTM with ocular infection has been reviewed by Kheir and colleagues, where they highlighted detrimental outcomes of NTM ocular infections due to delay in diagnosis and drug resistance [52].

Majority of infections caused by NTM are related to individuals with immunocompromised status [51]. Persons with chronic obstructive pulmonary disease (COPD), cystic fibrosis, bronchiectasis, primary or secondary immunodeficiency, or lung transplant are more susceptible to lung infections by NTM [49, 53]. Cystic fibrosis is a major contributor to pulmonary infections due to NTM, as the risk of NTM pulmonary infections is higher in children as well as adults suffering from cystic fibrosis [54]. As per the susceptibility of NTM pulmonary infection in cystic fibrosis patients, lung transplantation in such individuals require knowledge of past history of NTM exposure to avoid any kind of complications [55].

Association of NTM with HIV infection suggests some genomic interaction between HIV and mycobacterial genome which leads to multidrug resistant strains of mycobacteria [56]. Due to similarity of clinical symptoms as well as staining properties between NTM and *M. tuberculosis*, NTM have been recovered in many cases suspected with tuberculosis. Major complications in case of NTM infections are the lack of standard diagnostic criteria, streamlined drug pipeline and increasing drug resistance [42].

2.1.2.2.2 Epidemiology of NTM

An increase in incidences of NTM infections in the international scenario has been observed in recent years. The increase can be attributed to increment in NTM sources of infections, number of susceptible individuals, improvement of laboratory detection techniques, and awareness about NTM infections [57]. Although detailing the epidemiology of NTM infections is complicated due to hurdles like manifestation of variable symptoms, ubiquitous presence of NTM in the environment which overshadows the significance of a positive culture in patients, absence of a proper definition and negligence of NTM infections [58]

In Europe, the scenario of NTM infections is critical as number of NTM infections are increasing every year [59]. NTM species identified most frequently in European territory include *M. avium*, *M. gordonae*, *M. xenopi*, *M. intracellulare*, and *M. fortuitum* [59]. In France, Roax et al. also reported a higher prevalence of NTM infections in cystic fibrosis patients [60]. A 65-month epidemiological data from Greece found an incidence rate of 18.9 and 8.8 per 100000 inpatients and outpatients, respectively [61]. In Denmark, the rate of *M. avium* infections in pulmonary samples is high, whereas *M. marinum* was prevalent in extrapulmonary samples [2].

Among pathogenic NTM, the species of NTM found to be most prevalent in Brazil were *M. avium*, *M. abscessus*, and *M. fortuitum*. In nosocomial infections caused by NTM, comorbidities have been reported in HIV infected individuals [62]. Costa et al reviewed isolation of NTM species including, *M. avium* complex, *M. kansasii* and *M. fortuitum* from pulmonary infections [63]. Other data from the year 1993-2011, reported *M. kansasii*, *M. avium* complex, *M. abscessus*, and *M. fortuitum* to be more frequently isolated species [64].

Various reports from India signify the importance of NTM infections. As India is a TB endemic country, NTM infections have not been given the importance they deserve. As per the guidelines of the American Thoracic Society, NTM has come into limelight and various studies gave an estimate of NTM prevalence in different states of India. Data regarding epidemiology of NTM infections in all states is not available. In a study from Mumbai, *M. fortuitum* was found to be the most prevalent NTM among extrapulmonary tuberculosis samples [65]. Eye infections from NTM have also been reported in Southern India [66] and Eastern India [67]. Sengupta and co-workers reviewed an increased prevalence of NTM in India and highlighted the concern about increasing drug resistance among NTM [68]. A study of pulmonary and extrapulmonary samples in Himachal Pradesh from June 2013 to June 2014 showed 13% isolates to be NTM and suggested to keep an eye on the solemnity of NTM in clinical samples. The study also warned against ignoring NTM as contaminants [69]. Infections by NTM are not limited to immunocompromised patients. Musculoskeletal infections by NTM have also been reported in immunocompetent individuals. A retrospective data from tertiary center in Delhi have reported NTM members including *M. kansasii* and *M. chelonae* to cause infections among individuals without any infection of HIV [70]. Table 2.3 provides a list of important NTM reports from India.

Table 2.3: List of NTM incidences report from India. The table enlist important NTM incidence reports from India along with prevalent isolated NTM.

S.N.	Name of infection	Organism	Country/Year	Reference
1	Breast Implant Infection	<i>M. fortuitum</i> <i>M. chelonae</i>	Mumbai, India/ 2002-2010	[71]
2	Extrapulmonary Tuberculosis Infection	<i>M. fortuitum</i>	Mumbai, India/2010-2011	[65]
3	Endophthalmitis	<i>M. chelonae</i> <i>M. fortuitum</i>	Southern India/2004-2015	[66]
4	Pulmonary and Extrapulmonary Tuberculosis	<i>M. fortuitum</i>	New Delhi /2000- 2012)	[6]
5	Post-Surgical Wounds	<i>M. fortuitum</i>	Agra, New Delhi	[72]

6	Pulmonary and Extrapulmonary Infection	<i>M. kansasii</i> , <i>M. chelonae</i>	Delhi, India	[70]
7	Pulmonary and Extrapulmonary Infections	<i>M. fortuitum</i>	Mumbai, India (2005-2008)	[73]
8	Extrapulmonary Tuberculosis	<i>M. fortuitum</i>	Northern India	[3]
9	Post-Operative Wounds	<i>M. fortuitum</i>	Maharashtra, India	[74]
10	Pulmonary and Extrapulmonary infections	<i>M. chelonae</i> and <i>M. fortuitum</i>	Hyderabad, India (Jan-2013 to Dec 2014)	[4]

In other reports from Asian countries, *M. fortuitum* and *M. abscessus* found to be prevalent in pulmonary samples in Iran [75]. In another report from Iran by Nasiri et al., *M. simiae* and *M. fortuitum* were more prominent than other NTM [76], while similar study reported *M. simiae* and *M. fortuitum* along with *M. intracellulare* to be prevalent among infectious NTM [77]. *M. abscessus* and *M. fortuitum* were reported to be prevalent in Singapore in one report focusing on the relevance of NTM in clinical isolates [78].

In Africa, high rate of NTM isolates have been reported in children suspected to have tuberculosis, in Mozambique, which is a TB endemic country. The study also speculates TB misdiagnosis, as a reason for complications in treatment of NTM infections [79]. In a study, *M. avium* complex, *M. fortuitum*, and *M. abscessus* were found to predominant NTM isolates from African patients [80].

Epidemiological data from the United States of America reported the majority of NTM cases from older patients suffering from chronic obstructive pulmonary disease (COPD), of which, *M. abscessus* was responsible for most of the infections [81]. The rate of NTM pulmonary infections was reported to be 12.7/100000 individuals, which is a matter of concern. The U.S. National Institutes of Health recorded an 8.2% per year increase in cases of pulmonary NTM infections in adults aged 65 or above [82]. Donohue et al reported an increase in NTM incidence rate from 8.2 to 16 per 1,00,000 individuals, which is almost double, and found *M. avium*, *M. abscessus*, and *M. fortuitum* to be the prevalent organisms in clinical laboratory samples [83].

NTM isolation reports from Australia identified presence of *M. avium*, *M. kansasii* and *M. fortuitum* from pulmonary infections [84]. An association between NTM infections and climatic change has also been observed in Queensland, where, the incidence ratio of NTM infections increased from 11.1 to 25.88/1,00,000 individuals from the year 2011 to 2016. This increase in an incidence rate ratio of NTM, alarms for accurate diagnosis and treatment of these infections [85].



Figure 2.4: Predominant NTM isolated from different regions of the World. The figure shows globally prevalent NTM, where *Mycobacterium avium* complex (MAC), *M. fortuitum*, *M. abscessus* and *M. chelonae* reviewed to be most prevalent worldwide.

2.2 *Mycobacterium fortuitum*

M. fortuitum is a rapidly growing NTM with an ability to cause a range of infections in various hosts. Although *M. fortuitum* was first isolated in 1905 in a frog, its pathogenic behavior was recognized in 1938 by da Costa Cruz, who isolated *M. fortuitum* from skin abscess of a patient [86]. Since then, many case reports describing *M. fortuitum* as an isolate in various infections viz. pulmonary infection, extrapulmonary infection, and systemic infection have been documented. Most *M. fortuitum* infections are related to surgical and post-surgical treatments. *M. fortuitum* is present in natural habitats like soil, air, and water. Water acts as a reservoir of *M. fortuitum* and is responsible for most of the hospital associated and foot bath related infections [87].

2.2.1 Types of infections caused by *M. fortuitum*

M. fortuitum has the ability to cause a broad range of infections (Figure 2.5). Infections due to *M. fortuitum* includes both pulmonary as well as extrapulmonary infections, which are explained in detail in following section:

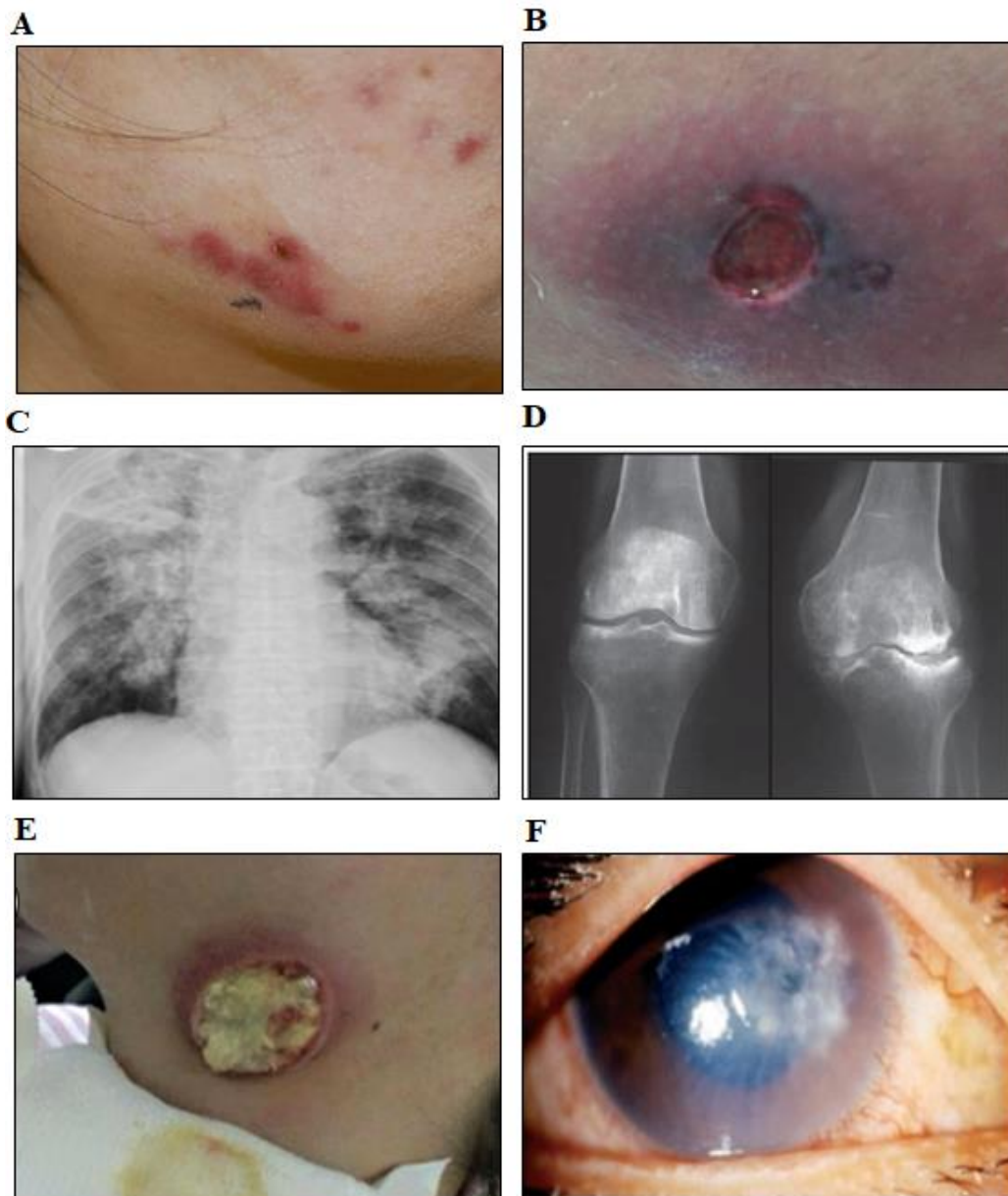


Figure 2.5: Infections caused by *M. fortuitum*. The figure represents different type of infections caused by *M. fortuitum*. (A, B) represents skin and soft tissue infections [94, 95], (C) represents pulmonary infections [96]; (D) represents bone infections [97], (E) represents lymph node infections [98], and (F) represents ocular infection [99].

2.2.1.1 Skin and soft tissue infections

M. fortuitum has made a recognized name in being one of the pathogens associated with skin and soft tissue infection. It causes cutaneous infections after surgery or trauma, which may extend to the lungs, lymph nodes, bones, joints, and meninges, often with fatal outcomes in immunocompromised individuals [88]. Post-breast implant breast infection are common due to *M. fortuitum* [88, 89]. Puncture wound act as a route for entry of *M. fortuitum* and the outcome vary from ulceration, cellulitis, abscesses to even draining sinus tracts [90, 91]. The estimated 321.5 billion surgical procedures would be required to combat the global disease burden treated through surgical procedures [92]. *M. fortuitum* is one of the pathogens associated with surgical procedures. Lack of mycobacterial culturing during diagnosis, as well as standard drug therapy for NTM cutaneous infections poses further challenges. Also, the requirement of prolonged antibiotic therapy for treatment of infections should not be neglected and considered for NTM diagnosis [10]. Clinicians caring for patients with chronic skin or soft tissue infections, especially in immunosuppressed patients or following a surgical procedure, should have a high index of suspicion for rapidly growing mycobacterial disease. Further, studies establishing the optimal duration of therapy and comparing specific regimens are warranted [93]

2.2.1.2 Blood stream infections

M. fortuitum has been isolated from the blood samples of patients suffering from cancer, autoimmune disorders, gastrointestinal disorders, intravenous drug usage, sickle cell anemia and chronic kidney disease [100-102]. *M. fortuitum* has a high predisposition to colonize and infect intravascular catheters and other intravenous devices, hence, presents a major source of blood-borne infections. Treatment of blood-borne infections by *M. fortuitum* can be accomplished by early species identification in blood and testing for antibiotic susceptibility tests. The Infectious Diseases Society of America (IDSA) recommended strict diagnostic criteria for catheter-related blood-borne infections by various microbes including NTM. Time duration required for the culturing of bacteria and variable time taken by NTM to show positive results are major challenges in the diagnosis of NTM, in catheter-related bloodborne infections. A case report of intravenous catheter-related blood infection documented a combination of at least two active antimicrobials given for a minimum of 4 weeks, plus removal of the intravascular catheter for treatment [103].

2.2.1.3 Bone infections

M. fortuitum has been reported to cause a variety of bone infections like osteomyelitis, otitis media, etc. following medical treatments such as surgery, stem cell transplant, and trauma. Spinal osteomyelitis in intravenous drug users due to *M. fortuitum* has also been documented [104, 105]. Case reports of co-infections by *M. fortuitum* with *M. chelonae* and *M. tuberculosis* in osteomyelitis patients are also available [106, 107]. Treatment of *M. fortuitum* bone infections requires around six weeks which is sometimes also associated with surgery, however, dual infection of *M. tuberculosis* and *M. fortuitum* requires longer drug therapy of about 9 months.

2.2.1.4 Ocular infections

M. fortuitum is one of the dominating NTM responsible for ocular infections [52]. Ocular infections due to NTM include periocular or adnexal infections, ocular surface infections, intraocular infections, and uveitis. Co-infection of *M. fortuitum* with *M. tuberculosis* in case of ocular tuberculosis has been reported in an immunosuppressed patient, who was not responding to anti-tuberculous therapy [11]. A case report related to *M. fortuitum* keratitis is documented by Sanghvi in a patient who was unresponsive to standard drug antibiotic therapy [108].

2.2.1.5 Disseminated infections

Spread of infection from one organ of the body to another organ is called as disseminated infection. Various incidence of disseminated infections by *M. fortuitum* have been reported in immunocompromised patients in the form of folliculitis and nodular lesions [9, 109]. In recent years, the cases of disseminating infections are emerging in patients with immuno-competent status as well [8, 110].

2.2.1.6 Pulmonary infections

Most pulmonary infections by *M. fortuitum* occur in patients with pre-existing lung diseases such as cystic fibrosis or tuberculosis [111]. Gastro-esophageal infection is also one of the factors responsible for pulmonary infections by *M. fortuitum* [112]. According to a report from India, 10% of the pulmonary infections by *M. fortuitum* were misdiagnosed as multidrug-resistant *M. tuberculosis* infection [73]. The epidemiological analyses of the prevalence of NTM among pulmonary infection suspects also reported *M. fortuitum* as one of

the prevalent NTM in India [7]. A similar type of study has been documented from Iran, where *M. fortuitum* was found to be the most prevalent NTM isolated from tuberculosis suspected patients [77]. In Feb 2019, an oral agent designated as SPR720 is developed by Spero Therapeutics, approved by FDA for treatment of NTM lung infections [113].

2.2.1.7 Nosocomial infections

The ubiquitous presence of *M. fortuitum* narrates the tolerance of this bacilli to harsh environmental conditions for survival. Being an important NTM to cause nosocomial infection, it confronts the sterilization procedures used to disinfect the surgical instruments [40]. The presence of such resistant bacteria in hospital settings not only causes infections to the patients admitted there but also contaminates the samples leading to misdiagnosis of other diseases [114]. Most important cause for *M. fortuitum* nosocomial infections includes presence of the bacilli in hot water supply and showerheads of hospitals. A few case reports related to nosocomial infection by *M. fortuitum* include a) peritonitis in patients having peritoneal dialysis, b) cutaneous infection through the use of contaminated needles for electromyography, c) osteomyelitis and arthritis through intra-articular injection of steroids, and d) disseminated infection in cancer patients through contaminated water supply [40].

2.2.1.8 Lymph node infections

M. fortuitum as an infectious agent in cervical lymphadenopathy has been reported by Nguyen and colleagues [115]. Few case reports describe *M. fortuitum* as a causative agent of lymphadenitis, mainly associated with an immunosuppressed status of the patient. In one such case report weakened immune response due to varicella-zoster virus infection was associated with *M. fortuitum* lymphadenitis [98]. In an epidemiological report, *M. fortuitum* was found to be one of the rapidly growing mycobacteria to cause cervico-facial lymphadenitis [116].

2.2.1.9 Cardiac Infections

Sporadic *M. fortuitum* cardiac infections in health care settings have been reported. Endocarditis in adults is usually fatal [117], however, Vuković et al. reported the recovery of *M. fortuitum* endocarditis in children [118]. Phadke and colleagues reviewed *M. fortuitum* as the most predominating NTM to cause infection in patients with cardiac device implantation [119]. In a recent study by Zhu et al, *M. fortuitum* was found to be most prevalent in cardiovascular implantable electronic device related infections [120].

2.2.2 Virulence of *M. fortuitum*

The information regarding the virulence mechanism of *M. fortuitum* is limited. *M. fortuitum* is an intracellular pathogen like *M. tuberculosis* and a literature survey shows sharing of virulence mechanism between *M. tuberculosis* and *M. fortuitum*. Intracellular survival in macrophage vacuoles by suppressing the immune response of the host demonstrates the virulent potential of *M. fortuitum*. Restriction of IFN- γ -induced nitric oxide production and inhibition of phagosome-lysosome maturation inside macrophages are two major mechanisms required for *M. fortuitum* intracellular survival [12].

Oxidative stress in the form of hydrogen peroxide production is one of the major immune responses towards intracellular pathogen, and the presence of catalase-peroxidase helps the bacteria in combatting this stress by catalyzing hydrogen peroxide to water. Extensive THP macrophage monolayer damage and an enhanced reactive oxygen species response was observed following *M. fortuitum* infection [121]. Nunez and colleagues described oxidative stress adaptation of *M. fortuitum* at the transcriptional level. They found over-expression of two genes including Catalase-peroxidase katG1 gene and transcription regulator furAII gene, when *M. fortuitum* was subjected to *in vitro* oxidative stress [122]. Sigma factors are important virulent determinants in case of *M. tuberculosis* and the number of sigma factors in *M. fortuitum* are more than in *M. tuberculosis*. Sigma factors play an important role in the recognition of promoters for transcription. Therefore, variation in active sigma factor populations may represent a powerful way to modulate the transcription profiles of an organism as per its physiological requirements [123].

The importance of cell wall and membrane proteins in virulence of pathogenic microorganisms has been demonstrated in various studies. Virulent cell wall proteins of *M. fortuitum* have not yet been studied extensively, however, di-o-acyl trehalose extracted from *M. fortuitum* showed inhibition of mouse T-cells proliferation. Inhibition of T-cell proliferation by di-o-acyl trehalose might be one of the reasons associated with T-cell hyporesponsiveness and immunosuppression in the case of mycobacterial diseases [124]. The role of outer membrane porin gene porM, required for diffusion of small and hydrophilic solutes, has been reported for the growth of *M. fortuitum*, where under-expression of porM gene led to the defective growth rate of *M. fortuitum* [125].

Apoptosis is one of the strategies used by pathogenic mycobacteria to overcome the immune response of the host. *M. tuberculosis* utilizes the re-programming of genetic behavior in favor of induction or repression of apoptosis to establish itself inside the host. Apoptosis induction helps the pathogen to disseminate inside the host, and its repression helps the pathogen to secure itself inside the host-cell [126]. Datta et al reported induction of macrophage apoptosis in *M. fortuitum* infected catfish, suggesting conservation of pro-apoptotic trait as a virulent factor to counteract immune response in pathogenic mycobacteria. They proposed that *M. fortuitum* triggers intracellular Ca^{+2} elevations, which results in the activation of Calmodulin (CaM), and generation of superoxide through protein kinase C- α (PKC- α), leading to apoptosis [127].

Antibiotic resistance genes play an important role in the survival of the pathogen under unfavorable conditions, and also trouble the physician in the treatment of the disease. In *M. fortuitum*, gene *aph(3'')-Ic* encoding for an aminoglycoside 3'-*O*-phosphotransferase was found to provide streptomycin resistance [128]. Macrolide resistance gene *erm* which codes for rRNS methylase has also been discovered in *M. fortuitum*, emphasizing the ability of *M. fortuitum* to adapt to unfavorable conditions [129]. Martin et al reported presence of an ORF homologous to Tn1696 transposon (Tn21 family) coding for site-specific integrase which provides resistance against sulphonamides [130]. The presence of efflux pump like *tap*, *tetV*, *ifrA*, and *efpA* in *M. fortuitum* also adds to resistance mechanisms against different antibiotics [131].

2.2.3. Models to study *M. fortuitum* infection

2.2.3.1 Fish model

Mycobacteriosis in freshwater and marine fish due to *M. fortuitum* has been well documented. [132]. Goldfish *Carassius auratus* has been established as a model to study *M. fortuitum* in 1998 by Talaat et al. [133]. The intravenous injection of 10^7 CFU/ml in *M. fortuitum* led to peritonitis in infected fish which is characterized by an accumulation of macrophage, lymphocytes and fibrous connective tissues around the intestine, liver, spleen, and pancreas. The persistence of infection by *M. fortuitum* has also observed in fish during 8 weeks of post-infection studies. Fish inoculated with 10^8 /mL CFU of *M. fortuitum* suffered from severe mycobacteriosis with high peritoneal scores, at 2 weeks, followed by a peritoneal chronic

granulomatous reaction starting 4 weeks post-infection. A severe mycobacteriosis was produced in fish inoculated with 10^9 /mL CFU of *M. fortuitum* and all fish died within 8 days post-infection with severe peritonitis. Necrotizing and caseous granuloma were observed in infected fish. In fish, the nervous system was not found to be involved [133]. *M. fortuitum* infection in a laboratory Zebrafish model showed signs of dropsy; dropsy is the medical term which describes fluid accumulation in the abdomen and protruding of scales from body wall in fish [134]. Mycobacterial infections in fishes are zoonotic, and hence, can be a source of infection to humans. Uma and Ronald isolated *M. fortuitum* from ornamental goldfish *C. auratus* with ulcerative granuloma in the dorsal tail [135].

2.2.3.2 Murine infection model

The infection of *M. fortuitum* in mice has characterized by Saito and Tasaka in 1969 [136]. They characterize the occurrence of *M. fortuitum* infection in the kidney as well as characteristic 'spinning disease' as symptoms of *M. fortuitum* infection in mice. Spinning disease is characterized by spinning rotation of mice when held through the tail, tilting of the neck as well as twitching, and shaking movement of the head of mice [136]. The occurrence of spinning neck in *M. fortuitum* infected mice was due to damage in the inner ear leading to loss of sense of balance. The murine BALB/c mouse infection model of *M. fortuitum* was further developed by Parti et al. [137] in 2005 and established the presence of a persistent form of infection of *M. fortuitum* in kidney of mice. Host immune response inside the kidney is such that the bacteria cannot proliferate but can reside in a non-proliferative form in the kidney till 60 days of post-infection. The study of immune response against *M. fortuitum* infection showed observed that CD4⁺ cells produced more IFN- γ as compared to CD8⁺ cells. Non-necrotic granuloma was observed in the kidney of the infected mouse model [137]. The characteristic granuloma formation in case of *M. fortuitum* infection was studied by Silva et al in 2010. They found the infection of *M. fortuitum* in the liver and spleen of infected mice. The granulomatous structure present in the liver of infected mice is characterized by lymphoid aggregate and macrophages. They also found a higher expression of IFN- γ in case of *M. fortuitum* infected mice. The observation of viable count of bacteria in liver and spleen showed a reduction from 7th day of post-infection [138] whereas Parti et al observed the constant viable count in kidney till 60 days highlighting characteristic pathogenesis of *M. fortuitum* in the kidney.

2.3 Membrane/secretory proteins as virulent factor

Membrane proteins encoding genes constitute 20% to 30% of bacterial, archaeon, and eukaryotic genomes. These proteins play various vital cellular functions required for survival, and hence, constitute about 50% of drug targets. Membrane proteins are involved in metabolite acquisition, molecular trafficking to host-cell membranes, cytoskeletal rearrangement, and production of cell adherence complexes. Cellular functions performed by membrane proteins are enlisted below:

2.3.1 Host-pathogen interaction

'Host-pathogen interaction' term indicates the possible ways by which a pathogen interacts with its host to cause disease. Pathogens discover alternative ways to infect an immunocompetent host. It can invade the host only after breaching the host immune response. Membrane proteins of pathogen act as armed forces with evolutionary adaptation capacity for entry inside the host-cell. Bacteria come across the plasma membrane of the host and interact with it for the initial infection process [139].

Macrophage as primary phagocytic cells of the immune system contributes a lot in the defense of host against various pathogenic organisms. These can be considered as the strongest candidate, the bacteria have to tackle with, however, various strategies were used by bacteria to cope up with the macrophages and to cause infection [140]. Among these pathogenic microbes, the most common is *M. tuberculosis*, the leading cause of deaths in developing countries [141]. Not only *M. tuberculosis*, but other NTM also reside inside the phagocytic cells and use these cells for their multiplication [142]. Besides using other strategies for survival of mycobacterium within macrophages such as inhibition of phagosome-lysosome fusion, the first and an important step of its pathogenesis is the use of macrophage receptors as an open gate for its entry [143]. Gateway of macrophages opens for mycobacteria as these cells recognize the pathogen-associated molecular patterns of mycobacterium through its pathogen recognition receptors such as toll-like receptors, complement receptors, scavenger receptors, mannose receptors, etc. [144]. The interaction of macrophages and mycobacterium is complex and can be responsible for the output of disease. Understanding the surface proteins of mycobacterium species which are not only involved in macrophage interaction but also adhesion, motility, molecular transport, and conjugation can be considered as novel drug targets and can be used as a vaccine candidate to combat diseases

caused by mycobacterium species [145]. Table 2.4 enlists some of the identified *M. tuberculosis* surface genes responsible for host-pathogen interactions.

Table 2.4: List of surface protein-encoding genes of *M. tuberculosis* involved in host-pathogen interactions [146-148].

S.N.	Name of gene	Brief details of the encoded protein
1	Rv0180	<ul style="list-style-type: none"> • Alanine and leucine rich transmembrane proteins • Regulation of lipoprotein gene (lprO) • Involved in macrophage invasion
2	Rv0227c	<ul style="list-style-type: none"> • Putative membrane protein with proteolytic activity • Host-pathogen interaction • Nutrient stress survival
3	Rv0679c	<ul style="list-style-type: none"> • Hypothetical membrane protein • Host-pathogen interactions • Immunomodulation
4	Rv1088	<ul style="list-style-type: none"> • PE family protein PE9 • Induces apoptosis • Immunomodulation
5	Rv1411c	<ul style="list-style-type: none"> • Antigen P27 protein LprG • Role in virulence • Triacylglycerol transporter • Immunomodulation
6	Rv1490c	<ul style="list-style-type: none"> • Conserved putative membrane protein • Role in macrophage interaction
7	Rv1510	<ul style="list-style-type: none"> • Hypothetical membrane protein • Role in host-pathogen interaction
8	Rv1980c	<ul style="list-style-type: none"> • Culture filtrate protein Mpt64 • Act as a diagnostic marker • Inhibits apoptosis of host-cell • Host-pathogen interaction
9	Rv2004c	<ul style="list-style-type: none"> • Putative surface protein • Signal transduction, probably codes for histidine kinase • Role in latency • Host-pathogen interaction
10	Rv2301	<ul style="list-style-type: none"> • Cutinase like protein • Lipid catabolism • Host-pathogen interaction • Immunomodulation
11	Rv2536	<ul style="list-style-type: none"> • Surface protein • Role in antibiotic resistance • Host-pathogen interactions

12	Rv2560	<ul style="list-style-type: none"> • Putative membrane protein • Host-pathogen interactions
13	Rv2969c	<ul style="list-style-type: none"> • Surface protein • Catalyzing oxidative folding of toxins and membrane proteins
14	Rv2707	<ul style="list-style-type: none"> • Alanine and leucine-rich transmembrane protein • Role in virulence • Host-pathogen interactions
15	Rv3166c	<ul style="list-style-type: none"> • Conserved membrane protein • Host-pathogen interaction
16	Rv3312A	<ul style="list-style-type: none"> • <i>M. tuberculosis</i> pili mtp • Adhesion and invasion inside the host
17	Rv3481c	<ul style="list-style-type: none"> • Integral membrane protein • Role in survival under stress conditions inside the host • Host-pathogen interaction
18	Rv3629c	<ul style="list-style-type: none"> • Secretory membrane protein • Role in virulence • Host-pathogen interaction
19	Rv3630	<ul style="list-style-type: none"> • Secretory membrane protein • Host-pathogen interaction
20	Rv3705c	<ul style="list-style-type: none"> • Hypothetical membrane protein • Host-pathogen interaction
21	Rv3804c	<ul style="list-style-type: none"> • MTB85A antigen • Immuno-stimulation • Host-pathogen interaction

Extracellular vesicles in thick cell wall containing microorganisms like mycobacteria have been reported to play an important role in host-pathogen interaction. A recent study by Athman and colleagues found mycobacterial extracellular vesicles to modulate host immune response in favor of pathogen [149].

2.3.2 Role of peptidoglycan in immune signaling and modification

Peptidoglycan (PGN) is a major component of the bacterial cell wall in both Gram-positive and Gram-negative bacteria. Modifications or variations to the basic PGN structure occur frequently amongst bacterial species. Many modifications are species-specific due to the expression of unique synthetic, modifying, or degradative enzymes. The benefits of such modifications include enhanced resistance to antibiotics and host degradative enzymes that target the bacterial cell wall. Resuscitation-promoting factors (Rpf) are PGN-hydrolyzing

enzymes involved in growth-state shift from dormancy into reactivation of *M. tuberculosis*. Defect in both RpfA and RpfB proteins resulted in inability of *M. tuberculosis* to enter the active phase from dormant state [150, 151].

2.3.3 Role of other components of the cell wall in immune signaling and modification

Cell wall-associated lipids, such as phosphatidyl-*myo*-inositol mannosides (PIM), and the glycolipids lipomannan (LM) and lipoarabinomannan (LAM), play a key role in modulating the host response during infection by interacting with different receptors on macrophages and dendritic cells [152]. Plasma lipopolysaccharide (LPS) binding protein enhances macrophage responses to LPS and LAM by transferring these microbial products to the cell surface receptor CD14. Similarly, soluble CD14 confers responsiveness to both LAM and LPS in CD14-negative cells [153]. In *M. smegmatis*, structural defects in LM and LAM resulted in loss of acid-fast staining, increased sensitivity to β -lactam antibiotics, and faster killing by THP-1 macrophages. Equivalent *M. tuberculosis* mutants were more sensitive to β -lactams, and also showed attenuated virulence in mice [154]. LM induces IL-12 release and induces apoptosis in the host [155]. Mycolic acids are the major structural lipids contributing to a protective layer of the cell wall. Mycolic acid cyclopropane ring is required for virulence and long-term persistence of pathogenic mycobacteria in mice [156]. Mycolic acid induces the accumulation of cholesterol inside peritoneal and alveolar macrophages. Macrophages containing cholesterol and lipid droplets resemble foamy macrophage derivatives observed in tuberculous granulomas. Mycolic acids help in the induction of Tumor Necrosis Factor- α (TNF- α), an important cytokine in response to mycobacterial infections.

2.3.4. Transport of nutrients

Outer-membrane channel proteins are thought to contribute for nutrient uptake in mycobacterium species. The overexpression of ATP binding ABC transporter proteins which helps in the import and export of various molecules across the cell membrane in a virulent strain of *M. tuberculosis* i.e. H37Rv as compared to avirulent strain H37Ra highlights the significance of these proteins in virulence of the bacilli [157]. Outer membrane channel protein CpnT helps the bacilli in surviving inside the macrophage by increasing the nutrient uptake from the host and also induces necrosis by secreting toxins, and thus, escapes phagocytosis [158].

2.3.5. Protection against osmotic and mechanical stresses

The mycobacterial products (ManLAM, trehalose dimycolate, and sulfolipids), phosphatase SapM, kinase PknG, and early secretory antigenic target-6 (ESAT-6) have been implicated in the inhibition of macrophage maturation [159]. Two-component signal transduction system (TCS) of mycobacteria plays an important role in combating the stress environment prevalent inside the host. A typical TCS comprises of a sensor histidine kinase and a response regulator that is localized in the plasma membrane and cytoplasm, respectively. Both components of the TCS have specific domains through which they sense environmental cues. The sensor kinase comprises a sensor domain, one or more transmembrane domains, and a cytoplasmic transmitter containing a dimerization motif and a kinase domain, and the latter can be again divided into two subdomains possessing a histidine phosphorylation box and an ATP-binding pocket. Signal recognition results in dimerization and auto-phosphorylation followed by the transfer of phosphate to the response regulator, thus enabling it to promote transcriptional, translational, and functional aspects [160, 161].

2.4 Immune Response against mycobacterial infections

The immune response of the host plays an important role in the outcome of infection by mycobacteria. Cytokines and chemokines act as messengers to stimulate the required immune response. These are a large group of signaling proteins, peptides and glycoproteins which are secreted by the immune cells of the body and help in activation and regulation of the immune system [162]. Cytokines are released by the host-cells since the onset of infection i.e. interaction with macrophages, till the bacterium resides in the host.

Cytokines released during mycobacterial infection can be differentiated into two classes: pro-inflammatory cytokines and anti-inflammatory cytokines. Pro-inflammatory cytokines are the cytokines released during the initial stages of infection by macrophages and have an impact on tissue damage and are imperative for anti-infectious processes [163], whereas, anti-inflammatory cytokines act as immunoregulatory cytokines that regulate the pro-inflammatory cytokines and protect the body from excessive tissue damage [164]. Important pro-inflammatory cytokines are IFN- γ , TNF- α , IL-12, and IL-2. Th2 cytokines also called as anti-inflammatory cytokines include IL-10, IL-4, and transforming growth factor- β (TGF- β). Another recently recognized T-cell population is Th17 cells that secrete IL-17, IL-17F, IL-21,

and IL-22. Crosstalk between antigen-presenting cells and effector T-cells through cytokines is required for the regulation of immune response for controlling infection. The outcome of mycobacterial infection depends upon the host immune response and extent of pro-inflammatory and anti-inflammatory cytokines release [165].

2.4.1 Pro-inflammatory cytokines

As the immune system of a host can recognize non-self cells, the immune response against non-self cells starts at the early stage of infection. Initial interactions of mycobacterium with antigen-presenting cells stimulates the expression of pro-inflammatory cytokines interferons, tumor necrosis factor, and interleukins. Brief process of induction of pro-inflammatory cytokines is provided in Figure 2.6.

2.4.1.1 Interferon (IFN) family

Interferons are a heterogeneous family of cytokines divided into type I and type II based on their structure, function, and cells of origin. While type I IFNs (IFN- α and IFN- β) are secreted by various cell types and through innate immune receptors, type II (IFN- γ) is mainly produced as a result of stimulation of T lymphocytes and Natural killer (NK) cells. Exogenous administration of IFNs result in higher susceptibility and may be pathogenic during *M. tuberculosis* infection, due to lack of responsiveness of IFN- γ to macrophages [166]. IFN- γ connects the innate and adaptive immune response of the body. IFN- γ plays a protecting role during mycobacterium infection. It is responsible for the induction of adverse conditions such as the production of reactive nitrogen intermediates (RNI) and reactive oxygen species (ROS) inside macrophages to kill the infectious invaders [167]. IFN- γ also produces immunomodulatory and chemotactic molecules that promote the up-regulation of receptors for TNF- α and Natural resistance-associated macrophage protein (NRAMP-1) molecules. Macrophages play a vital role in the tuberculous granuloma formation, where they are in proximity with activated T-cells. In this microenvironment, IFN- γ secreted by activated T-cells can synergize with *M. tuberculosis* to down-modulate IL-10 production and allow IL-12 synthesis from macrophages. At the same time IFN- γ can potentiate the antimycobacterial activity of the macrophages and also elevate other macrophage pro-inflammatory responses. Distinct cytokine response of dendritic cells and macrophages following *M. tuberculosis* infection may allow these two cell types to be effective at different stages of an immune response towards the pathogen [168].

It has been shown that the effector cells mainly secrete IFN- γ , whereas effector memory cells secrete IFN- γ and IL-2, and central memory cells secrete IL-2. Central memory cells are characteristic of latent tuberculosis infection. The increase in IFN- γ /IL-2-secreting T-cells after anti-tuberculosis treatment can also serve as a biomarker of treatment response. However, the immunological response during active tuberculosis is predominated by TNF- α and can be used to distinguish between active and latent tuberculosis [169, 170].

2.4.1.2 Tumor Necrosis Factor α (TNF- α)

TNF- α , an autocrine cytokine, helps in controlling mycobacterial infection by stimulating the release of various cytokines and helps in the formation of granuloma, however, TNF- α should be produced in a controlled way, otherwise, it can lead to disseminated tuberculosis [168]. TNF- α acts synergistically with IFN- γ to stimulate the production of nitric oxide by macrophages and influences the expression of chemokines, such as CCL5, CCL9, CXCL10, and CCL2, which induce migration to, and maintenance of immune cells at the infection site [171]. TNF- α tries its level best to limit the infection by apoptosis of infected cells, a direct event for killing the bacilli along with its safe harbor [172]. TNF- α is an important cytokine for the host as it helps in restricting the infection by contributing to granuloma formation, effective phagocytosis, and apoptosis of infected cells. Owing to significant importance of TNF- α , its release by host-cell is done in regulated manner as decrease in TNF- α gives opportunity to pathogenic mycobacterium to multiply inside the host and cause necrosis of cell while an increase in TNF- α leads to a process named necroptosis i.e. macrophages sacrifice themselves along with the infecting mycobacterium due to excessive reactive oxygen intermediate production [173].

2.4.1.3 Interleukins

IL-12 also called as IL-12p70, is the main class of interleukins that acts as a link between innate and acquired immune response by stimulating phagocytosis and activating NK cells and T-cells through binding with IL-12R β 1 receptors on them, for initiating the release of IFN- γ , the main cytokine in controlling infection [174]. Once IFN- γ is released from T-cells, it behaves in an autocrine manner and increases its own production and TNF- α production by binding with IL-12 receptors on T-cells. IL-12 is one of the important cytokines in maintaining the granuloma and limits the pathogen within granuloma, preventing its dissemination and helps the host to control the infection [174, 175]. IL-12 also protects CD4⁺

cells from antigen-induced apoptotic death [176]. Lack or a reduced amount of IL-12 leads to reduced Th1 cell activity and increased susceptibility towards intracellular pathogens [177]. IL-12 stimulates T-cell, NK cells as well as macrophages to release immune-effector cytokines. IL-12 and IL-18 cooperate and induce the secretion of IFN- γ from T-cells, NK cells, B-cells, macrophages and dendritic cells [178]. IL-18 is constitutively expressed in macrophages in its inactive form, after stimulation with foreign cells it gets converted to its active form and binds with IL-18R receptors to stimulate the release of IFN- γ . IL-18 and IL-23 also stimulate Th1 cells and increase the release of TNF- α and IFN- γ . IL-2, a pro-inflammatory cytokine is also involved in the clonal expansion of antigen-specific T-cells. Macrophage-derived IL-1 also enhances IL-2 production, IL-2R expression, and subsequent clonal expansion of the CD4⁺ T-cells.

Various cell wall components of the mycobacterium play an important role in the induction of immune response. Cell wall components induce cytokine release, such as lipoproteins stimulates IL-12 production, LM induces IL-12 and TNF- α production, LAM induces IL-10 production, trehalose di-mycolates releases IL-1 β , TNF- α , and IL-6, phenolic glycolipids release TNF- α , IL-6 and CCL2, and ESAT 6/ CFP 10 family proteins induce the production of TNF- α . A heat shock protein HSP-70 of mycobacterium binds with CD40 receptor on antigen-presenting cells and stimulates the production of IL-12 and some chemokines. This type of interaction is favorable for induction of Th1 cells during low infection dose [179].

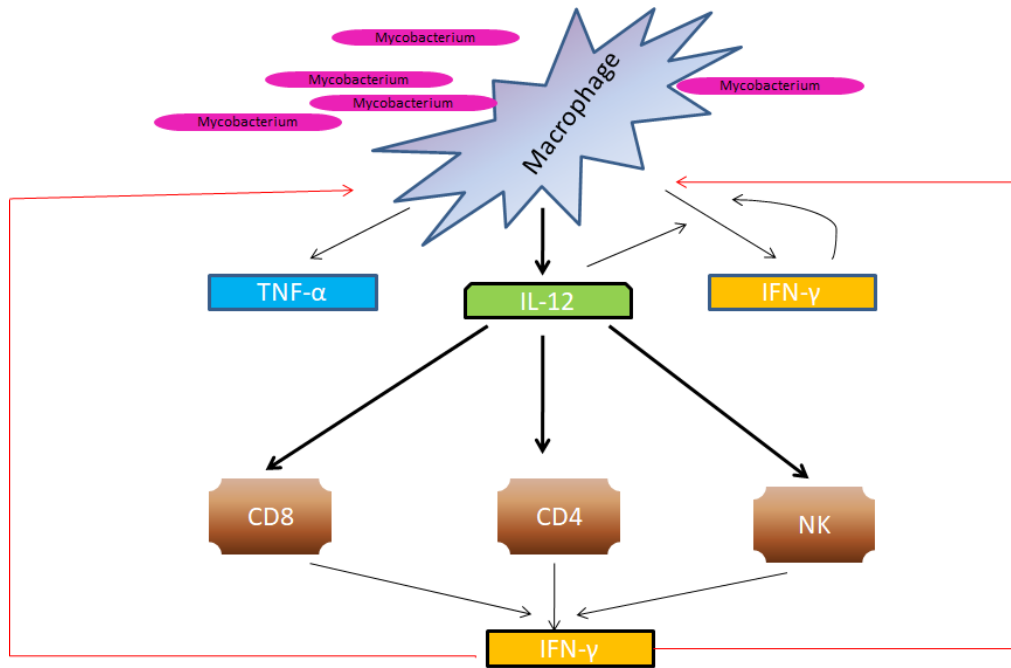


Fig 2.6: Pro-inflammatory cytokines in *M. tuberculosis* infection. The figure represents release and regulation of pro-inflammatory cytokines after interaction and invasion of host by pathogenic mycobacteria.

2.4.2 Anti-inflammatory Cytokines

Cytokines released during the initial phase of infection lead to inflammation and tissue damage, therefore an immunoregulatory mechanism is present in human body to prevent excessive tissue damage. This role is played by anti-inflammatory cytokines such as IL-10 and TGF- β which controls the immune response and protects the cells from destructive effects of pro-inflammatory cytokines. It is released by infected and non-infected macrophages during infection and secreted by Th2, Th1, Th9, and Th17 cells. IL-27 and TGF- β also regulate the release of IL-10 from T-cells [180]. IL-10 suppresses the expression of IL-12 by macrophages, thus restricts the production of other pro-inflammatory cytokines, however, in granuloma IFN- γ can suppress the activity of IL-10 and maintain a required concentration of IL-12 for an antimycobacterial response [181]. IL-10 down-regulates the immune response during infection by inhibition of TNF alpha by modulation of STAT-3 transcription, inhibition of chemokine release and suppression of activated macrophages in combination with other factors such as TGF- β . TGF- β is shown to synergize with IL-10 to promote immune tolerance and limit pathological inflammation [182]. It has been found that the presence of TGF- β *in vitro* increases the growth of intracellular bacilli, whereas, its absence is beneficial in preventing the growth of intracellular bacteria. The effect of TGF- β

on the growth of mycobacterium is due to decreased phagocytosis by macrophages, and reduced production of IFN- γ and TNF- α [183].

IL-10 knockout mice were found to be more resistant to *M. tuberculosis* infection than wild type [184]. As an immune evasion strategy, mycobacterium increases the production of IL-10 by host-cells for its benefit. IL-10 can interfere with antigen presentation by inhibiting the MHC II expression of macrophage cells infected with mycobacterium. Thus, IL-10 can enhance the intracellular survival of bacilli by inhibition of phagosomal maturation, reducing nitric oxide production, blocking IFN- γ signaling in macrophage, suppression of Th1 responses by impairing antigen presentation, and IL-12 production. IL-10 can also inhibit macrophage apoptosis that is required for the efficient development of T-cells response [185]. However, low-levels of IL-10 can trigger host antimicrobial response and prevent tissue damage. Hence, decreasing the IL-10 level during tuberculosis therapy might benefit the rapid clearance of bacteria [186]. Lack of IL 10 leads to excessive apoptosis of macrophages and excessive tissue damage [187].

IL-27 is a regulatory cytokine and the absence of IL-27 leads to increased T-cell proliferation [188]. It also induces the production of IL-10 from T-cells and is released in large amounts in active tuberculosis. IL-27 plays an important role in regulation of other cytokines, however, antigen specific T-cells lacking IL-27R are more protective against tuberculosis, can enter parenchymal cells more efficiently and can interact with antigen containing myeloid cells. IL-27R signaling also leads to a decrease in the level of IL-2 and has a detrimental effect on the effector T-cells [189].

2.5 Genetic strategies for identifying new drug targets

2.5.1 Bioinformatics tools

Advancement in high throughput techniques has resulted in availability of genome sequences of many bacterial species. Accessibility of genome sequence allows identification of conserved virulent genes among multiple pathogens through comparative genomics. There are various databases which assist in the identification and/or screening of virulent factors (Table 2.5), as a potential drug candidate [190].

Table 2.5: List of databases for identification of genes/proteins involved in virulence.

S.N.	Name of Database	URL link	Description
1	Virulence Factor Database (VFDB)	http://www.mgc.ac.cn/VFs/	Provides automatic pipeline for identification of virulent factors of bacteria
2	Victors Database	http://www.phidias.us/victors/	Provides screening of virulent factors of bacteria, virus and fungi based on host-pathogen interacting proteins
3	Pathogen Finder	https://cge.cbs.dtu.dk/services/PathogenFinder/	Executes bacterial pathogenicity estimation based on protein sequence
4	Toxin and Toxin Target Database (T3DB)	http://www.t3db.ca/	Combines detailed toxin data with comprehensive toxin target information pollutants, pesticides, drugs, and food toxins.
5	Bacterial Toxin Prediction Server (BTXpred)	http://crdd.osdd.net/raghava/btxpred/	Predicts bacterial toxins and its function from primary amino acid sequence
6	Database for Bacterial Endotoxins for Humans (DBETH)	http://www.hpppi.iicb.res.in/btox/	Provides a comprehensive database for human pathogenic bacterial exotoxins
7	Virmugen DB	http://www.violinet.org/virmugendb/	Predicts a gene that encodes for a virulent factor of a pathogen and has been proven feasible to make a live attenuated vaccine
8	Pathogen-Host Interaction Database (PHI-base)	http://www.phi-base.org/	Provides expertly curated molecular and biological information on genes proven to affect the outcome of pathogen-host interactions

2.5.2 Gene knockout strategies

Inactivation of gene function due to some mutation is called as gene knockout, which has been utilized in various genetic studies like functional genomics. Gene knockout is broadly used to determine the significance of a particular gene regarding its function associated with a

particular disease or phenotype. Gene knockouts studies can be done using wet-lab experiments (Table 2.6) as well as using *in silico* approaches (Table 2.7).

Table 2.6. Wet lab strategies used for gene knockout studies [191].

S.N.	Name of Technique	Mechanism
1	PCR based strategies	Knock out genes by finding a selectable marker which then will be exchanged to change the promoter
2	Lambda (λ) Red Recombineering Strategy	Use of bacteriophage λ to inactivate chromosomal genes in various bacteria and fungi by homologous recombination
3	Zinc Finger Nuclease Technology	Use of engineered DNA-binding proteins that assist the targeted editing of a genome by generating double-stranded breaks in DNA based on user-defined sequences

Table 2.7. *In silico* approaches used for gene knockout studies [191].

S.N.	Name of Approach	Details
1	OptKnock	Based on knocking out of a group of genes
2	OptGene	Allows input of the genome-scale stoichiometric model
3	OptStrain	A hierarchical computational framework, aiming at pathway modifications through addition and deletion of a microbial network
4	OptReg	The computational framework uses OptKnock formulation as a starting point and uses three sets of binary variables for each reaction
5	OptORF	Identify metabolic engineering strategies based on a minimal number of metabolic and transcription factor knockouts to improve biochemical production
6	MOMAKnock	Bi-level framework derived from OptKnock. Predict gene knockout strategies to improve targeted chemical product microbial strains
7	RobustKnock	Implement on gene knockout strategies by calculating the attendance of opposing pathways in the network.
8	Network-Free Inference	Analysis of functional network to infer the knockout effect
9	Genetic Design through Local Search (GDLS)	A huge number of genetic manipulations in a design

2.5.3 Antisense technology

Antisense technology is a powerful tool to inhibit gene expression and may be used for studying gene function (functional genomics) and for therapeutic purposes (antisense gene therapy). Manipulation in gene functions based on mRNA sequence is utilized in antisense technology. Whenever mRNA forms a duplex with a complementary antisense RNA sequence, translation is blocked. This can be used to disrupt the function of any gene. Disruption of gene function helps in understanding the essentiality of the gene for the pathogen, which leads to the identification of potential drug targets. The technology uses agents like antisense oligonucleotides, ribozymes, short interfering RNA (siRNA), micro RNA (miRNA), etc. Antisense technology has been applied in the case of pathogenic mycobacteria for drug target identification [192, 193].

2.5.4 Complementation

To study the function of a gene, mutation generated through various methods is generally followed by a complementation study to validate the proposed function of the gene. In mutants, a secondary mutation in a gene other than the target gene can be the reason for the observed phenotype. Hence, the complementation, where, mutated gene function is further recovered in mutant and observed for phenotype similar to wild type strain is used to confirm gene function [194]. *In vivo* complementation is performed using integration-proficient vectors, which allow the stable propagation of genomic libraries as well as individual genes in bacteria during animal infections [195]. The non-pathogenic *M. smegmatis* was used as the host in complementation experiments. In a study, essentiality of FabG1 gene in *M. tuberculosis* has been described by Parish et al, using complementation approach [196]. This approach was also used by Sakhti and colleagues, where they determine role of lipoprotein LpqS in virulence of *M. tuberculosis* [197].

2.5.5 Transposon mutagenesis

Transposon elements (TE) are mobile nucleotide sequences with an ability to move within a genome from one location to another. TE were identified by Barbara McClintock during their discovery of transposition in maize [198]. Transposons are ubiquitous i.e. they are present in all living organisms including eubacteria, archaebacteria, and eukaryotes. TE can be simple, composite or conjugative based on the variability of a nucleotide sequence.

- **Simple TE:** Contains gene for transposition and inverted repeats on both sides

- **Composite TE:** Contains gene for transposition along with insertion sequences that bound for additional genetic information
- **Conjugative TE:** Contains hybrid properties of transposon, plasmids, and bacteriophages

Transposon mutagenesis is a powerful tool for generating randomized gene mutations in bacterial genomes due to the ability of transposons to insert randomly or near-randomly in genomic DNA. Various composite bacterial transposons such as Tn3, Tn5, Tn7, Tn10, Tn552, etc. have been utilized for mutagenesis. Transposon Tn5 has been widely used in medical microbiology for identifying essential genes in bacteria such as *Burkholderia cenocepacia*, *E. coli*, *Streptococcus mutans*, *M. tuberculosis* etc. [199-202]. Transposon Tn5 consists of two inverted and identical sequences IS50L and IS50R at both ends. These two sequences contain specific end sequences (ES) required for transposition. IS50L and IS50R bracket the gene encoding for antibiotic resistance. IS50R functions for transposition with the help of transposase (Tnp) enzyme as well as transposition inhibition with inhibitor (Inh), while, IS50L contains a C-terminal truncated version of Tnp and Inh. The process of transposition is provided in Figure 2.7.

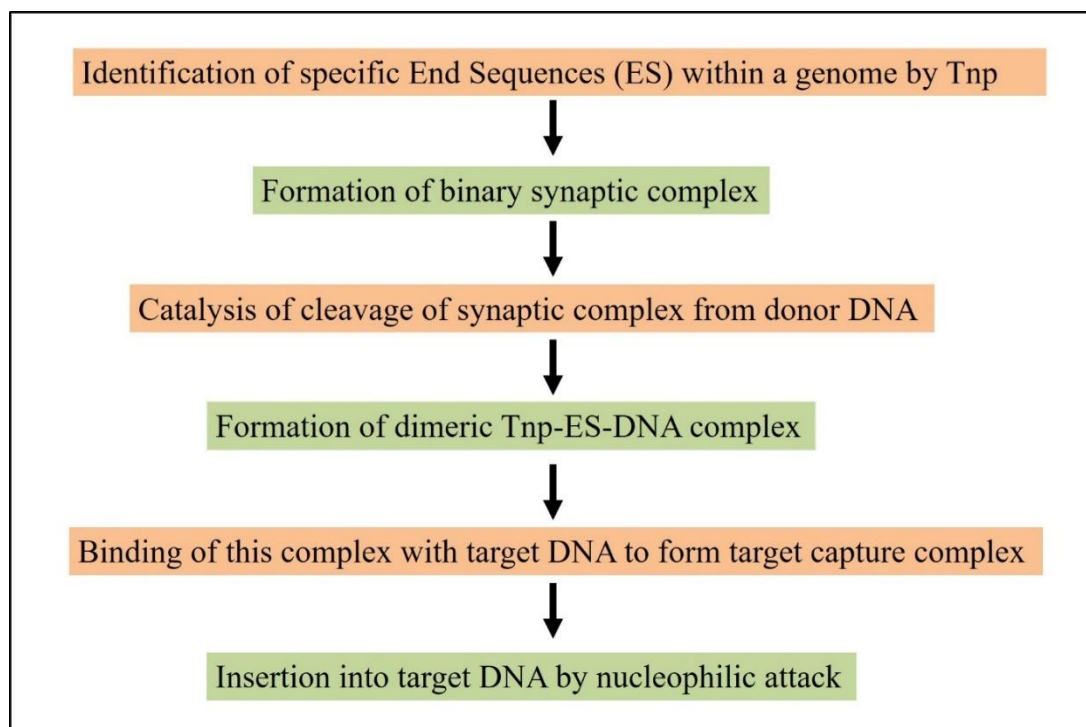


Figure 2.7: Flow diagram of the mechanism of transposition. The figure represents steps required for transposition events (Adapted from Reznikoff 2008 [203]).

2.5.6 CRISPR Interference

CRISPR/Cas (Clustered Regularly Interspaced Short Palindromic Repeat/CRISPR associated) system is present in majority of bacteria and archaea which helps in providing immunity against foreign DNA elements by selective cleavage [204]. The mechanism of resistance through CRISPR/Cas involves three stages:

- Adaptation stage: Small DNA fragments get integrated into short DNA repeats of host genome with the help of conserved Cas proteins. Integration of short DNA fragments lead to occurrence of repeat sequences interspersed by short unique spacers (proto-spacers) in host genome. Unique proto-spacer adjacent motifs (PAMs) helps in selection of proto-spacers from foreign invading nucleic acids.
- CRISPR RNA biogenesis: A long primary transcript of CRISPR locus i.e. pre-creRNA is expressed. This long pre-creRNA is then digested into short creRNAs with the help of single endonuclease or multiple protein complexes.
- Interference: The mature creRNAs guide the Cas protein complexes to bind with complementary target DNA or RNA sequences that match the spacers leading to their cleavage.

CRISPR interference (CRISPRi) is a simple and cost-effective approach for targeted gene regulation in all microorganisms. In this approach, small guide RNA (sgRNA) is expressed to target the gene of interest in a bacterial cell having catalytically inactive Cas9 protein (dCas9). This sgRNA binds specifically with target gene through a short nucleotide sequence homologous to target gene. This leads to recruitment of dCas9 to the site. This sequence of events results in interference with either transcription initiation or elongation, leading to lower levels of RNA of the gene targeted [205].

Complete repression of target genes in *M. tuberculosis* through CRISPRi using dCas9 of *Streptococcus pyogenes* has been reported by Chaudhary and co-workers [206]. The use of CRISPRi as genetic strategy for the identification of novel drug targets in *M. tuberculosis* has been validated [207] to accelerate the discovery of new antitubercular agents. Utilization of *Streptococcus thermophilus* CRISPR-Cas9 has also been demonstrated for gene editing in *M. marinum* and *M. tuberculosis* [208].

2.5.7 Conditional Mutagenesis

The generation of conditional mutants is one of the effective approaches to study bacteria and identify drug targets. Availability of various genetic strategies helped in the generation of conditional mutants of Genus *Mycobacterium* for characterization of essential genes. Many plasmids and transposon have been used previously for conditional mutagenesis in pathogenic mycobacteria. A tetracycline regulatable system has been successfully adapted for use in *M. bovis* and *M. smegmatis* for the construction of conditional mutations confirming its use in regulation of essential genes in mycobacteria [209]. Based on the regulatable promoters, a transposon was constructed by Shute and colleagues to generate conditional mutants in *M. smegmatis* [210]. Plasmid containing tetracycline-repressive expression system along with Xer Site-Specific recombinase system was constructed by Meng et al. [211] to generate label-free controllable expression strains of *M. tuberculosis*. Using this plasmid, *M. tuberculosis* mutants with inability to form colonies and sensitivity to antibiotic d-cycloserine has been identified [211].

2.6 Genes used in reporter fusion and promoter trap strategies

Reporter genes are nucleic acid sequences which encodes for a protein that can be easily assayed. These are used to monitor the efficacy of gene delivery vehicles for cloning and expression of gene of interest. Reporter gene methodology utilizes gene delivery vehicles like plasmid with a promoter less gene encoding a protein which, in most cases, catalyzes an easily assayable enzymatic reaction. This is often done through constructing a genetic fusion in which expression of the target gene also drives expression of the reporter gene product. Measurement of reporter gene product gives a direct readout for expression of the target gene. Even with the advent of technologies such as DNA microarrays, reporter genes continue to provide a powerful tool for studying gene expression [212]. Specific promoter sequences from known genes are cloned upstream of the promoter less reporter gene, so that the activity of the gene of interest can be simply measured. Some of the reporter genes which are commonly used in bacterial system are provided in Table 2.8.

Table 2.8: Reporter genes commonly used in bacterial systems. (Adapted from [204])

S.N.	Name of Reporter Gene	Advantages
1	β -Galactosidase (LacZ)	Simple assays using wide range of substrates
2	Chloramphenicol acetyltransferase (CAT)	Lack of background activity in most bacterial species
3	Alkaline phosphatase (PhoA)	Simple assay in wide variety of formats; High sensitivity (Substrate dependent)
4	Green fluorescent protein (GFP)	<i>In situ</i> measurement of activity; single-cell sensitivity possible
5	Bacterial luciferase (LuxAB)	<i>In situ</i> measurement of activity; rapid assay possible
6	Kanamycin resistance (NPT-II)	May be used for studying protein targeting

2.6.1 β -Galactosidase (lacZ)

β -Galactosidase is an enzyme which catalyzes β -1,4 cleavage of lactose to monomeric sugars glucose and galactose. Its activity can be easily monitored using 5-bromo-4-chloro-3-indolyl- β -D-galactoside (X-gal), methylumbelliferyl- β -D-galactoside (MUG), fluorescein digalactoside (FDG), or o-nitrophenyl- β -D-galactoside (ONPG). These are artificial LacZ substrates that are metabolized to produce measurable color changes [212]. β -galactosidase reporter system has been extensively used to monitor gene expression in response to various environmental conditions, including the activity of promoters during intracellular growth of mycobacteria within macrophages [213, 214]. The β -galactosidase activity can be easily assayed in cell extracts or intact mycobacterial cells [215, 216].

2.6.2 Alkaline phosphatase (phoA)

In *E. coli*, alkaline phosphatase is encoded by *phoA* gene. Alkaline phosphatase is a dimeric periplasmic protein and its activity requires translocation of alkaline phosphatase across cytoplasmic membrane to periplasmic space. Hence, *phoA* gene of *E. coli* contains export signal in the form of N'-terminal signal sequence for translocation of encoded protein i.e. alkaline phosphatase. However, absence of this signal sequence in *phoA* serves to play role as reporter gene, and genetic fusion of *phoA* reporter gene with export signals of membrane protein or secretory protein encoding genes lead to its translocation and activation thereof [17]. Alkaline phosphatase activity can be easily detectable by biochemical based quantitative and phenotypic assay. Quantitative assays for alkaline phosphatase activity rely on the rate of hydrolysis of *p*-nitrophenyl phosphate (PNPP) in permeabilized cells [217]. Mycobacterial

colonies expressing *phoA* can be identified by screening for blue colonies on culture plates supplemented with chromogenic substrate 5-bromo-4-chloro-3-indolyl phosphate (XP). This selection works well in *M. smegmatis* [218] and was used for isolating secretory signal corresponding to the exported 19 kDa lipoprotein and 28 kDa protein from mycobacteria [218]. Identification of virulence genes *in vivo* has been accomplished by combining *phoA* fusion along with transposons, using *TnphoA* [219].

MATERIALS AND METHODS

3.1 Materials

3.1.1 Bacterial strains and plasmids

Bacterial strains and plasmids used in the present study are enlisted in the following tables where Table 3.1 enlists bacterial strains, and Table 3.2 enlists plasmids used.

Table 3.1: Bacterial strains used in the current study.

Name of Bacteria	Source
<i>Mycobacterium fortuitum</i> ATCC 6841	Central Drug Research Institute (CDRI), Lucknow, India
<i>Escherichia coli</i> DH5 α	Institute of Microbial Technology (IMTECH), Chandigarh, India

Table 3.2: Plasmids used in the current study.

Name of Plasmid	Phenotype/marker	Reference
pRT291	pRK290 derivative, carrying Tnp _{phoA} / Km ^r	Taylor <i>et al.</i> , 1989
pUC19	Amp ^r	MBI Fermentas

3.1.2 Culture media and buffers

Culture medium, buffer, stains, and antibiotics used in the current study are enlisted in Appendix.

3.1.3 Chemicals

Chemicals and biochemicals used for the present study were procured from Promega, Axygen, Thermo Fisher Scientific, and Genei which include molecular weight markers, X-Gal, XP, IPTG, enzymes-RNase, Lysozyme, and proteinase K. Restriction endonucleases were purchased from New England Biolabs. PCR master mix used was procured from Promega. Dehydrated media and other ingredients used for the growth of bacteria were purchased from HiMedia and Difco Laboratories. Antibiotics were purchased from HiMedia. General biochemicals and solvents used were procured from Merck, HiMedia, Loba Chemie, and SRL.

3.1.4 Primers

Table 3.3 enlists the primers used in the current study

Table 3.3: Primers used in the current study.

Sr. No.	TnphoA specific Primers	
1	RS6	5'ACATTGCCGCCGATACCG3'
	RS7	5'TGGATGGCTTTCTTTCTTGCCG3'
	K36	5'ATCGCTAAGAGAATCACGCAG3'
	pUC19 Universal Primers	
2	M13Fwd	5'GTAAAACGACGGCCAG3'
	M13Rev	5'CAGGAAACAGCTATGAC3'

3.2 Methods

3.2.1 Media and growth conditions

Luria-Bertani (LB) broth, supplemented with 0.5% glycerol (Fischer Scientific) and 0.2% Tween-80 (Bio Basic Inc) (LBGT) was used to grow *M. fortuitum*. Middlebrook 7H9 medium was used for *in vitro* stress experiments. Nutrient agar (NA) supplemented with 0.05% Tween-80 (NAT) was used as solid media to grow *M. fortuitum*. LB and NA were used for growing *E. coli* cells. Bacterial cells were grown at 37°C with constant shaking at 200 rpm. Determination of cell viability was done by serial dilution of cultures in normal-saline supplemented with 0.02% Tween-80 [Tween Normal saline (TNS)] followed by spreading on solid media to determine CFU (Colony Forming Units) at different time points. Mycobacteria forms clumps during growth as its unique growth characteristic, hence, the cultures were vortexed properly for obtaining homogenous bacterial suspension and then used for CFU determination.

3.2.2 Zeihl-Neelson (AFB) staining

A drop of saline was kept on a grease free glass slide and a loopful of mycobacterial culture was added into it to make a smear. The smear was air-dried and heat fixed. Carbol fuchsin was poured onto the slide and the slide was heated (5-8 minutes) till the appearance of vapours. After heating, the slide was kept at room temperature for 5 minutes for cooling.

Extra stain was removed by rinsing with tap water. The primary stain was decolorized by adding acid alcohol for 30 seconds. After washing the slide again with water, counterstain malachite green was added to the smear for 3 minutes. The slide was washed with tap water to remove extra malachite green. The smear was air-dried and observed under microscope. Observation of pink rods indicates the presence of mycobacterial cells.

3.2.3 Construction and screening of transposon mutant library

3.2.3.1 Electroporation of plasmid into *M. fortuitum*

Transposon TnphoA containing plasmid pRT291 was transformed into *M. fortuitum* ATCC 6841 cells through electroporation. The protocol used for electroporation was followed as described previously [220]. Briefly, *M. fortuitum* was grown in LBGT till mid logarithmic phase at 37°C. The culture was then kept on ice for 30 minutes. The cells were collected by centrifugation at 5000 xg for 10 minutes at 4°C. Washing of cells was done with 5% glycerol twice by centrifugation at 5000 xg for 10 minutes at 4°C. The competent cells thus obtained were then resuspended in 1 mL 5% glycerol and kept at 4°C.

400 µL of competent cells were added in the electroporation cuvette of 0.2 cm electrode gap. 25 ng of plasmid pRT291 was added to the competent cells followed by 5 minutes incubation on ice. Gene Pulser (Bio-Rad) was used to give an electric shock to the cells using the following conditions:

Voltage	2500V
Capacitance	25 µF
Resistance	1000 Ω

The electric shock was given for 2 seconds twice with 5 minutes interval between the two electric shocks. After the electric shock, the cells were kept on ice for 5 minutes, inoculated into 2 mL of LBGT and incubated at 37°C for 6 hours. The cultures were then spread on selection plates containing Kanamycin (30 µg/mL), XP (5-bromo-4-chloro-3-indolyl phosphate), and 5% glucose.

3.2.3.2 Biochemical assay for screening of the mutant library

Primary screening of the transposon mutants was done based on blue color production by mutants containing an insertion of the transposon into membrane protein-encoding genes on

NAT in the presence of substrate XP. The blue clones were further processed for quantitative alkaline phosphatase assay for secondary screening of the mutants. Alkaline phosphatase assay of mutants was performed as previously described by Kaufman and Taylor [221], with some modifications. The mutants and wild type *M. fortuitum* were grown in MB7H9 medium till mid logarithmic phase. 500 μ L of each culture was centrifuged at 15000 xg for 10 minutes. The supernatant was removed, and the cell pellet was treated with 0.1% SDS and 2 mg/mL lysozyme for lysis. The mixture was vortexed properly, followed by the addition of 100 μ L 1M tris buffer and 1 mL 2 mM *p*-nitrophenyl phosphate. Further, the suspension was kept at 37°C till yellow color appears (10-20 min). After the appearance of yellow color, 100 μ L 10N NaOH was added to stop the reaction. Optical density of the sample was measured at 420 nm, and alkaline phosphatase units were calculated as $(1000 \times \text{Optical density at 420nm}) / (\text{minutes of incubation} \times \text{Optical density at 600nm (Initial culture)} \times 0.5 \text{ mL})$.

3.2.4 *In vivo* infection studies

3.2.4.1 Animals

All protocols and the number of mice used for *in vivo* infection studies were approved by the Institutional Animal Ethics Committee (IAEC). Female BALB/c mice of 18–20 g weight were utilized and were procured from the Institute of Microbial Technology (IMTECH), Chandigarh (India), National Institute of Pharmaceutical Education and Research (NIPER), Chandigarh (India), and Central Research Institute (CRI) Kasauli, Himachal Pradesh (India). Pathogen-free sterile environment maintained in institute's animal house facility was used for all studies. Three mice were kept per cage and given food and water *ad-libitum*.

3.2.4.2 Infection

M. fortuitum ATCC 6841 and the shortlisted mutants were inoculated in LBGT followed by incubation till mid logarithmic phase (Optical density of 0.4 at 600nm). Pellet was collected by centrifugation at 3000 xg for 5 minutes. The cell pellet was weighed and resuspended in 0.05% TNS to have a final concentration of 5×10^7 cells/mL. Female BALB/c mice were intravenously infected with 10^7 cells/mice in a final volume of 200 μ L. After infection, the mice were observed for the appearance of symptoms and sacrificed 10 days and 25 days post-infection (PI) to determine the bacillary load, tissue damage, and cytokine profiling.

3.2.4.3 Bacillary load determination

The bacillary load per gram of kidney tissue was determined 10 days and 25 days PI. Three mice per group were sacrificed at each time point by chloroform euthanization. The mice were dissected, and kidneys were isolated aseptically from each mice. The weight of the kidney was determined, followed by homogenization of kidney tissue in 0.05% TNS using a glass homogenizer. After proper homogenization of kidney tissue, serial dilution of this suspension was made followed by plating of serial dilutions on NAT plates. The plates were incubated followed by counting of colonies and calculation of CFU per gram kidney tissue weight.

3.2.4.4 Histopathology

To have an insight into the tissue damage in mice infected with wild type *M. fortuitum* and shortlisted mutant strains, kidneys were isolated and stored in a 10% formalin solution prepared in normal-saline. Preserved kidney tissues were processed as described previously [222] for histopathological studies. Briefly, fixing of tissues in 10% neutral-buffered formalin was done followed by dehydration in a graded concentration of alcohol. The tissues were then cleared in xylene and embedded in paraffin wax. 5 µm thick sections of paraffin embedded tissue were prepared and stained with hematoxylin and eosin to observe tissue pathology.

3.2.4.5 Cytokine profiling

Cytokine profiling was done using KrishGen Biosystems sandwich ELISA kits of IFN- γ , TNF- α , and IL-10 cytokines as per manufacturer's instructions. Mice were sacrificed 10 days and 25 days PI, followed by the collection of blood through cardiac puncture. Collected blood samples were kept at 37°C for 2 minutes, to allow clotting of RBC, and then centrifuged at 3000 xg for 2 minutes at 4°C. The upper pale colored layer of serum was aspirated. To prevent cytokine degradation, serum samples were immediately frozen at -80°C until analyzed for cytokine quantification. All samples were analyzed in triplicate and the concentration of cytokine was determined in pg/mL using a standard curve.

3.2.5 Molecular methods used for identification of genes affected by mutation

Genes of the mutants affected by transposon mutagenesis were identified through cloning of the mutated gene in pUC19 followed by sequencing. The strategy used for the identification of the mutated gene is provided in Figure 3.1.

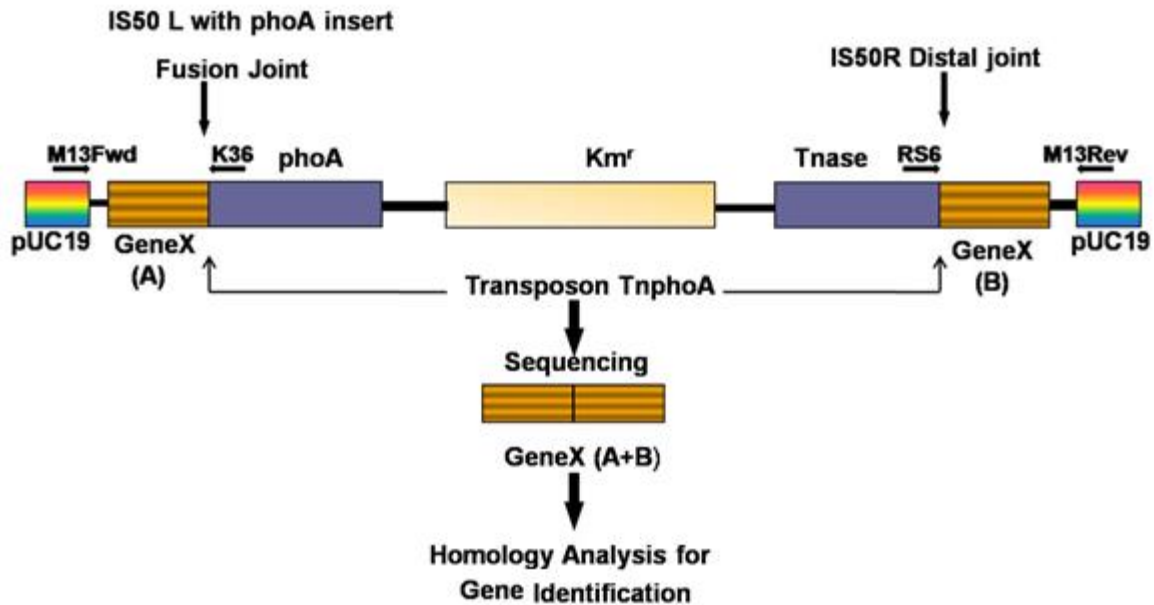


Figure 3.1: Strategy for identification of the mutated gene. The figure shows transposon mutagenesis strategy used in the present study for the identification of gene involved in *M. fortuitum* virulence. The transposon is a derivative of Tn5 with a region encoding *E. coli* alkaline phosphatase (*phoA*) lacking signal sequence, expression signals inserted into the left IS50 element (IS50L), kanamycin resistance gene (Km^r) and transposase enzyme (Tnase) sequence. Active insertions into membrane gene interrupt the ‘Gene X’ and result in the production of a hybrid protein from Gene X - *phoA* fusion. Sequencing of Gene X with outward primers (K36 and RS6), and inward primers (M13Fwd and M13Rev) after cloning into pUC19 vector, followed by homology study led to the identification of the mutated gene.

3.2.5.1 Genomic analyses of mutants

To identify the gene mutated due to transposon mutagenesis, genomic analyses using various molecular methods was done. The protocol used for the genomic analyses of the mutants is provided in the flowchart below (Fig. 3.2)

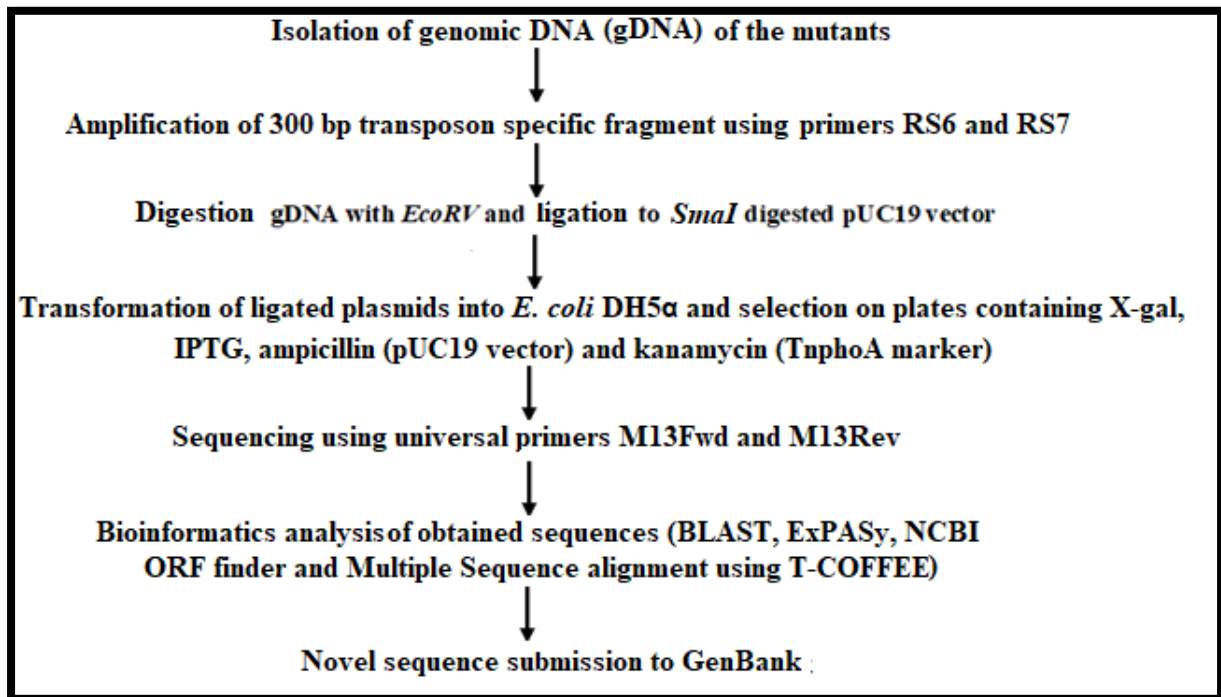


Figure 3.2: Flow chart for identification of the mutated gene.

A. Genomic DNA isolation

Wild type *M. fortuitum* and shortlisted mutant strains were inoculated in LBGT and incubated at 37°C till its maximum growth. The cultures were centrifuged at 5500 xg for 10 minutes and obtained pellets were suspended in 200 µL of TES buffer, which was incubated at 80°C for one hour. Lysozyme (2 mg/mL) was added to the cell suspension and incubated at 37°C for two hours. After two hours, 1.5% SDS and 100 µg/mL proteinase K were added and incubated at 50°C for 1 hour. Buffered phenol was added to the cell suspension and mixed, followed by centrifugation at 12000 xg for 10 min. After centrifugation three phases were obtained; of which, the aqueous layer was collected and extracted twice with chloroform: isoamyl alcohol (24:1) solution. DNA was precipitated from the aqueous layer using an equal volume of isopropyl alcohol and pelleted through centrifugation at 12000 xg for 15 min at 4°C. The pellet was washed using 70% ethanol twice, air dried, and resuspended in autoclaved water.

B. PCR amplification

PCR master mix (Promega) was used for the amplification of a desired 300 bp DNA fragment in mutants using a Thermocycler (Applied Biosystems). Following reaction mixture was prepared for PCR amplification:

Primer RS6	25 pmol
Primer RS7	25 pmol
Template DNA	0.10-10 ng
2X master mix	25.0 μ L
Nuclease free water to 50 μ L (final volume)	

Following conditions were used for PCR amplification:

Initial denaturation	95°C for 4 min	
Denaturation	95°C for 1 min	} 30 cycles
Annealing	52°C	
Extension	72°C for 1 min	
Final extension	72°C for 5 min	

C. Agarose gel electrophoresis

Agarose gel electrophoresis was done for observation of DNA using gel electrophoresis apparatus (Medox). Briefly, required amount of agarose powder (Loba Chemie) was weighed, suspended in 1X TAE buffer and dissolved by heating. Ethidium bromide was added to the molten agar and the mixture was poured into the comb fitted casting tray. The gel was kept at room temperature for 10-15 minutes. After solidification, the comb was removed from the casting tray and placed in an electrophoresis tank containing 1X TAE buffer. The DNA samples were mixed with 6X loading dye (final concentration) and loaded into the wells. Electrophoresis was carried out at a constant voltage of 5-10 V/cm. The electrophoresed DNA was analyzed under the UV Gel Documentation system (Alpha Innotech) and photographed. For DNA extraction from gel, low melting agarose was used and gel extraction kits (MACHEREY-NAGEL, Germany) were used. The protocol used for gel extraction was followed as per the manufacturer's instructions.

3.2.5.2 Cloning of transposon inserted DNA segment

A. Plasmid isolation

Alkaline lysis method [223] with minor modifications, was used for isolation of plasmid from *E. coli* cells. Inoculation of *E. coli* cells was done in antibiotic containing LB broth and incubated overnight. Cells were collected by centrifugation at 5500 xg for 10 minutes. Pellet was resuspended in an appropriate volume (V) of alkaline lysis solution I. The suspension

was vortexed properly, followed by the addition of (2V) of alkaline lysis solution II. The suspension was then mixed gently and incubated at room temperature for 5 minutes. Prechilled (1.5V) alkaline lysis solution III was added, mixed, and incubated on ice for 45 minutes. After incubation, the cell lysate was centrifuged at 12000 xg for 25 minutes. The pellet was discarded, and the supernatant was collected in a new centrifuge tube. Precipitation of the plasmid DNA was done by the addition of an equal volume of chilled isopropanol and incubated at -20°C overnight. After precipitation, plasmid DNA was pelleted by centrifugation at 12000 xg for 20 min, washed with 96% ethanol followed by washing with 70% ethanol. The pellet was air dried and suspended in autoclaved water. The presence of plasmid DNA was checked by agarose gel electrophoresis. The isolated plasmid was stored at -20°C until further use.

B. Restriction digestion

Restriction digestion of DNA with specific enzymes was done in the buffer provided by the manufacturer. DNA with a concentration of 1 µg was digested using ~5 units of enzymes in a total reaction volume of 30 µL and incubated at a specific optimum temperature for 3 hours. After 3 hours, the reaction was stopped by heating at 65°C for 10 min, for inactivation of restriction enzyme. For the current study, gDNA isolated from the shortlisted mutants was digested with *EcoRV*, and the pUC19 vector was digested with *SmaI* to generate blunt ends. Digestion of plasmid DNA was confirmed through agarose gel electrophoresis using proper DNA molecular size markers.

C. Ligation

Ligation of insert and vector was done as per the instructions provided by kit manufacturer (Promega). Insert to vector ratio used in the present study was 3:1. A reaction mixture of 20 µL final volume contains:

Insert DNA	1-2 µg
Vector DNA	0.1-0.5 µg
10X T ₄ DNA ligase buffer	2 µL
T ₄ DNA Ligase	5 Unit

The reaction mixture was incubated at 16°C for 16 hours followed by inactivation of ligase at 65°C for 10 min.

D. Plasmid transformation into *E. coli*

Protocol used for transformation of the ligated product into *E. coli* DH5 α was followed as described by Hanahan [224] with some modifications. Briefly, seed culture was prepared by inoculating a single colony of *E. coli* in LB broth followed by overnight incubation. Further, inoculation from seed culture in a dilution of 1:50 was done in fresh LB media and incubated till optical density reaches to 0.6 at 600 nm. The cells were harvested by centrifugation at 5500 \times g for 10 min at 4°C, followed by washing with chilled transformation buffer I (TFBI). The cell pellet was suspended in transformation buffer II (TFBII). The suspension was then incubated over ice for 30 min to prepare competent bacterial cells. The competent cells were collected by centrifugation and resuspended in fresh TFBII.

For transformation, 1 μ g DNA was added to 200 μ L of competent cells and incubated on ice for 30 min. After incubation, the cells were subjected to 42°C temperature for 90 seconds in water to give heat shock to the cells. About 800 μ L of LB broth was added to the vials after heat shock and incubated at 37°C for 40 min. The transformation mixture was plated on LB agar plates containing Ampicillin (pUC19 marker) and Kanamycin (transposon marker) followed by incubation at 37°C.

3.2.5.3 Sequencing

Selected clones of transformed *E. coli* cells were used for the isolation of plasmid. After confirmation of plasmid for the presence of transposon containing segment of DNA, the mutated gene was sequenced from both ends using universal primers M13Fwd (5'TGTAAAACGACGGCCAGT3'), and M13Rev (5'CAGGAAACAGCTATGAC3'); and transposon specific outward primers K36 (5'ATCGCTAAGAGAATCACGCAG3'), and RS6 (5'ACATTGCCGCGGATACCG3'). For Sanger sequencing, the plasmids were outsourced to Xcelris genomics, Ahmedabad (India).

3.2.6 Bioinformatics tools used for homology study

Table 3.4 enlists bioinformatics tools used for the analysis and identification of *M. fortuitum* transposon mutated gene after cloning and sequencing.

Table 3.4: List of tools used for bioinformatics analysis

S. N.	Tools/ Online servers	Reference
1	BLAST	https://blast.ncbi.nlm.nih.gov/Blast.cgi
2	ORF finder	https://www.ncbi.nlm.nih.gov/orffinder/
3	ExPASy Translate tool	https://web.expasy.org/translate/
4	Reverse Compliment	https://www.bioinformatics.org/sms/rev_comp.html
5	T-COFFEE	http://tcoffee.crg.cat/
6	Jalview	http://www.jalview.org

The sequence obtained were analyzed through nucleotide BLAST (BLASTN) and nucleotide translation protein BLAST (BLASTX) of NCBI. ORF finder and ExPASy translate online server were used to identify ORFs (open reading frame) and translate ORFs into their encoded amino acid sequence, which was further subjected to multiple sequence alignment using T-COFFEE tool and visualized using Jalview software.

3.2.7 Growth kinetics of mutants under *in vitro* stress conditions

Survival and growth kinetics of the attenuated mutants along with wild type *M. fortuitum* (WTMF) was determined to have an insight into the role of the mutated gene in survival under various *in vitro* stress conditions.

3.2.7.1 Acidic stress

WTMF and the shortlisted mutants were subjected to *in vitro* acidic stress conditions as described previously by Geiman et al. [225] with some modifications. Briefly, WTMF and the mutant strains were grown in MB7H9 medium till mid-logarithmic growth phase and centrifuged at 5500 xg for 10 minutes. Individual pellet were then washed twice with Phosphate Buffered Saline (PBS) and resuspended into 5 mL MB7H9 medium. Each culture suspension was then used to inoculate 100 mL MB7H9 medium with different pH 6.5, 5.5, 4.5, and 3.5, and incubated at 37°C with shaking. Samples were collected from each flask after 2, 4, 6, 12, 24, and 36 hours, and CFU of the collected samples was determined by serial dilution followed by plating on NAT plates.

3.2.7.2 Oxidative stress

WTMF and the shortlisted mutants were subjected to *in vitro* oxidative stress as described previously by Kawaji et al. [226] with minor modifications. Briefly, WTMF and mutant strains were grown in MB7H9 medium till mid-logarithmic phase and centrifuged at 5500 xg for 10 minutes. Individual pellet were then washed twice with PBS. Each culture suspension was then inoculated into 100 mL MB7H9 medium with 10mM H₂O₂. The cultures were then incubated at 37°C, and CFU was determined after 2, 4, 6, 12, 24, and 36 hours by plating on NAT medium.

3.2.7.3 Nutrient starvation

WTMF and the shortlisted mutants were subjected to *in vitro* nutrient starvation as described previously by Geiman et al. [225] with some modifications. Briefly, WTMF and mutant strains were grown in MB7H9 medium till mid-logarithmic phase and centrifuged at 5500 xg for 10 minutes. Individual pellet were then washed twice with PBS. Each culture suspension was then inoculated into 100 mL PBS and incubated at 37°C. CFU was determined after 2, 4, 6, 12, 24, and 36 hours by plating on NAT medium.

3.2.7.4 Detergent stress

WTMF and the shortlisted mutants were subjected to *in vitro* detergent as described previously by Geiman et al. [225] with some modifications. Briefly, WTMF and mutant strains were grown in MB7H9 medium till mid-logarithmic phase and centrifuged at 5500 xg for 10 minutes. Individual pellet were then washed twice with PBS. Each culture suspension was then inoculated into 100 mL of 0.05% SDS containing MB7H9 medium and incubated at 37°C. CFU was determined after 2, 4, 6, 12, 24, and 36 hours by plating on NAT medium.

3.2.7.5 Heat stress

WTMF and the shortlisted mutants were subjected to *in vitro* heat stress as described previously by Geiman et al. [225] with minor modifications. Briefly, WTMF and mutant strains were grown in MB7H9 medium till mid-logarithmic phase and centrifuged at 5500 xg for 10 minutes. Individual pellet were then washed twice with PBS. Each culture suspension was then inoculated into 100 mL MB7H9 medium and incubated at 45°C. CFU was determined after 2, 4, 6, 12, 24, and 36 hours by plating on NAT medium.

3.2.7.6 Hypoxic stress

WTMF and the attenuated mutants were subjected to hypoxia-induced NRP (Non-replicating Persistence) model described by Sood et al. [15] with minor modifications, for determination of cell viability of mutants under hypoxic stress. Briefly, cultures were grown till an optical density of 0.7 - 0.9 at 600 nm under aerobic conditions. 1.5 µg/mL methylene blue (Loba Chemie) was added to the cultures as an indicator of oxygen deterioration. Sterile glass vials with 15 mL capacity were taken, and 7.5 mL of actively growing methylene blue containing culture was transferred to these vials to maintain a constant headspace ratio of 0.5. To ensure hypoxic conditions inside the vials, the vials were tightly closed with rubber septa, and sealed with vacuum grease. Vials were incubated at 37°C and oxygen deterioration inside vials was observed through decolorization of methylene blue. The vials were taken after a regular time interval of three days till the observation period of 27 days, and CFU was determined by plating on NAT plates.

3.2.8 Prediction of transmembrane helix and *in silico* interaction studies

M. fortuitum short-chain dehydrogenase (MfSdr) was identified to be mutated in the attenuated mutant MT726. TMpred (https://embnet.vital-it.ch/software/TMPRED_form.html) program was used for the prediction of transmembrane helices in the amino acid sequence of MfSdr.

M. fortuitum short-chain dehydrogenase was characterized by *in silico* interaction study using Search Tool for the Retrieval of Interacting Genes/Proteins (STRING) version 10.5 (<https://string-db.org>). As the *M. fortuitum* database is not available in STRING, hence, MfSdr amino acid sequence was submitted to STRING for homology in *M. tuberculosis*. STRING showed maximum hits with *M. tuberculosis* probable short-chain dehydrogenase Rv2509. Thus, the protein interaction map was generated using Rv2509. The interaction parameter was set to a medium confidence level of 0.5 in the STRING database.

3.2.9 Molecular modeling

Three-dimensional high-quality structure of MfSdr was predicted using the Robetta (<http://rosetta.bakerlab.org>) server. Predicted models were further analyzed using PyMOL (The PyMOL Molecular Graphics System, Version 2.0 Schrödinger, LLC) based on root mean square deviation (RMSD) values with available short-chain dehydrogenase structures of

pathogenic mycobacterial species including *M. avium* carveol dehydrogenase (PDB ID: 5EJ2), *M. avium* carveol dehydrogenase bound to NAD (PDB ID: 3T7C), and *M. paratuberculosis* carveol dehydrogenase (PDB ID: 3PGX).

3.2.10 Molecular docking

For identification of potential inhibitors of *M. fortuitum* short-chain dehydrogenase (MfSdr), docking studies were performed using Autodock version 4.2.6, and docked complexes were visualized using Python Molecular Viewer (1.5.6) software.

A. Preparation of ligand and receptor

FDA approved drug library of 3134 molecules was taken from the ZINC database in SMILE format. Three-dimensional structure of FDA approved drugs were generated through 3D Corina for ligand library preparation. Three-dimensional structure of known *M. tuberculosis* short-chain dehydrogenase inhibitor i.e. tricyclazole was retrieved from PubChem database in SDF format, followed by conversion to PDB format using Open Babel software. The predicted structure of MfSdr was used as a receptor. All the ligands, inhibitors, and receptors were converted into PDBQT for docking.

B. Prediction of the binding site

PyMOL was used to predict possible binding sites by comparing MfSdr structure with available short-chain dehydrogenase structures of Mycobacterium species. *Mycobacterium avium* short-chain dehydrogenase (PDB ID: 3T7C) showed the closest similarity to MfSdr, Nicotinamide Adenine Dinucleotide (NAD) from 3T7C was complexed with MfSdr structure and used for grid preparation.

C. Docking studies

Autodock version 4.2.6 in combination with PMV software was used for the screening of drug library against MfSdr structure. The Gasteiger atomic charges were assigned for ligands (inhibitors and FDA approved drug library). The binding site in the 3D structure of MfSdr on X, Y & Z coordinates was estimated to be located at 4.725Å, 7.589Å, and 8.726Å respectively. Grid map of MfSdr was constructed and the size of the grid box was kept at 126 x 126 x 126. The grid was set to be sufficiently large to cover significant portions of the binding sites. Lamarckian genetic search algorithm was employed. Virtual screening of drug

library was done using two rounds of docking, where number of energy evaluation was set to 2,500, 000 per run. Fifty and hundred independent docking runs were performed during the first and second rounds of screening respectively, whereas population size was set to 150 and 250 for respective screenings. All other parameters were set to default values.

The binding free energies were evaluated for the binding conformations of ligand, and the low-energy conformations were selected from the largest cluster. In each docking log file (DLG) file obtained after docking, the structure having the lowest energy docked conformation from each cluster was selected. Visualization of ligand-receptor binding was done using MegaMol.

RESULTS

A library of transposon mutants was constructed and screened for *in vivo* virulence, immunoprofiling, and histopathology. Mutants with attenuated virulence were further subjected to genomic and bioinformatics analyses for identification of gene mutated due to transposon mutagenesis. The growth behavior of the mutants was further studied under *in vitro* stress conditions to have an insight into the probable role of the mutated gene in survival under unfavorable conditions. One mutant showing maximum attenuation in virulence was characterized by *in silico* studies for the identification of inhibitors against the respective mutated gene.

The results are compiled under following subheadings

4.1 Identification of mutants defective in *in vivo* virulence

4.2 Analyses of mutants for identification of potential drug targets

4.3 Structure prediction, interaction and molecular docking studies to identify potential inhibitors

4.1 Identification of mutants defective in *in vivo* virulence

4.1.1 Construction of transposon mutant library and shortlisting of mutants

TnphoA based transposon mutagenesis of *M. fortuitum* ATCC 6841 resulted in the construction of a library of about 5000 mutants. Primary screening of transposon mutants on selection plates containing XP as substrate and kanamycin as antibiotic selection marker led to the identification of 186 blue mutants having insertion of the transposon in membrane protein encoding genes (Figure 4.1).

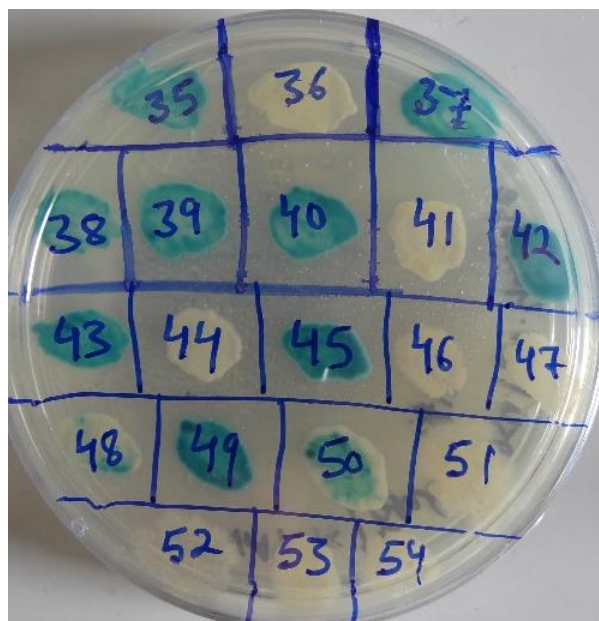


Figure 4.1: Primary screening of *M. fortuitum* transposon mutants on selection plates containing XP. Blue colored mutants represent transposon insertion in membrane protein-encoding genes due to alkaline phosphatase activity, while white colored mutants contain mutation in genes other than membrane/transmembrane/secretory protein-encoding genes.

Secondary screening was done by quantitative analyses of alkaline phosphatase activity of identified 186 blue colored mutants which resulted in shortlisting of 20 mutants with high alkaline phosphatase activity for further study. Table 4.1 shows alkaline phosphatase activity of the shortlisted 20 mutants in Miller Units (MU). Considering the permission for the limited number of mice by Institutional Animal Ethics Committee (IAEC), six mutants namely, MT721, MT723, MT724, MT725, MT726, and MT727 showing the highest alkaline phosphatase activity (>800) were shortlisted for *in vivo* virulence study.

Table 4.1: Alkaline phosphatase activity of transposon mutants. Table shows alkaline phosphatase activity expressed in Miller Units (MU) of the top 20 mutants. Six mutants (written in **bold**) showing the highest alkaline phosphatase activity were shortlisted for *in vivo* studies.

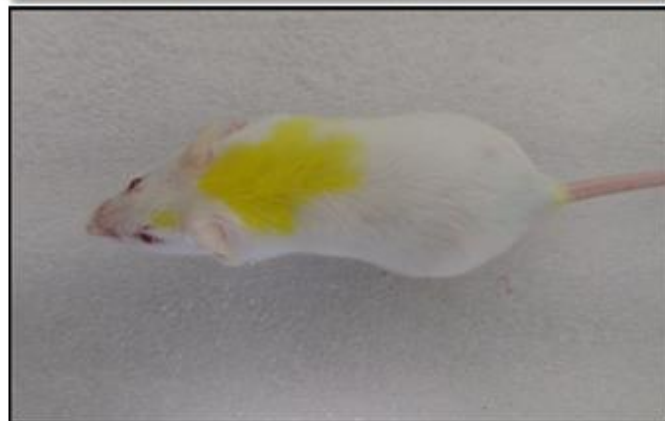
S. N.	Mutant Name	pNPP Assay values (MU)	S. N.	Mutant Name	Alkaline phosphatase activity (MU)
1	MT661	257.8	11	MT723	971.2
2	MT662	333.2	12	MT724	982.1
3	MT663	365.7	13	MT725	830.0
4	MT664	466.9	14	MT726	918.2
5	MT666	303.2	15	MT727	957.6
6	MT711	525.8	16	MT728	336.6
7	MT712	476.1	17	MT741	777.1
8	MT713	442.1	18	MT761	540.84
9	MT721	953.4	19	MT762	573.7
10	MT722	559.95	20	MT763	645.01

4.1.2 Mutants MT726, MT725, and MT727 showed virulence attenuation

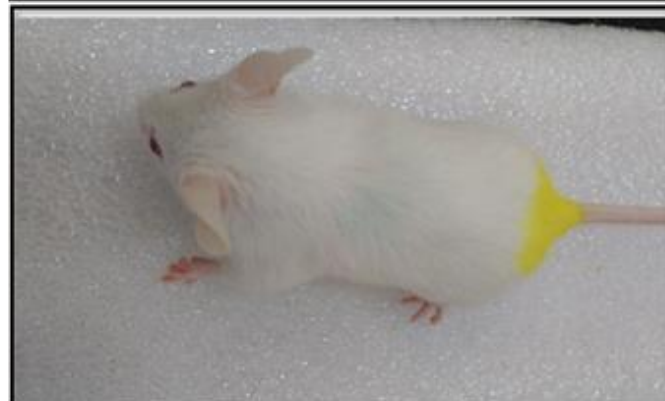
Wild type *M. fortuitum* (WTMF) infected mice showed restlessness, loss of weight, neck tilting and spinning movement of the head. Spinning movement is a characteristic feature of *M. fortuitum* infection in mice model. Mice infected with mutant MT725 and MT726 showed fewer symptoms in the form of neck tilting only and no spinning movement was observed (Figure 4.2). However, mice infected with mutant MT727, MT725, MT723, and MT724 showed similar symptoms as shown by wild type infected mice. No mortality was observed in mice infected with either wild type or mutants until the observation period of 25 days.



Wild type
M. fortuitum



Mutant MT726



Mutant MT725



Mutant MT727

Figure 4.2: Symptoms in mice infected with wild type *M. fortuitum* (WTMF) and the mutants. The figure shows characteristic neck tilting in mice infected with WTMF, whereas mutant MT726 and MT725 shows less neck tilting. Mutant MT727 shows symptoms similar to WTMF.

Based on bacillary load obtained, three mutants namely MT726, MT725, and MT727 showed attenuation in the maintenance of infection in comparison to the wild type *M. fortuitum*. Mutant MT726 showed attenuation in virulence as a decrease of 1.8 log bacillary load was observed after 10 days PI, followed by clearance of infection 25 days PI. Mutant MT725 and MT727 showed bacillary load similar to the wild type till 10 days PI, however, a decrease of 2.3 and 1.8 log in bacillary load was observed respectively 25 days PI (Figure 4.3). Three mutants namely MT721, MT723, and MT724 showed symptoms and bacillary load similar to wild type.

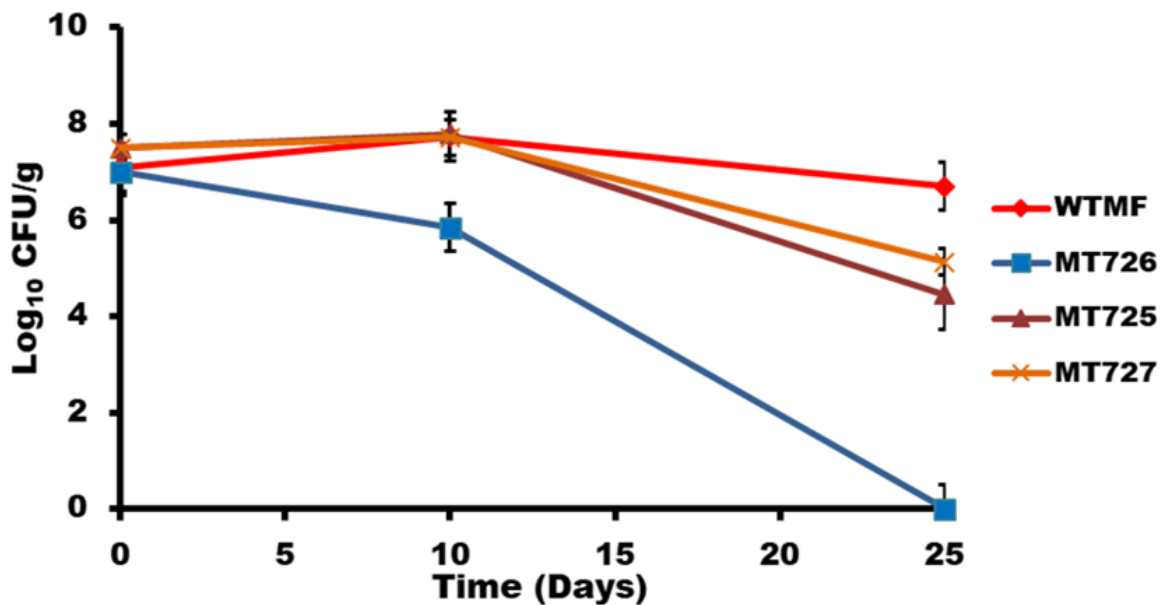


Figure 4.3: Bacillary load in kidney tissue of mice infected with WTMF and mutants. The figure shows maintenance of infection in case of wild type *M. fortuitum* (WTMF) till 25 days, whereas mutant MT726 shows clearance of infection 25 days PI. Mutant MT725 and MT727 show 2.3 and 1.8 log decrease at 25 days PI time point in comparison to WTMF. [Data shows a mean of three independent experiments with standard deviation in error bars].

4.1.3 The mutants showing virulence attenuation also showed reduced tissue pathology

Histopathology of wild type *M. fortuitum* infected kidney tissue showed damage in the form of dilated tubules, constricted blood vessels, leukocyte infiltration and granuloma formation at 10 days PI, followed by pronounced granuloma formation with fibrous necrotic center 25 days PI. Mutant MT726 showed leukocyte infiltration in kidney tissues 10 days PI with no conspicuous granulomatous structures 25 days PI. Mutant MT725 showed leukocyte infiltration and formation of granulomatous structures 10 days PI, whereas, at 25 days PI the mutant showed reduced leukocyte infiltration and granuloma formation. Mutant MT727 showed tissue pathology and cell damage similar to wild type infected kidney of mice at 10 and 25 days PI (Figure 4.4).

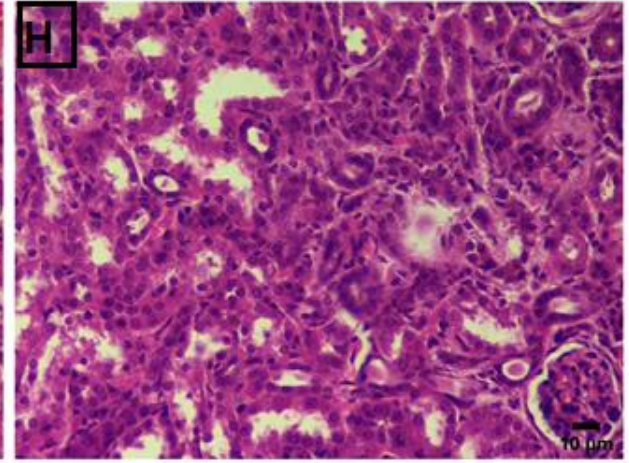
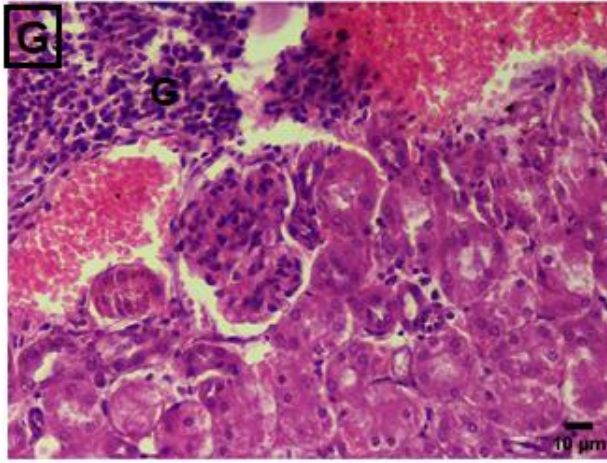
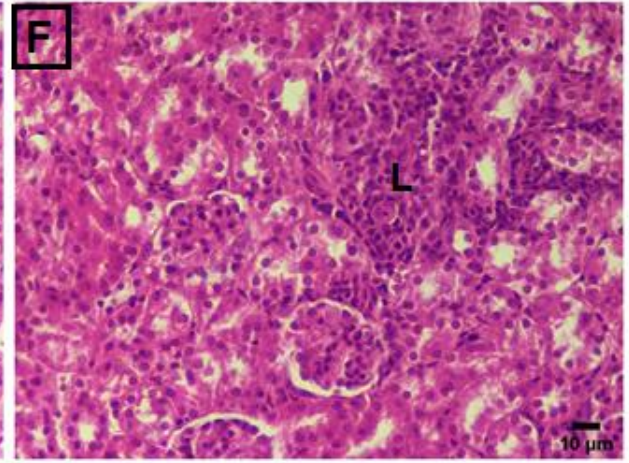
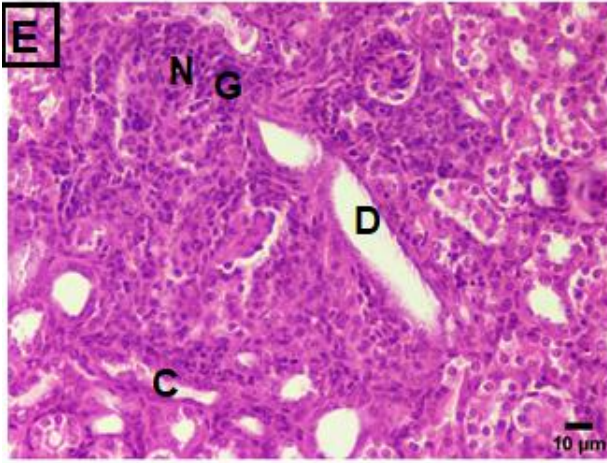
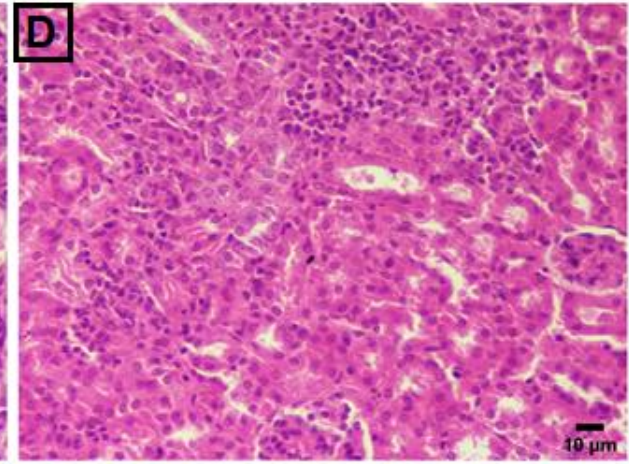
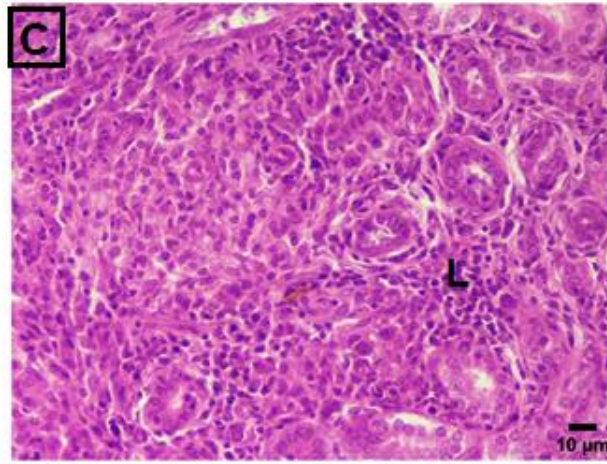
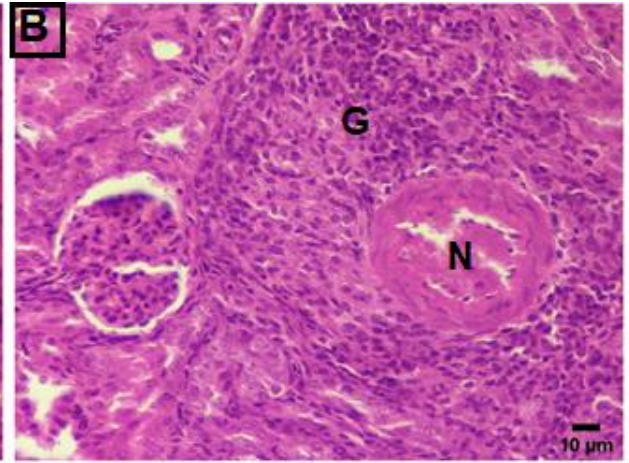
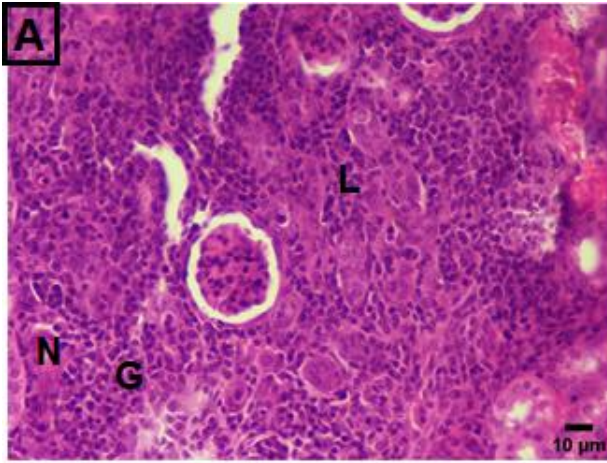


Figure 4.4: Histopathology of kidney tissue infected with WTMF and attenuated mutants (MT726, MT725, and MT727). The figure shows kidney tissue histopathology (Hematoxylin and eosin staining) 10 days and 25 days PI in mice infected with wild type *M. fortuitum* (A, B); mutant MT726 (C, D); mutant MT725 (E, F); mutant MT727 (G, H). G-Granuloma formation; N-Necrotic center; L-Leukocyte infiltration; D-Dilated tubules; C-Congested vessels. Original magnification: 400X; Horizontal scale bar: 10 μ m.

4.1.4 Attenuated mutants showed lower levels of IFN- γ and TNF- α

Analysis of cytokine concentration in blood serum of mice infected with mutants showed deviation in comparison to the mice infected with wild type *M. fortuitum* (Figure 4.5).

Mutant MT726, MT725, and MT727 showed 5.2, 4.3 and 1.8-fold reduction in IFN- γ levels at 10 days PI in comparison to the wild type respectively. In addition, TNF- α concentration also varied in blood serum of mice infected with wild type and mutants. 2-fold, 1.1-fold and 3.7-fold decrease in TNF- α serum concentration were observed in mice infected with mutant MT726, MT725, and MT727 respectively at 10 days PI. At 25 days PI, low concentrations of IFN- γ and TNF- α in mice serum infected with wild type as well as mutants were observed.

In the case of the anti-inflammatory cytokine, IL-10, no appreciable difference was observed in serum concentrations of mice infected with wild type and mutants.

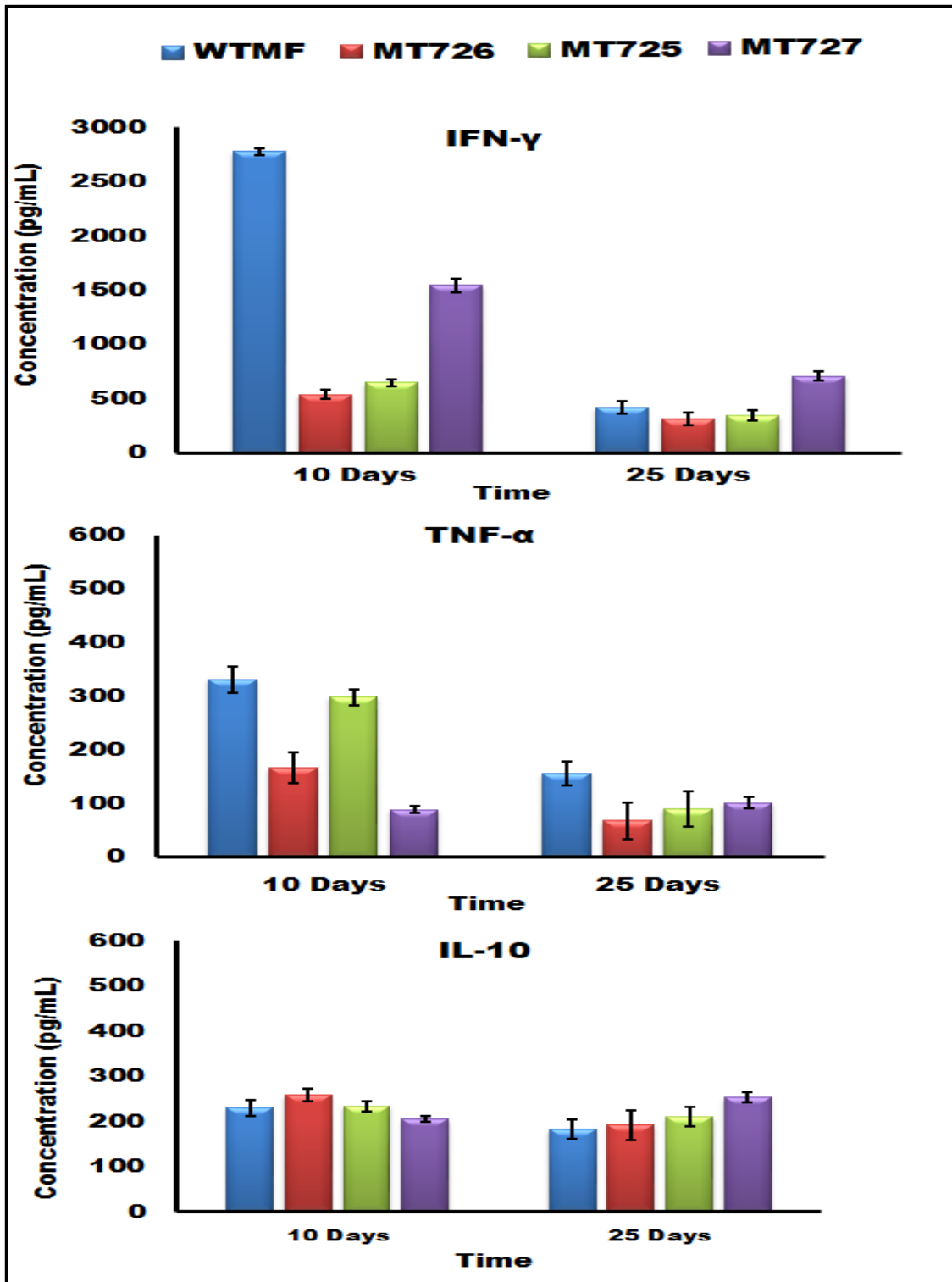


Figure 4.5: Cytokine profiling of WTMF and attenuated mutants (MT726, MT725, and MT727). The figure shows low IFN- γ and TNF- α concentration in mice serum infected with the mutants in comparison to wild type *M. fortuitum* (WTMF) at 10 days PI. At 25 days PI, low concentration of IFN- γ and TNF- α in mice serum infected with WTMF as well as mutants was observed. No appreciable difference in IL-10 concentrations was observed in serum concentration of mice infected with WTMF and the mutants. [Data shows a mean of three independent experiments with standard deviation in error bars].

4.2 Analyses of mutants for identification of potential drug targets

4.2.1 PCR amplification confirmed the presence of transposon in mutants

Genomic DNA of attenuated mutants (MT726, MT725, and MT727) and wild type *M. fortuitum* was isolated, followed by PCR amplification with transposon specific primers. A transposon specific PCR product of 300bp was amplified from the gDNA of the mutants (Figure 4.6). Genomic DNA of wild type *M. fortuitum* was taken as a negative control, where, no PCR product was obtained, confirming the insertion of the transposon in the mutants.

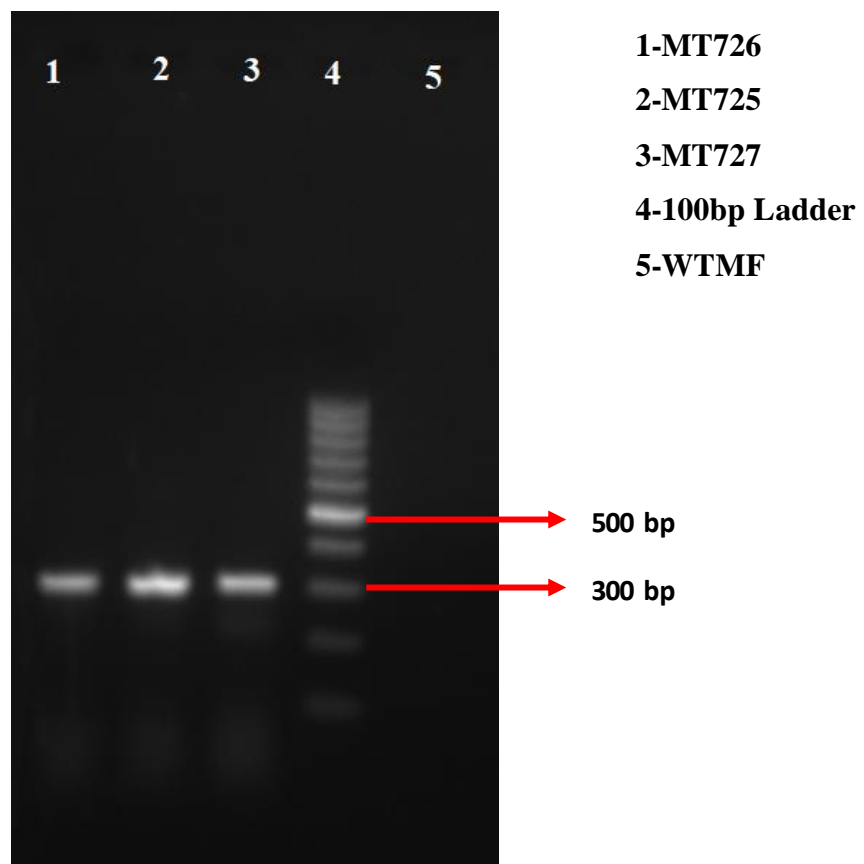


Figure 4.6: Amplification of transposon specific PCR product. The figure shows the amplification of a 300 bp PCR product, indicating transposon insertion in gDNA of mutants (MT726, MT725, and MT727). Wild type *M. fortuitum* (WTMF) taken as negative control shows no amplification.

4.2.2 Genomic analyses led to identification of ORFs mutated in attenuated mutants

Three nucleotide sequences were obtained after cloning and sequencing of transposon inserted DNA fragments of attenuated mutants (MT726, MT725, and MT727). The homology study of the nucleotide sequence is given in the following sections.

4.2.2.1 Short-chain dehydrogenase was found to be mutated in mutant MT726

Sequencing of the DNA fragment mutated by insertion in mutant MT726 led to the identification of a 417 bp ORF translating to 138 amino acids (Figure 4.7). Alignments using BLASTX showed the closest homology with short-chain dehydrogenase of *M. fortuitum* CT6 strain followed by other mycobacterial species. Multiple sequence alignment of the translated amino acid sequence of obtained ORF with *M. fortuitum* CT6 strain and *M. tuberculosis* short-chain dehydrogenase amino acid sequences showed a percent identity of 99.28% and 79.71% respectively (Figure 4.8).

Hence the novel nucleotide sequence was identified as probable short-chain dehydrogenase of *M. fortuitum* (MfSdr) and submitted to GenBank with accession number KY250516.

```
Nucleotide sequence (417 bp)  
CTAGCCGCCGCCGAGCTTCTTGTAGACCGCACCCACGATCGGGGTGACGATGGCGCGCG  
GCGCGTAGCCGCTGGCCATCGACATGGCCTTGGACGTCACGCCGGGCACCACGCGCATC  
TTGTTCTTCTCCAGGCCGTCCAGGGACAGCTTGGCGGTGTATTCGGTTGAGATCCAAAGG  
AAGTCGGGGATCAGCCGTTTCGACCAGGGACTGCTCCGCCTCGTCGGGCAGCTCGGTGCG  
GACCGGGCCCGGCGCCAGCACGGTGACGTGCACGCCCGCGCCATTGAGTTCGCCGCGCA  
GCGACTCGCTGAATGTGTTGGCGAATGCCTTGGACGCGGCATAGGTGGCGTTGTTGGGTA  
TCGGTGAGTTACCGGCGGCCGAACCGGAGGTGAGGATCCCGCCGGAGCCGCGCTTGACC  
AT  
Translated protein sequence (138 Amino acid Residues)  
MVKRSGGILTSGSAAGNSPIPNNATYAASKAFANTFSESLRGELNGAGVHVTVLAPGPVRT  
ELPDEAEQSLVERLIPDFLWISTEY TAKLSLDGLEKNKMRVVPGVTSKAMSMASGYAPRAIV  
TPIVGAVYKKLGGG
```

Figure 4.7: Nucleotide sequence (GenBank accession number KY250516) and translated protein sequence of probable *M. fortuitum* short-chain dehydrogenase (MfSdr). The figure shows a nucleotide sequence of 417 bp and corresponding translated protein sequence of 138 amino acid residues of MfSdr, found to be mutated in the mutant MT726.



Figure 4.8: Multiple sequence alignment of *M. fortuitum* short-chain dehydrogenase (MfSdr). The figure shows 99.28% and 79.71% homology of MfSdr (M.Ft) with short-chain dehydrogenase of *M. fortuitum* strain CT6 (M.Ftc) and *M. tuberculosis* (M.Tb) respectively.

4.2.2.2 Anthranilate synthase complex was found to be mutated in mutant MT725

A nucleotide sequence of 1186 bp was obtained in mutant MT725. Analysis of the nucleotide sequence for the presence of ORFs resulted in the prediction of two ORFs with 384 and 567 base pairs (Figure 4.9), coding for 127 and 188 amino acids respectively (Figure 4.10).

Nucleotide Sequence (1186 bp)

GAGGATCCCATCGGTAGAATTGCTGAAACGGCAAGTGCCAAGTCACCAAGTATATGGAAGTGGAGCTCTCCG
CTAIGTCATGCATTTGACCAGCGTGGTCAAGGGACGTTTGCTTCCAGTACTCAATGCCATGGATGCCTTGAA
AGCTACACTTCCAGCTGGAACAGTGT CAGGAGCTCCAAAGATTCGGGCCATGAGACGCATCTATGAACTGGA
GACGGAAAAACGAGGCGTATACGCAGGAGCAATCGGCTACTTGTCTGCGACGGGTGATATGGATTTCGCCAT
TGCCATCCGAACTATGATTCTCAAAAATCAAACAGCCTATGTGCAGGCTGGGGCAGGGATTGTCTATGATTCT
ATCGCCAAAACGAATACCAAGAAACCATTAAACAAGGCTAAATCTATGACTAGAATTGGAGAACTAAGACC
ATGA
ATGATTTTATGATTGATAACTATGATTCTTTTACTTATAACTTGGCTCAATACATTGGGAATTTTGCAGAGGTGCAGGTTTTGA
GAAATGATGATCCCAAGCTGTATGAAGAAGCTGAAAAAGCAGATGGTCTGGTTTTTCTCCCGTCTGGTTGGCCAATTGA
TGCCGGAAAGATGGAAGACATGATTCTGTGACTTTTCAGGCAAGAAGCCAATTCTAGGGATTTGTTGGGTCATCAAGCCATC
GCAGAAGTCTTTGGTGGGAAGCTAGGCTTGGCTCCAAAAGTCATGCATGGGAAGCAGAGCCATATCAGCTTTGAAAGCGCC
ATCTGTTCTCTATCAAGGCATTGAGGATGGTCTCCAGTCATGCGTTACCACAGTATTTGATTGAAGAAATGCCAGAAGACT
TTGAAGTGACAGCTCGTTCTGACTGATGACCAAGCTATTATGGGAATTC AACACAAAAGCCTGCCGATTTATGGCTTCCAGTA
CCATCCAGAAAGTATCGGAACGCCAGATGGCTTGTCTTCTATTCGGAATTTATCGAGAAGGTTGTAAGTGAGGAAACTA
GGATGAAAGAGATTATTGAAAACTAGCAAAATTTGAACATTTATCAGGTGTGGAATGACGGACGTCATTGAGCGT
ATCGTAACTGGCCGTCGTTTTACAATCACTAGTGAATTCGCGGCCCGCTGCAGGTCGACTCATATGGGAGAGCTCCC
AACGCTTGGAAAAACGCCCCG

Figure 4.9: Complete nucleotide sequence obtained after cloning and sequencing of mutant MT725. Homology analyses identified two Open Reading Frames (ORFs)- Anthranilate synthase component I (MftrpE) (GenBank accession number KY250521) represented in **bold** font; Anthranilate synthase component II (MftrpG) (GenBank accession number KY250520) represented in *italics*. The overlap of nucleotide sequences between the

two ORFs is highlighted. Start and end sequences represented in normal font do not form part of the identified ORFs.

<p>Translated protein sequence of MfTrpE (127 amino acid residues) MEVELFRYVMHLTSVVKGRLLPVLNAMDALKATLPAGTVSGAPKIRAMRRIYE LETEKRGVYAGAIGYLSATGDMDFALAIRTMILKNQTAYVQAGAGIVYDSIAQN EYQETINKAKSMTRIGELRP</p> <p>Translated protein sequence of MfTrpG (188 amino acid residues) MILLIDNYDSFTYNLAQYIGNFAEVQVLRNDDPKLYEEAEKADGLVFSPPGWP IDAGKMEDMIRDFSGKKPILGICLGHQAIAEVFGGKGLLAPKVMHGKQSHISFE APSVLYQGIEDGRPVMRYHSILIEEMPEDFEVTARSTDDQAIMGIQHKSLPIYGF QYHPESIGTPDGLSSIRNFIEKVVK</p>
--

Figure 4.10: Translated protein sequence of putative *M. fortuitum* anthranilate synthase component I (MfTrpE) and anthranilate synthase component II (MfTrpG).

BLASTX analysis of 384 bp ORF showed the closest homology to anthranilate synthase component I (TrpE) of *Mycobacterium abscessus* subspecies *abscessus*. Thus, the ORF was identified as a putative homolog of anthranilate synthase component I of *M. abscessus* in *M. fortuitum* (MftrpE) and submitted to GenBank (Accession number KY250521).

Sequence similarity-based analysis of 567 bp ORF using BLASTX showed its closest homology to anthranilate synthase component II (TrpG) of *M. abscessus* subspecies *abscessus*. Hence, the sequence obtained was identified as a putative homolog of anthranilate synthase component II of *M. abscessus* in *M. fortuitum* (MftrpG) and submitted to GenBank (Accession number KY250520).

Multiple sequence alignment of the amino acid sequence of MfTrpE with *M. abscessus* and *M. tuberculosis* TrpE showed a percent identity of 95.28% and 50.85% respectively. Further, MfTrpG showed 93% and 48.44% identity with TrpG sequences of *M. abscessus* and *M. tuberculosis* respectively (Figure 4.11). TrpE in combination with TrpG forms anthranilate synthase complex in prokaryotic organisms [227] and is involved in the first step of the tryptophan biosynthesis pathway. Thus, in the present study, anthranilate synthase complex was found to be affected by mutation in MT725.

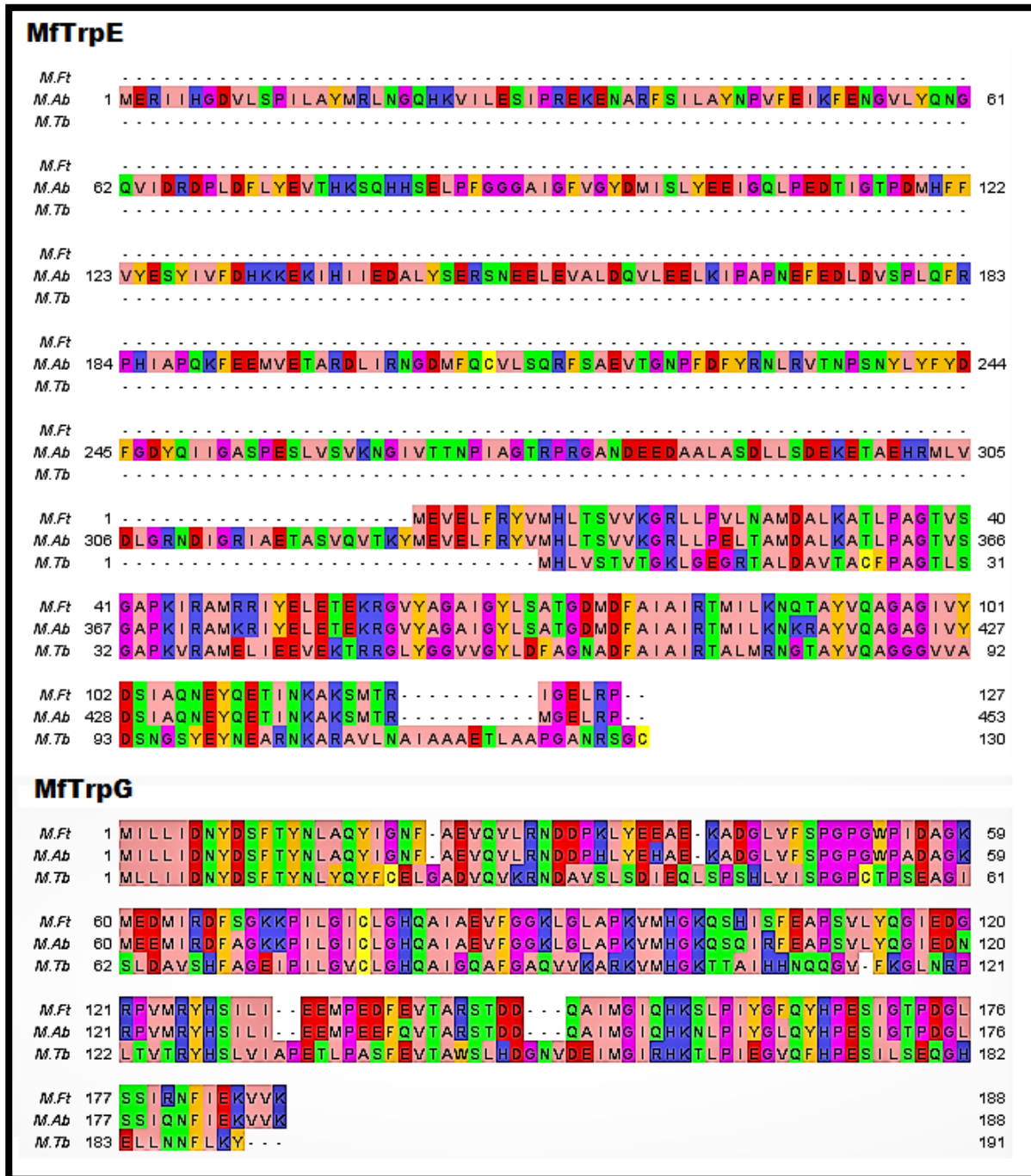


Figure 4.11: Multiple sequence alignment of *M. fortuitum* Anthranilate synthase component I (MfTrpE) and *M. fortuitum* Anthranilate synthase component II (MfTrpG) with *M. abscessus* and *M. tuberculosis* TrpE and TrpG. The figure shows 95.28% and 50.85% homology of MfTrpE (M.Ft) with TrpE of *M. abscessus* (M.Ab) and *M. tuberculosis* (M.Tb) respectively; 93% and 48.44% homology of MfTrpG with TrpG of M.Ab and M.Tb respectively.

ORFs MftrpE and MftrpG showed an overlap of four base pairs

Analyses of MftrpE and MftrpG ORFs showed MftrpE to be spanning from nucleotide 56 to 439, and MftrpG ORF starting within the reading frame of MftrpE i.e. from nucleotide 436 to 1002. Sequence analyses revealed the presence of overlap of four base pairs 'ATGA' between MftrpE and MftrpG ORFs, where 'ATG' might be the start codon of MftrpG, and 'TGA' might be the stop codon for MftrpE (Figure 4.12).

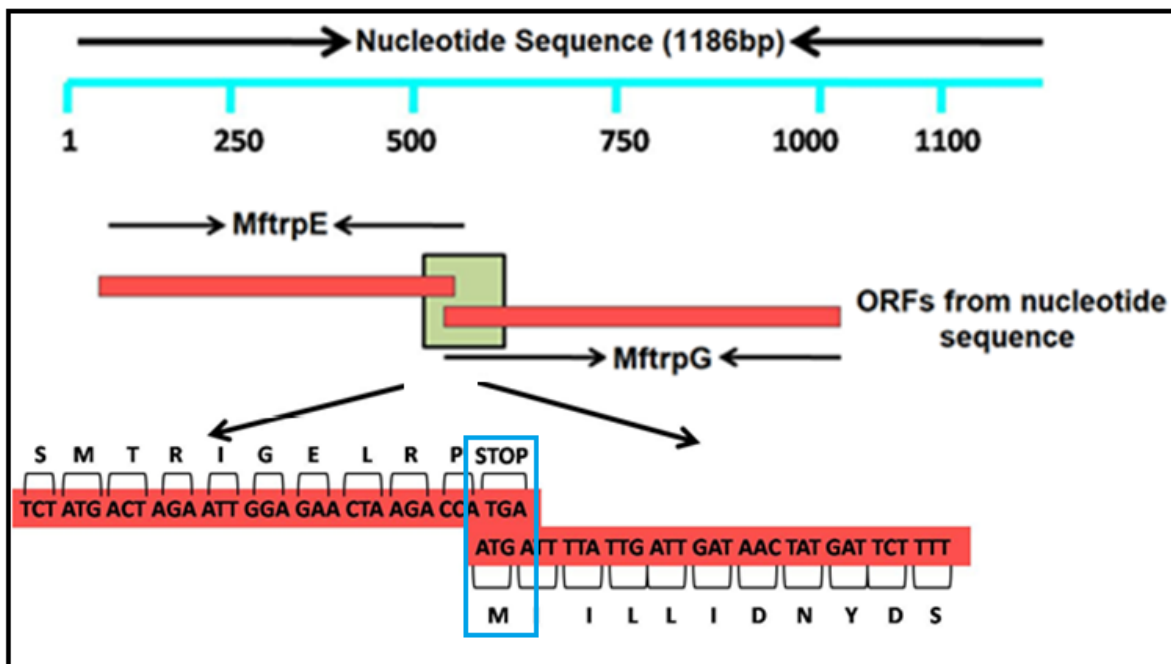


Figure 4.12: Overlap of nucleotide sequence between two ORFs coding for *M. fortuitum* Anthranilate synthase component I (MftrpE) and Anthranilate synthase component II (MftrpG) of tryptophan operon in *M. fortuitum*. The figure shows an overlap of nucleotide sequence 'ATGA' between MfTrpE and MfTrpG.

4.2.2.3 Ribosomal maturation factor RimP was found to be mutated in mutant MT727

The sequencing of mutant MT727 led to the identification of a 312 bp ORF translating to 103 amino acids (Figure 4.13). Homology study of the gene using BLASTX showed 61% homology with ribosomal maturation factor rimP of *M. abscessus* subspecies *abscessus*, and 36% identity with *M. tuberculosis* rimP. Multiple sequence alignment of the translated product obtained by ExPASy translate tool showed 60.8% identity with *M. abscessus* subspecies *abscessus* and 27.9% identity with *M. tuberculosis* RimP protein sequences respectively (Figure 4.14). As the percentage identity of the novel identified gene was most significant with *M. abscessus* subspecies *abscessus*, hence, the sequence obtained was

identified as a homolog of *M. abscessus* subspecies *abscessus* RimP in *M. fortuitum* and designated as MfRimP. The identified sequence was submitted to GenBank as ‘Putative ribosomal maturation factor RimP of *Mycobacterium fortuitum*’ with accession number MH052677.

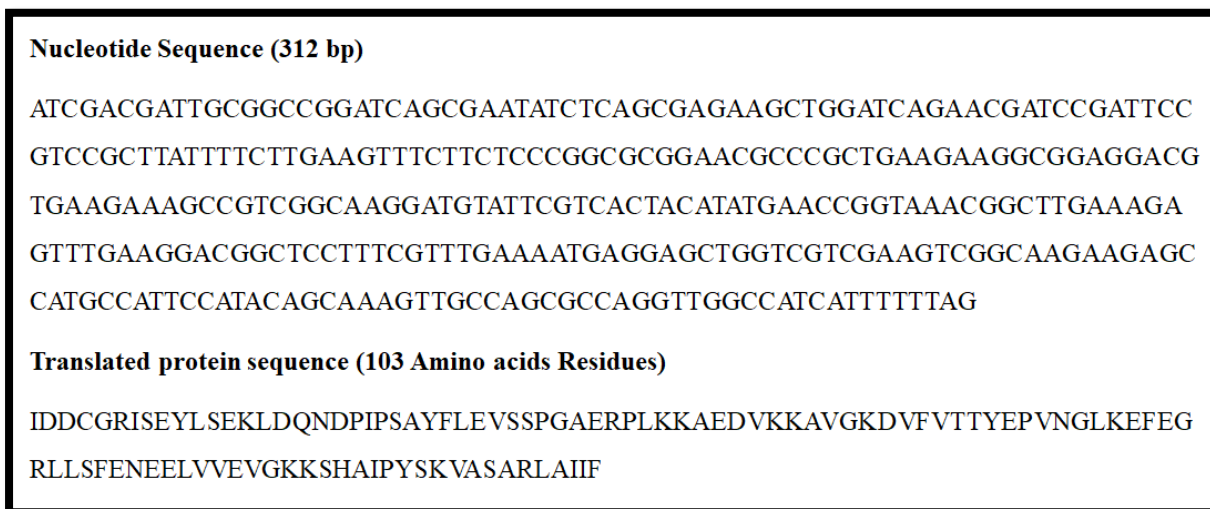


Figure 4.13: Nucleotide Sequence (GenBank accession number MH052677) and translated protein sequence of putative ribosomal maturation factor (RimP) of *M. fortuitum*. The figure shows a nucleotide sequence of 312 bp and corresponding translated protein sequence of 103 amino acid residues of MfRimP, found to be mutated in the mutant MT727.

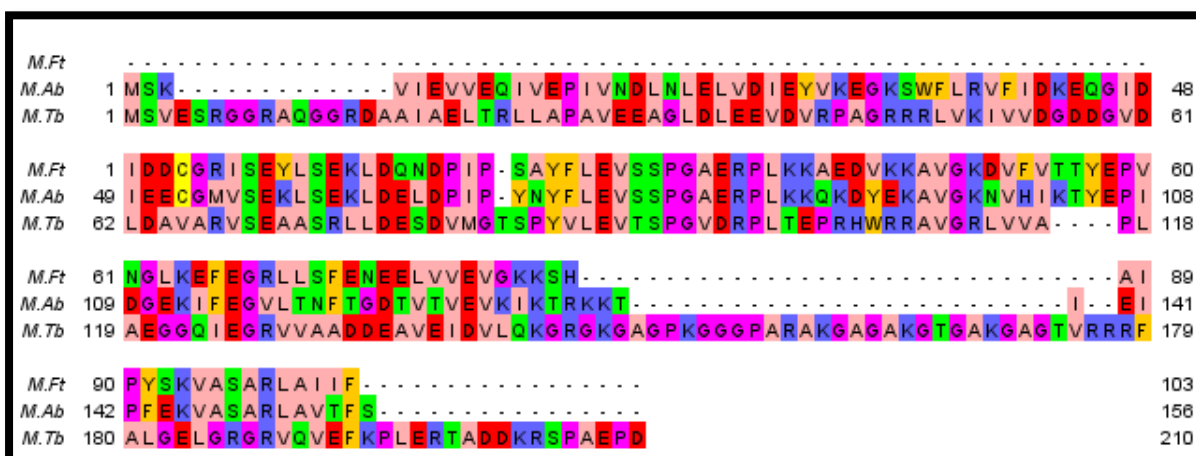


Figure 4.14: Multiple sequence alignment of *M. fortuitum* Ribosomal maturation factor (MfRimP) with RimP of *M. abscessus* and *M. tuberculosis*. The figure shows homology of 60.8% and 27.9% of MfRimP (M.Ft) with RimP of *M. abscessus* (M.Ab) and *M. tuberculosis* (M.Tb) respectively.

Thus, the genomic and bioinformatics analyses of the attenuated mutant led to the identification of *M. fortuitum* short-chain dehydrogenase (Mfsdr) in mutant MT726, *M. fortuitum* anthranilate synthase encoding genes MftrpE and MftrpG in mutant MT725, and *M. fortuitum* ribosomal maturation factor (MfrimP) in mutant MT727.

Three mutants MT721, MT723 and MT724, which did not show any attenuation in mice infection model were also subjected to cloning and sequencing protocols leading to the identification of three novel gene sequences of *M. fortuitum* ATCC 6841 (Table 4.2) and were submitted to GenBank.

Table 4.2: Genes identified in mutants MT721, MT723, and MT724.

Mutant	Gene Identified	GenBank ID
MT721	<i>M. fortuitum</i> Anthranilate phosphoribosyltransferase	KY250522
MT723	<i>M. fortuitum</i> Transcription termination/antitermination protein NusA	MK574079
MT724	Peptidase S9, prolyl oligopeptidase protein	KY250519

4.2.3 Response to different *in vitro* stress conditions by mutants and wild type *M. fortuitum* (WTMF)

4.2.3.1 Mutants showed growth defect under *in vitro* acidic stress

Analyses of growth behavior of attenuated mutants to survive under *in vitro* acidic stress resulted in reduced growth of all mutants under acidic stress of pH 4.5 and 3.5, whereas mutant MT726 also showed growth sensitivity under acidic stress condition of pH 5.5. (Figure 4.15).

Growth analyses of mutants under acidic stress of pH 6.5

Exposure of mutants to pH 6.5 revealed no appreciable difference in growth behavior in comparison to the wild type *M. fortuitum* (WTMF), showing growth behavior similar to WTMF.

Growth of mutants under in vitro acidic stress of pH 5.5

Mutant MT725 and MT727 showed growth behavior similar to the wild type at pH 5.5, whereas, a reduction of 1.3 log CFU was observed after 12 hours from initial CFU in case of mutant MT726. A continuous decline in MT726 growth was observed. Comparison of growth behavior with WTMF revealed a decrease of 3.61 log in the mutant MT726 post 36 hours of stress, suggesting growth defect at pH 5.5, suggesting a role of the mutated gene in survival under acidic stress conditions.

Growth of mutants under in vitro acidic stress of pH 4.5

Exposure of mutants to pH 4.5 resulted in reduced growth of the mutants in comparison to WTMF. WTMF showed multiplication of the bacilli without any reduction in CFU throughout the observation period.

All the three mutants MT726, MT727 and MT725 showed a continuous decline in their CFU at pH 4.5 from 12 hours to 36 hours of the observation period. In comparison to WTMF, the highest reduction of 4.74 log in CFU was shown by mutant MT726, followed by a 3.8 log and 2.6 log decrease by MT727 and MT725 respectively. Growth limiting effect shown by the mutants at pH 4.5 suggests an involvement of the respective mutated gene in survival under acidic stress conditions.

Growth of mutants under in vitro acidic stress of pH 3.5

The mutants showed defect in growth behavior under acidic stress conditions of pH 3.5 in comparison to the WTMF. Survival of WTMF reduced to 3.25 log from its initial CFU, post 24 hours of stress, and was unable to sustain its growth until 36 hours. In comparison to WTMF, all mutants showed an inability to grow at pH 3.5. Mutant MT727 showed an inability to survive beyond two hours of stress, indicating a drastic effect of acidic pH on its growth and survival. Mutants MT726 and MT725 were unable to sustain their growth beyond six hours of stress exposure.

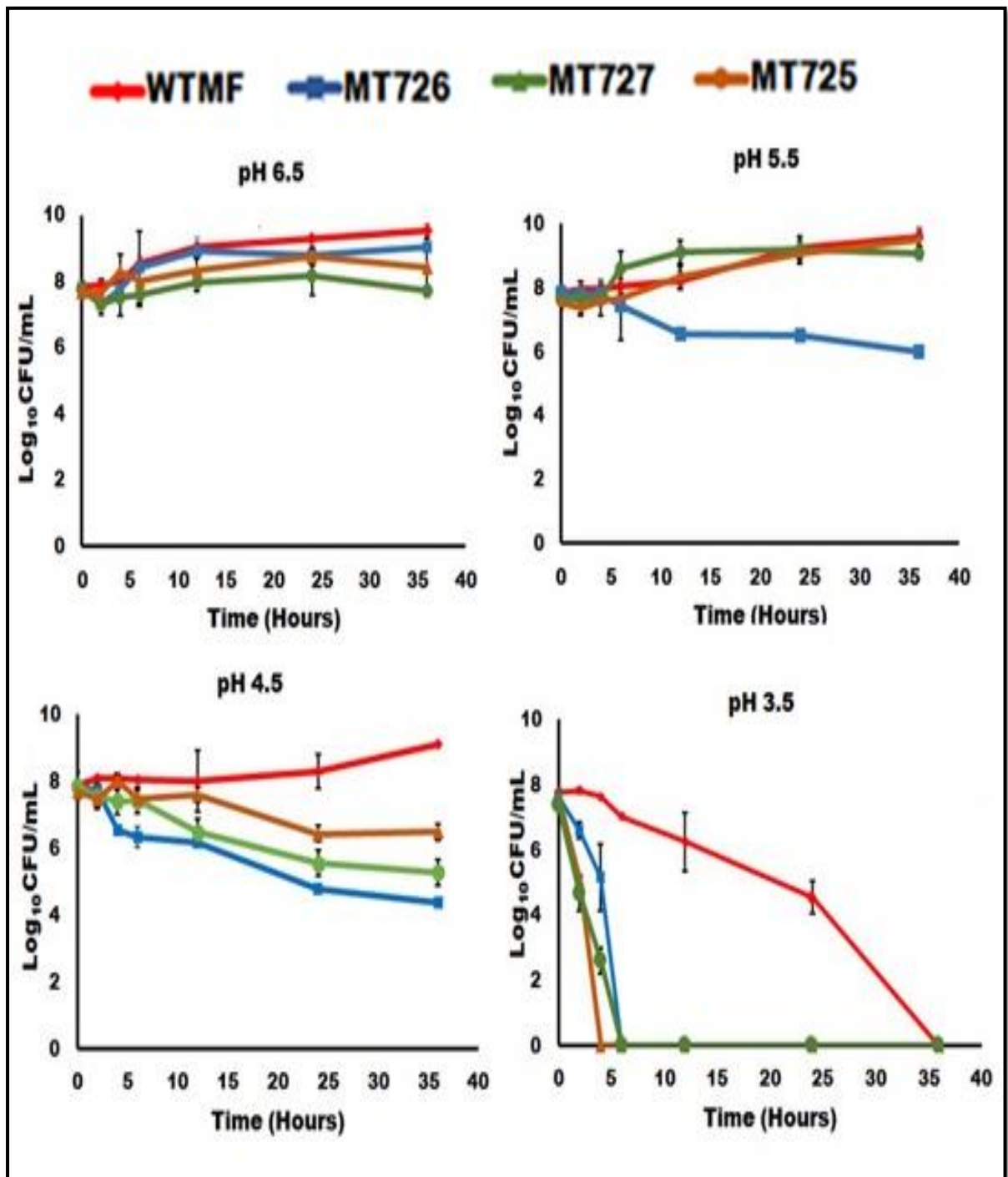


Figure 4.15: Growth kinetics of mutants under *in vitro* acidic stress. Mutants show growth behavior similar to wild type (WTMF) at pH 6.5. Mutant MT726 showed growth defect at pH 5.5, whereas a decrease in growth of all mutants was observed at pH 4.5 in comparison to WTMF. At pH 3.5, all three mutants showed an inability to survive beyond six hours of stress. [Data shows a mean of three independent experiments with standard deviation in error bars].

4.2.3.2 Mutants showed no growth defect under oxidative and heat stress

Under oxidative stress, the WTMF showed constant growth kinetics throughout the observation period, indicating the ability of *M. fortuitum* to resist oxidative stress, prevalent inside the host. All mutants also showed growth behavior similar to WTMF, suggesting the non-involvement of mutated genes in survival under oxidative stress (Figure 4.16).

Under heat stress, the WTMF showed a continuous reduction in growth followed by the inability to maintain its growth beyond 24 hours, indicating the inability of *M. fortuitum* to resist *in vitro* heat stress. All mutants also showed growth behavior similar to WTMF, suggesting no role of mutated genes in survival under heat stress (Figure 4.16).

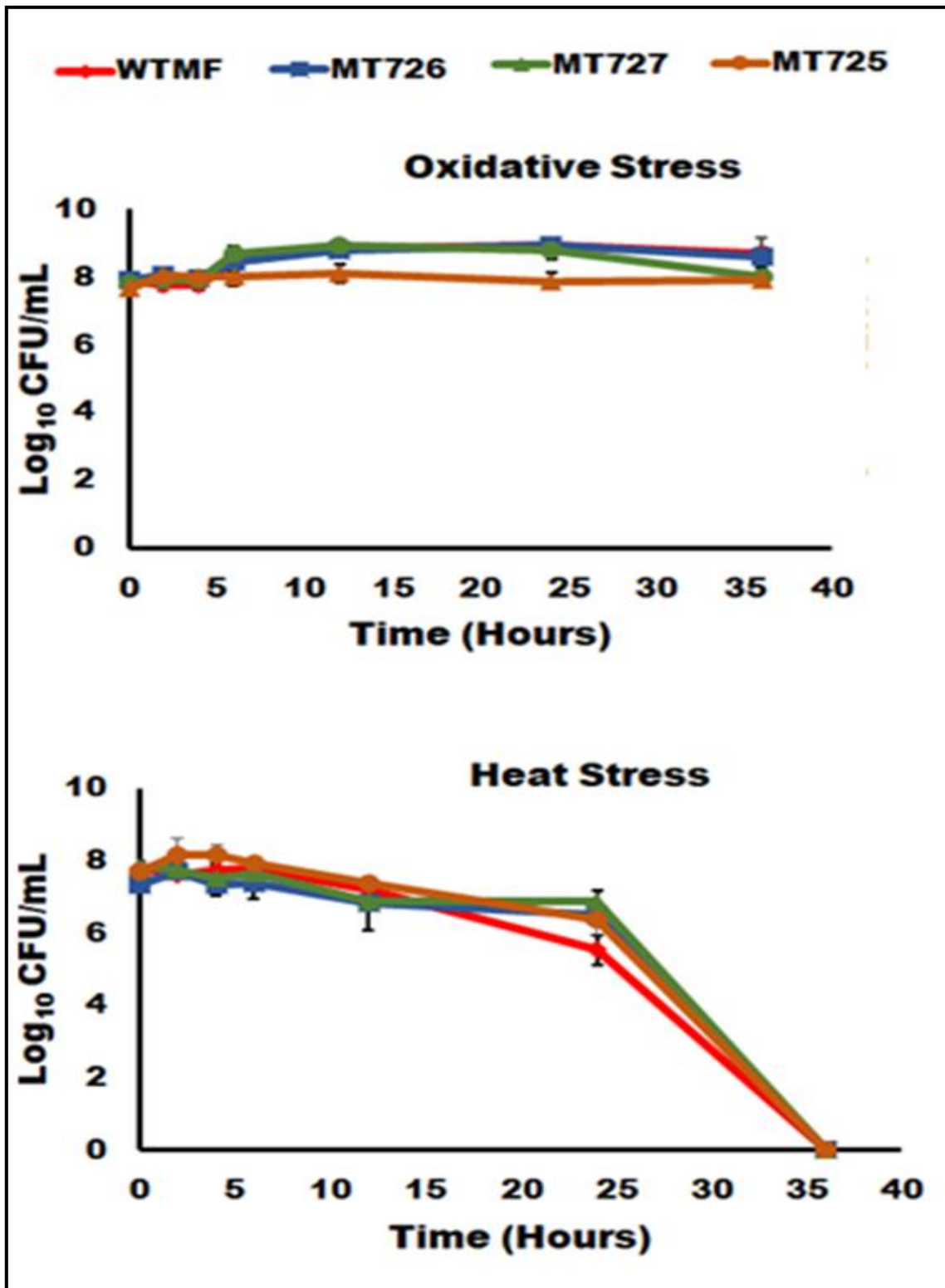


Figure 4.16: Growth kinetics of the mutants under *in vitro* oxidative and heat stress conditions. Under *in vitro* oxidative and heat stress wild type *M. fortuitum* (WTMF) and the mutants show similar growth behavior. WTMF and the mutants (MT726, MT725, and MT727) show no effect of oxidative stress on their growth, no CFU was recorded after 36 hours of exposure to heat stress. [Data shows a mean of three independent experiments with standard deviation in error bars].

4.2.3.3 Mutant MT727 showed growth defect under *in vitro* detergent stress

Under *in vitro* detergent stress, the WTMF showed constant growth behavior till the observation time period. Mutant MT725 and MT726, showed no appreciable difference in growth behavior in comparison to WTMF, indicating no role of the respective mutated gene in survival under detergent stress. However, mutant MT727 showed a decrease of 3.98 log in comparison to WTMF after 36 hours of stress, suggesting the involvement of the mutated gene in survival under detergent stress (Figure 4.17).

4.2.3.4 Mutant MT726 showed slight deviation in growth under *in vitro* nutrient starvation

Under nutrient starvation, the WTMF showed constant CFU throughout the observation period, indicating the ability of *M. fortuitum* to survive under nutrient starvation. Mutant MT725 and MT727 showed growth behavior similar to WTMF, suggesting no role of mutated genes in survival under nutrient limiting conditions. Mutant MT726 showed a decrease of 1.6 log after 36 hours from its initial CFU (Figure 4.17).

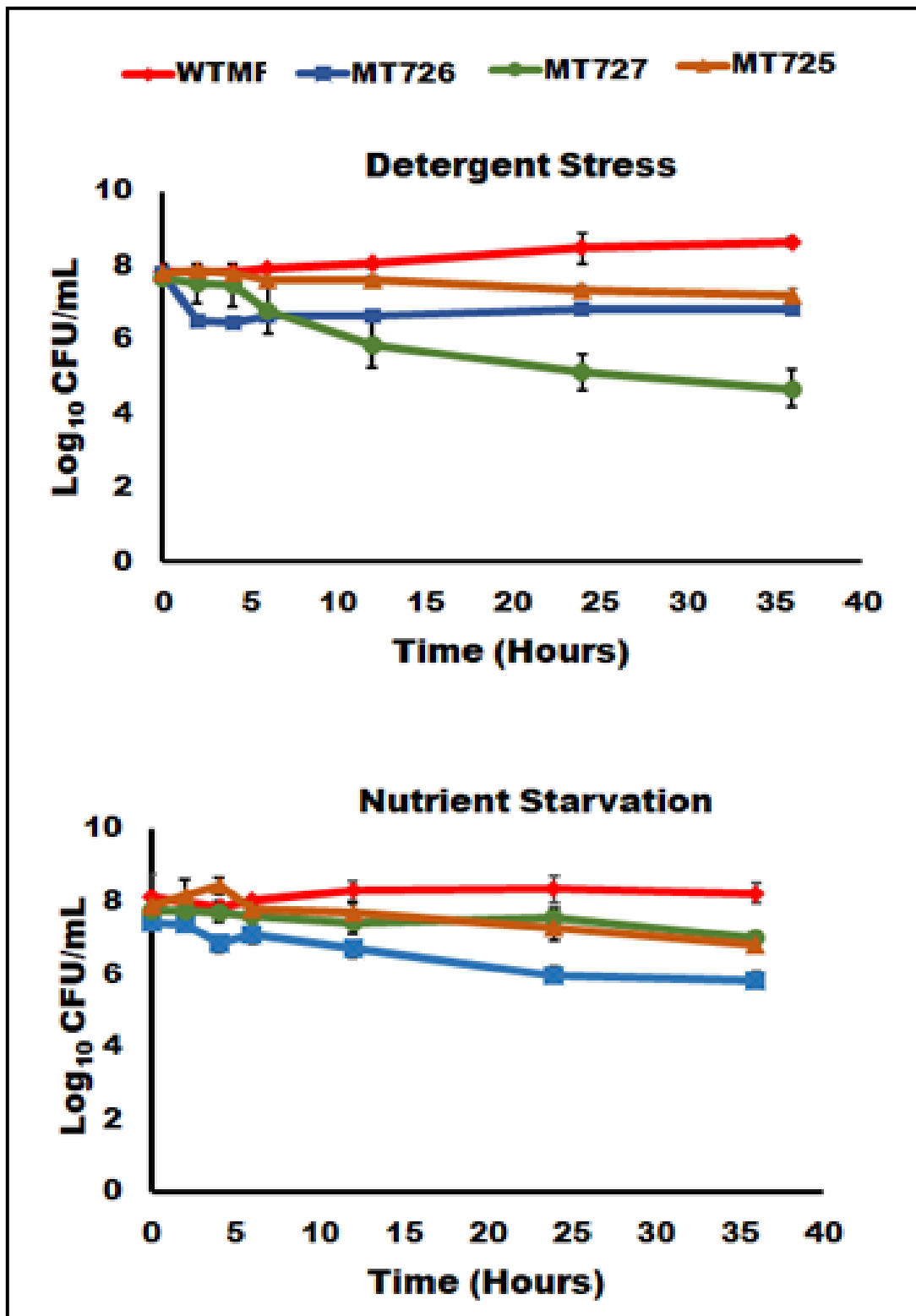


Figure 4.17: Growth kinetics of mutants under *in vitro* detergent stress and nutrient starvation conditions. Under *in vitro* detergent stress, mutant MT727 showed a 3 log decrease in CFU in comparison to wild type *M. fortuitum* (WTMF). Under nutrient starvation, constant growth behavior was observed in all mutants except mutant MT726 which showed 1.6 log reduction post 36 hours from initial CFU. [Data shows a mean of three independent experiments with standard deviation in error bars].

4.2.2.5 Mutants showed sensitivity to *in vitro* hypoxic stress

Under hypoxic stress, WTMF showed maintenance of constant CFU during the observation period of 27 days, indicating its ability to persist under *in vitro* hypoxic stress conditions. However, the mutants showed a deviation in growth behavior in comparison to the WTMF (Figure 4.18).

After nine days of stress, mutant MT726 showed a reduction of 3.5 log from its initial CFU under *in vitro* hypoxic stress conditions. The mutant showed stabilization of its growth till 15 days, however, it was unable to maintain its growth beyond 15 days. Mutant MT727 showed a decrease in 4.1 log CFU at 12 days observation point in comparison to its initial CFU. Mutant MT725 showed an inability to grow for an extended period of time under hypoxic stress conditions and was unable to sustain beyond 9 days.

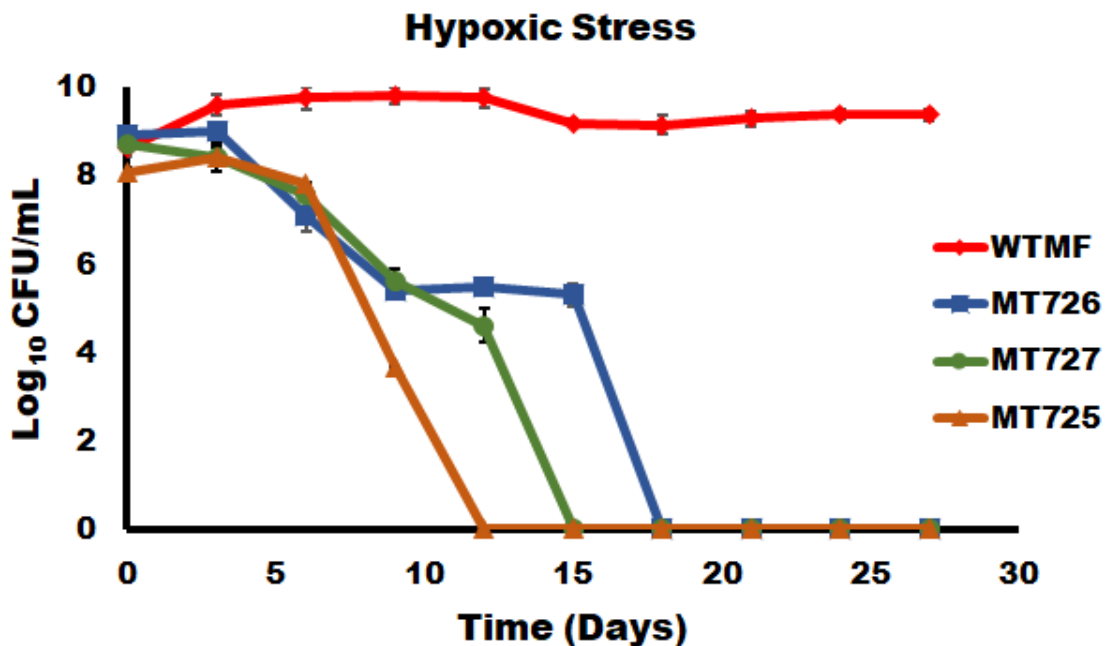


Figure 4.18: Growth kinetics of mutants (MT726, MT727, and MT725) under *in vitro* hypoxic stress. The figure shows the inability of mutants to persist under *in vitro* hypoxic stress for long duration of time. [Data shows a mean of three independent experiments with standard deviation in error bars].

4.3 Structure Prediction, interaction and molecular docking studies to identify potential inhibitors

Mutant MT726, showed highest level of attenuation in mice infection model, hence the ORF mutated in MT726 i.e. Mfsdr was subjected to *in silico* structural and functional analyses followed by docking studies to identify potential inhibitors.

4.3.1 MfSdr showed the presence of transmembrane helix

M. fortuitum short-chain dehydrogenase (MfSdr) showed the presence of one N-terminal transmembrane helix in its amino acid sequence (114-132) from outside to inside orientation with a score of 626. A score above 500 is considered significant to indicate the presence of transmembrane helix (Figure 4.19).

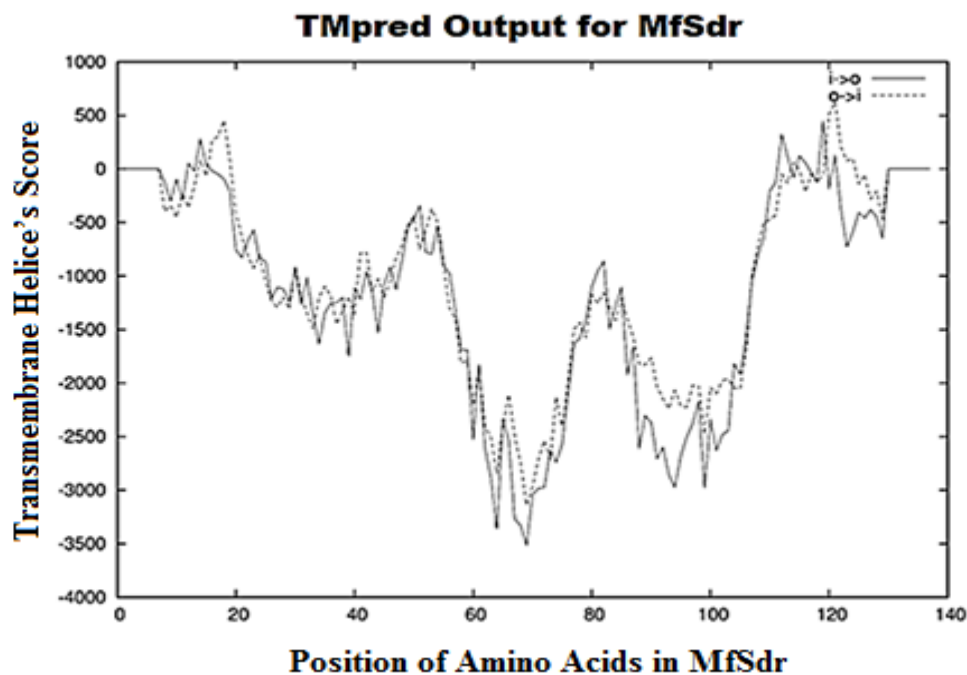


Figure 4.19: Transmembrane helix prediction in the amino acid sequence of *M. fortuitum* short-chain dehydrogenase (MfSdr). The X-axis shows position of amino acid, and Y-axis depicts the transmembrane helix's score. Score more than 500 is considered to have possible transmembrane helix. MfSdr shows the presence of a possible transmembrane helix between amino acid 114 to 132 (outside to inside orientation).

4.3.2 Short-chain dehydrogenase shows functional interaction with proteins involved in mycolic acid biosynthesis

Functional interactions of *M. tuberculosis* short-chain dehydrogenase Rv2509 (MfSdr homologue in *M. tuberculosis*) were majorly observed with proteins involved in mycolic acid biosynthesis. *M. tuberculosis* short-chain dehydrogenase Rv2509 interacting proteins includes probable conserved transmembrane protein Rv2709, polyketide synthase (pks13), putative inactive phenol phthiocerol synthesis polyketide synthase type I (pks1), probable conserved integral membrane leucine and alanine rich protein Rv2508, cyclopropane mycolic acid synthase 2 (cmaA2), long-chain-fatty-acid-AMP ligase (fadD32), trehalose monomycolate exporter (MmpL3), alpha-(1->3)-arabinofuranosyltransferase (aftC), probable conserved membrane protein Rv3802c, and uncharacterized oxidoreductase fabG2 (Figure 4.20). Functions of interacting proteins are provided in Table 4.3.

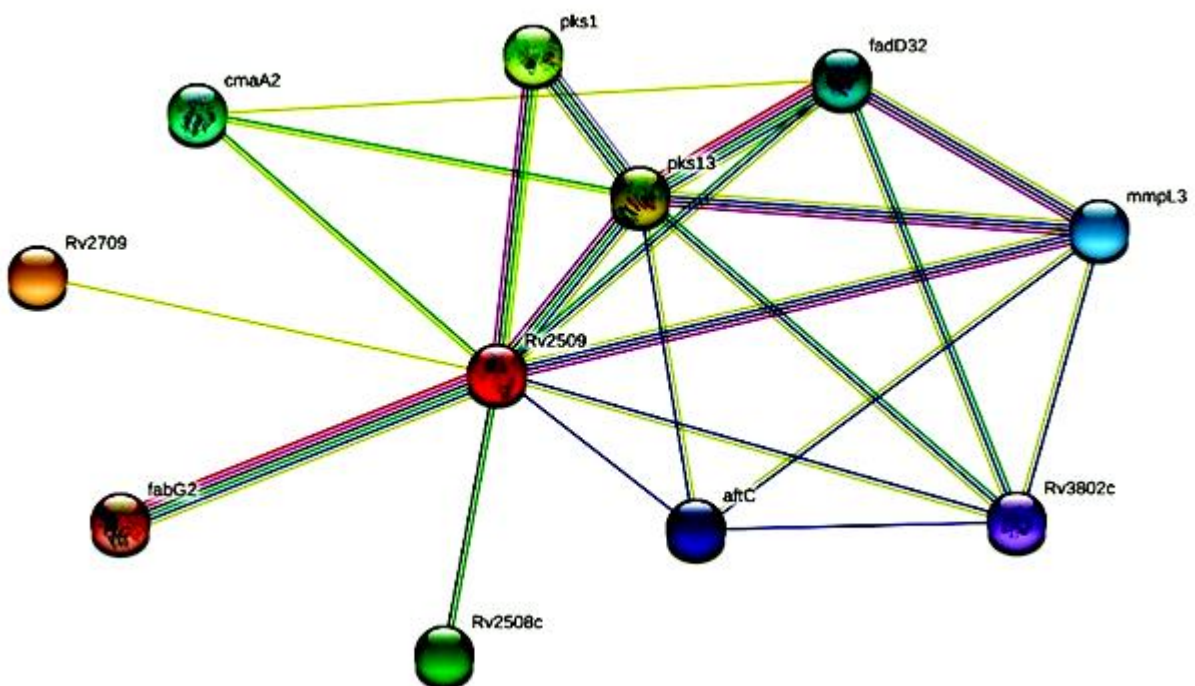


Figure 4.20: Protein-protein interaction studies of *M. tuberculosis* Rv2509, a homolog of *M. fortuitum* short-chain dehydrogenase (MfSdr) using STRING. The figure shows the interaction map of Rv2509 protein with Rv2709, pks13, pks1, Rv2508c, cmaA2, fadD32, mmpL3, aftC, Rv3802c and fabG2. Here, each node represents the proteins produced by a single protein-coding gene locus and edges represent specific and meaningful functional associations. The red-colored node represent query protein and the first shell of interacting proteins (proteins binding directly to input protein); empty nodes represent proteins of unknown 3D structures (Rv2709, Rv2508c, mmpL3, aftC) whereas filled nodes represents predicted 3D structure of protein (pks13,

pks1, cmaA2, fadD32, Rv3802c, and fabG2). Color of edges signifies the properties of interactions; where sky blue represents known interactions from curated databases, magenta indicates known interactions that are experimentally determined, green represents predicted interaction as protein neighborhood, blue shows predicted interaction as protein co-occurrence, lime shows data available from text mining, red shows predicted gene fusion and black shows co-expression of proteins.

Table 4.3: List of proteins interacting with *M. tuberculosis* Rv2509, a homolog of *M. fortuitum* short-chain dehydrogenase and their reported functions (as taken from Mycobrowser database <https://mycobrowser.epfl.ch>).

Gene Name	Encoded Proteins	Function
Rv2709	Probable conserved transmembrane protein	Unknown Function
pks13	Polyketide synthase	Final Steps of mycolic acid synthesis
pks1	Putative inactive phenolphthiocerol synthesis polyketide synthase type I	Phthiocerol biosynthesis
Rv2508c	Conserved integral membrane Protein	Unknown Function
cmaA2	Cyclopropane mycolic acid synthase 2	Mycolic acid synthesis
FadD32	Long-chain-fatty-acid-AMP ligase	Activation of long-chain fatty acids as acyl-adenylates (acyl-AMP) for further chain extension
mmpL3	Trehalose monomycolate exporter MmpL3	Transports trehalose monomycolate (TMM) across the inner membrane
aftC	Alpha-(1->3)-arabinofuranosyl Transferase	Involved in the biosynthesis of the arabinogalactan (AG) region of the mycolyl arabinogalactan-peptidoglycan (mAGP) complex
Rv3802c	Probable conserved membrane Protein	Lipid catabolism
fabG2	Uncharacterized oxidoreductase	Fatty acid biosynthesis pathway

4.3.3 Predicted secondary structure of MfSdr

Five models namely, model 1, model 2, model 3, model 4 and model 5 of MfSdr were obtained through Robetta. Root mean square deviation (RMSD) based structural analyses of

models, resulted in the rejection of model 1 and model 5, as these two structures showed more structural dissimilarity with other models. Model 2, model 3 and model 4 were further analyzed on the basis of RMSD with available mycobacterial short-chain dehydrogenase including *M. avium* carveol dehydrogenase (PDB ID: 5EJ2), *M. avium* carveol dehydrogenase bound to NAD (PDB ID: 3T7C), and *M. paratuberculosis* carveol dehydrogenase (PDB ID: 3PGX). Model 4 showed lowest RMSD value with 3T7C, and hence, considered as *M. fortuitum* short-chain dehydrogenase/reductase (MfSdr) structure.

Structural analysis of MfSdr protein showed the presence of two chains: chain A and chain B. Chain A and chain B were present as mirror images of each other, with both chains showing the presence of characteristic Rossmann fold. Rossmann fold in MfSdr structure consists of alternating seven parallel β -strands and eight α -helices; where β -strands form an extended β -sheet and α -helices surround both faces of the sheet (Figure 4.21).

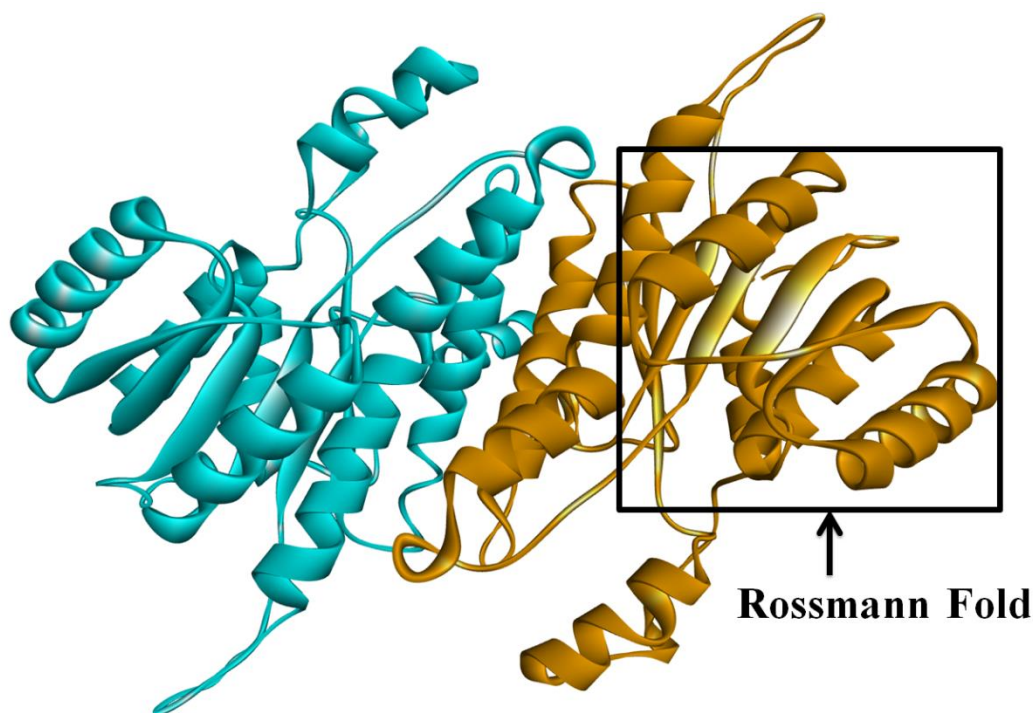


Figure 4.21: Secondary structure of *M. fortuitum* short-chain dehydrogenase (MfSdr). The figure shows presence of chain A (Blue) and chain B (brown) in the predicted secondary structure of MfSdr. Predicted MfSdr secondary structure shows the presence of characteristic Rossmann fold.

4.3.4 Potential inhibitors were identified against MfSdr through molecular docking studies

High throughput *in silico* screening of FDA approved drug library was done to determine their binding affinity with MfSdr. Tricyclazole, an inhibitor of *M. tuberculosis* short-chain dehydrogenase was taken as reference for docking analysis. The comparative binding energy of FDA approved drugs and inhibitors in the first round of docking resulted in shortlisting of 424 drugs to bind more efficiently than tricyclazole. The second round of docking of the shortlisted 424 drugs led to the identification of 118 drugs with better binding efficiency. Of these 118 molecules, the top five inhibitors with the lowest binding energy are proposed as potential inhibitors of MfSdr (Table 4.4). Visualization of interaction between ligand (drugs) and receptor (MfSdr) obtained from MegaMol are provided in Figure 4.22.

Table 4.4: Potential inhibitors of *M. fortuitum* short-chain dehydrogenase (MfSdr) identified by virtual screening using Autodock version 4.2.6. The table shows Ergocalciferol, Tacrolimus, Paricalcitol, Doxercalciferol and Ursodeoxycholic acid with better binding affinity in comparison to tricyclazole (reference inhibitor) based on binding energy scores of docked structures.

ZINC ID	Common name	Binding Energy (Kcal/mol)
ZINC000004629876fda	Ergocalciferol	-17.13
ZINC000169289411fda	Tacrolimus	-16.74
ZINC000013911941fda	Paricalcitol	-16.67
ZINC000004641374fda	Doxercalciferol	-16.47
ZINC000003914809fda	Ursodeoxycholic acid	-15.42
Tricyclazole	Reference	-6.08

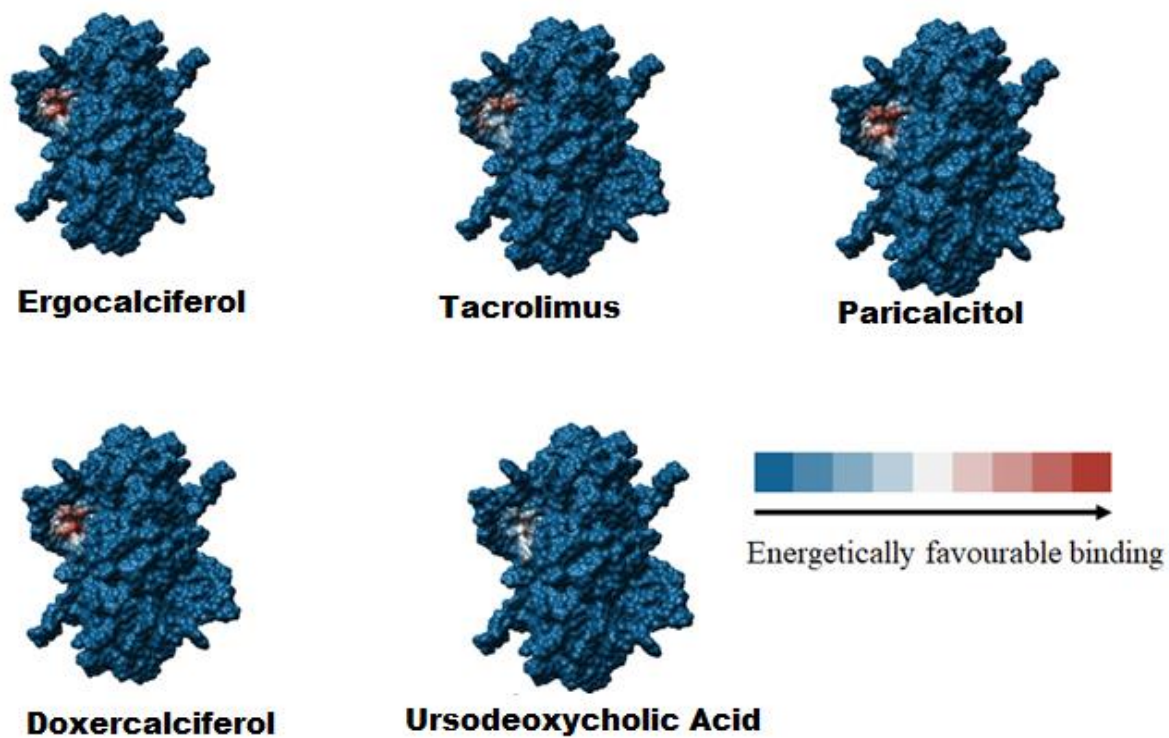


Figure 4.22: Visualization of ligand-receptor interactions using MegaMol. The figure shows ligand-receptor interaction based on energetically favorable binding. The color scale represents min 0 (blue) to max 68 (red) values based on minimum binding energy.

DISCUSSION

M. fortuitum is one of the most important pathogenic NTM with a diverse host range. It is responsible for a variety of infections including skin and soft tissue infections, bone infections, lymph node infections, blood born infections, eye infections, brain infections, etc. [3, 7]. Immunocompromised individuals are more sensitive to *M. fortuitum* infections [228], in addition, infections in immuno-competent individuals have also been well documented [229, 230]. Post-surgical infections such as keratitis, endocarditis, etc. due to *M. fortuitum* are prominent, which are majorly attributed to its biofilm forming capability [40].

NTM infections including *M. fortuitum* are increasing in an emerging trend, however, the absence of a standard diagnostic criteria makes these infections unreportable, especially in TB endemic countries [69, 231]. Increasing drug resistance of *M. fortuitum* leads to long term drug treatment, drug toxicity as well as increases the treatment cost [42]. Understanding of virulence of *M. fortuitum* will provide a foundation for the development of new drug targets against this pathogen. Information regarding virulence and mechanism of pathogenesis of *M. fortuitum* is very scarce, hence, identification of virulent genes of the bacteria would aid in the understanding of its pathogenesis, as well as developing effective drug targets against the infection in specific, and related pathogenic mycobacteria in general.

M. fortuitum is an intracellular pathogen and utilizes macrophages as its favorable niche for the establishment of infection [12, 232]. Macrophages, being defense cells of the body are equipped with an arsenal of multiple stress conditions to prevent the growth of a pathogen. Generation of reactive oxygen species and reactive nitrogen intermediates decrease in intracellular pH, presence of antimicrobial peptides, deprivation of nutrients, and increased intracellular temperature are the prevalent stress conditions inside macrophages [233]. In *M. tuberculosis*, many genes have been identified which play an essential role in survival under different stress conditions prevalent inside the host [233] (Table 5.1).

Table 5.1: *M. tuberculosis* genes involved in survival under stress conditions [233]. The table shows a list of genes involved in survival of *M. tuberculosis* under respective stress conditions.

Type of Stress	Gene involved in stress response
Acidic Stress	Rv3671c, Rv2224c, Rv2136c, ponA2, mgtC, ompA
Oxidative Stress	katG, sodA, sodC, mel2
Nutrient Starvation	relA
Cell Membrane Stress	whiB3, kasB
Hypoxic Stress	dosS/dosT/dosR

The ability of *M. fortuitum* to resist stress conditions prevalent inside macrophages highlights its virulence potential.

Bacterial cell membrane protein play a crucial role in interaction and invasion of the host cell, hence, are imperative for virulence of bacteria. In addition, these proteins are involved in various vital processes such as transport of nutrients, cellular communication, signaling, etc. Resistance to various unfavorable conditions is also provided by membrane proteins [234, 235]. Hence, functional and physically intact cell membrane proteins are essential for the survival of bacteria. Changes in the membrane or surface proteins of pathogenic mycobacteria modulate its fluidity, permeability, and antigenicity, and thus affects the resistance of mycobacterial pathogens to various stress conditions [233]. Knowledge regarding implication of mycobacterial membrane proteins led to the discovery of successful antibacterial agents, which inhibit membrane proteins and halt the growth of mycobacterial cells [145], elucidating the role of membrane proteins as a potential drug target(s). Thus, the present study was carried out with an aim to identify *M. fortuitum* membrane proteins involved in virulence of the bacteria, which might be used for the development of new drugs as treatment for *M. fortuitum* infections.

Transposon mutagenesis a valuable tool for understanding the essentiality of any gene for a specific phenotype. The technique has been successfully applied for the identification of virulent genes in bacterial pathogens like *M. tuberculosis* [236], *M. marinum* [20], *Salmonella* spp. [237, 238], *Staphylococcus aureus* [239, 240], *Vibrio cholerae* [241, 242], and

Streptococcus pneumoniae [243, 244]. Leucine responsive protein-encoding gene *lrp* was identified in *M. fortuitum* to play a role in virulence [14].

TnphoA based transposon mutagenesis is one of the important techniques used for the characterization of membrane protein-encoding genes of bacteria as it contains a reporter alkaline phosphatase (*phoA*) gene. The expression of *phoA* can be observed visually due to the blue color of mutants with transposon insertion in membrane protein-encoding genes, on selection plates containing XP, a substrate of alkaline phosphatase [17].

In the present study, a library of about 5000 mutants was constructed by TnphoA based transposon mutagenesis. Primary screening based on the determination of the phenotypic presence of alkaline phosphatase in mutants, due to their blue color formation on selection plates led to the identification of 186 mutants, with a transposon insertion in membrane protein-encoding genes. Secondary screening of the 186 mutants based on biochemical quantitative alkaline phosphatase assay led to shortlisting of twenty mutants with high alkaline phosphatase activity. Considering the approval of a limited number of mice by the Institutional Animal Ethics Committee (IAEC), six mutants (MT721, MT723, MT724, MT725, MT726, and MT727) with the highest alkaline phosphatase activity were selected for the study of their virulence potential using a murine infection model.

The ability of *M. fortuitum* to cause acute as well as chronic infection in a mouse model has been described previously by Parti et al. [14]. Characteristic features of *M. fortuitum* infection in the form of nephritis, following the intravenous route of inoculation were reproduced in the present study as described previously [14]. Symptoms including restlessness, weight loss, neck tilting, and spinning movement of the head were observed. Wild type *M. fortuitum* showed maintenance of bacillary burden in kidney tissues until 25 days PI, which indicates the ability of *M. fortuitum* to maintain the infection. Mutant MT726 showed virulence attenuation as reduced bacillary load was observed at 10 days PI followed by clearance of infection at 25 days PI. Mutant MT725 and MT727 showed attenuation at later stage of infection as reduced bacillary load was observed at 25 days PI. Thus, from bacillary load determination, three mutants (MT726, MT725, and MT727) with virulence attenuation were observed.

The other three mutants namely MT721, MT723, and MT724 did not show any deviation in their pathogenesis in comparison to wild type in terms of observed symptoms and bacillary load. As no attenuation was observed, these three mutants were not subjected to further analysis.

The presence of cytokines in blood serum indicates the level of immune response generated by pathogen. Pro-inflammatory cytokines such as IFN- γ , TNF- α , and IL-12 indicate inflammation and tissue damage. Whereas, anti-inflammatory cytokines such as IL-10 and TGF- β act as regulators of pro-inflammatory cytokines and hence prevent excessive tissue damage [245]. Analyses of blood serum cytokine concentration showed a lower concentration of pro-inflammatory cytokines (IFN- γ and TNF- α) in mutant MT726, MT725 and MT727, in comparison to the wild type during early stages of infection. The decreased level of IFN- γ in the mutant infected mice signifies reduced antigenic presentation of the bacteria to the host, as well as reduced T-cell activation. The results of decreased level of IFN- γ and TNF- α are similar to the study by Hu et al where a mutant defective in *GroEL* gene showed decreased expression of TNF- α and IFN- γ [246]. At a later stage of infection i.e. 25 days PI, reduction in pro-inflammatory cytokines in comparison to the early stage of infection was observed in both wild type as well as mutants. No appreciable difference was observed in serum IL-10 concentration of wild type and mutant infected mice, which is similar to a previous study, where mice showed similar IL-10 concentrations during the early stages of infection, in wild type as well as virulence attenuated mutant of sigE in *M. tuberculosis* [247].

Severity and progression of infection caused by *M. fortuitum* were analyzed through histopathology of kidney tissue, which showed nephritis, where destructive tissue pathology in the form of granulomatous structures and leukocyte infiltration was observed in mice tissue infected with wild type. Granuloma is an organized collection of inflammatory mononuclear cells infiltrate, which prevents the spread of infection by surrounding mycobacteria containing macrophages in the necrotic center. The presence of granulomatous structures following *M. fortuitum* infection has been described in previous studies [12, 14].

The histopathological study indicated more reduction in pathological damage in kidney tissue of mice infected with mutant MT726 followed by MT725, confirming virulence attenuation in

both of these mutants. Mutant MT727 showed tissue pathology similar to wild type, indicating no attenuation in its tissue damaging abilities.

In vivo virulence studies based on characteristic symptoms, tissue bacillary load, immunoprofiling and histopathology led to the identification of mutant MT726 showing a higher level of attenuation in virulence followed by mutant MT725 and MT727, in comparison to the wild type *M. fortuitum*. Attenuated mutants MT726, MT725 and MT727 were subjected to genomic and bioinformatics analyses to identify the mutated ORFs.

For genomic and bioinformatics analyses, the transposon inserted DNA segment of each mutant was cloned in pUC19 followed by sequencing. Protein sequences are more conserved in comparison to their corresponding nucleotide sequences. Hence, BLASTX, which translates nucleotide sequence into protein sequence, is a more sensitive tool for alignment in comparison to nucleotide BLAST (BLASTN) [248, 249]. Hence, the homology study of nucleotide sequences obtained after the sequencing of the mutants was done based on protein sequence alignment, using BLASTX to identify corresponding protein homologs.

These three mutants were further subjected to *in vitro* stress conditions to understand the probable role of identified ORFs in survival under such conditions. Role of identified ORFs in survival under stress conditions are discussed mutant wise in the following section.

Characterization of mutant MT726

Sequence similarity-based homology of nucleotide sequence obtained after cloning and sequencing of the TnphoA inserted segment of mutant MT726 showed its closest homology with short-chain dehydrogenase of *M. fortuitum* CT6 strain. Hence, the ORF/gene mutated in the mutant MT726 was identified as probable short-chain dehydrogenase of *M. fortuitum* ATCC 6841 (MfSdr) and submitted to GenBank (Accession ID: KY250516).

In vivo virulence studies showed a high level of attenuation by mutant MT726 in the murine infection model used for the present study. Hence, we propose a probable role of *M. fortuitum* short-chain dehydrogenase (Mfsdr) for *in vivo* survival and virulence of *M. fortuitum*. Findings can be correlated with previous studies, where, an association of short-chain

dehydrogenase with virulence was observed in *Burkholderia pseudomallei*, as a deletion mutant of short-chain dehydrogenase showed an inability to interact with the host cell [250].

To have an insight into the importance of MfSdr in survival under stress conditions prevalent inside the host, mutant MT726 was subjected to various *in vitro* stress conditions. The mutant showed susceptibility to *in vitro* acidic, nutrient starvation, and hypoxic stress conditions, indicating the role of MfSdr in combating these stress conditions. Discovery of a probable role of MfSdr in *M. fortuitum* corroborates with previous findings, where probable short-chain dehydrogenase (Rv2509) mutant in *M. tuberculosis* showed a reduced growth rate in comparison to the wild type [251]. Similar observations have been reported in *M. smegmatis* where Rv2509 homolog of *M. smegmatis* was found to be essential for its *in vitro* growth [252]. In *Pseudomonas aeruginosa*, short-chain dehydrogenase has been reported to be involved in biofilm formation [253].

Characterization of mutant MT725

Sequence similarity-based homology of nucleotide sequence obtained by cloning and sequencing of mutant MT725 identified two ORFs with the closest homology to anthranilate synthase component I and anthranilate synthase component II of *M. abscessus*. Hence, the two ORFs namely *M. fortuitum* anthranilate synthase component I (MftrpE) and anthranilate synthase component II (MftrpG) were identified to be mutated in the mutant MT725. Nucleotide sequences of MftrpE and MftrpG were submitted to GenBank (Accession ID: KY250521 and KY250520 respectively).

Anthranilate synthase component I (trpE) and component II (trpG) code for the anthranilate synthase complex in most bacterial species [254]. Genes trpE and trpG form a part of tryptophan operon which consists of anthranilate synthase component I (trpE) and component II (trpG); tryptophan synthase α subunit (trpA), tryptophan synthase β subunit (trpB), indole glycerol phosphate synthase (trpC), anthranilate phosphoribosyl transferase (trpD) and phosphoribosyl anthranilate isomerase (trpF). In the present study, we identified, *M. fortuitum* anthranilate synthase component I (MftrpE) and component II (MftrpG), which codes for anthranilate synthase (MfAS) of tryptophan operon to be mutated in mutant MT725.

Tryptophan operon is characterized by genetic organization either in the form of gene overlap or gene fusion in bacteria [227]. Analyses of nucleotide sequences of MftrpE and MftrpG revealed the presence of overlap of 'ATGA' between these two ORFs, indicating genetic organization in the form of gene overlap. The presence of overlap between trpE and trpG has also been reported in *Streptococcus pneumoniae*, *Staphylococcus aureus*, *Campylobacter jejuni* and *Corynebacterium glutamicum* [227]. In addition, the overlap between trpE and trpD has also been documented in *Bacillus subtilis*, *Nitrosomonas europaea*, *Ralstonia metallidurans* and *Coxiella burnetii* [227, 255].

The requirement of the tryptophan operon in the virulence of intracellular pathogens including *M. tuberculosis*, *Francisella tularensis*, and *Chlamydia trachomatis* has been reviewed by Olive and Sasseti [256]. Generation of tryptophan starvation conditions through immune response inside the host highlights the need for *de novo* tryptophan biosynthesis by the pathogens to cause infection [257, 258].

Attenuation of virulence shown by a trpE deletion mutant of *M. tuberculosis* has been demonstrated previously [259, 260] which can be co-related with our results showing attenuation of virulence in MT725. Mutations in the tryptophan synthesis gene in *Klebsiella pneumoniae* [261] and *M. tuberculosis* renders the pathogen incapable of causing infection in mice [260].

Mutant MT725 showed a growth defect under acidic and hypoxic stress conditions. The limited growth of trpE deletion mutant of pathogenic *M. tuberculosis* inside macrophages highlights the potential role of trpE gene in survival under stress conditions prevalent inside macrophages [259]. Based on the growth defect observed under acidic stress conditions in mutant MT725, MfAS might play a role in survival under acidic stress in *M. fortuitum*, which can also be correlated with the study showing upregulation of trpE under acidic stress in *M. avium* subspecies *paratuberculosis* [262]. Glutamate is formed as a co-product by a reaction catalyzed by anthranilate synthase complex in tryptophan operon, and conversion of glutamate to ammonia can help in neutralization of acidic stress [263, 264]. Thus, the formation of glutamate by MfAS might be a mechanism by which it provides resistance to *M. fortuitum* under acidic stress environment. The role of tryptophan synthesizing genes has not yet been reported under *in vitro* hypoxic stress conditions, and to the best of our knowledge,

this is the first report showing growth defect under *in vitro* hypoxic stress conditions in *M. fortuitum*.

Characterization of mutant MT727

Sequence similarity-based homology of nucleotide sequence obtained by cloning and sequencing of mutant MT727 identified, closest homology with ribosomal maturation factor rimP of *M. abscessus*. Hence, the nucleotide sequence found to be mutated in mutant MT726 was identified as probable ribosomal maturation factor of *M. fortuitum* ATCC 6841 (MfRimP) and submitted to GenBank (Accession ID: MH052677).

Ribosomal maturation factor RimP plays an important role in the central metabolism of bacteria. It helps in the biogenesis of the 30S ribosomal subunit, an essential component required for bacterial protein synthesis [265]. Ribosomal maturation factors RimM and RimP are required during the early and late stages of ribosomal maturation, respectively [266]. The work done previously [267] showed reduced growth of RimM deletion mutant under normal growth conditions, which signifies the essentiality of ribosomal maturation factors for the growth of bacteria. RimP has been reported to increase the affinity of 30S ribosomal protein s12 (RpsL) with 16S rRNA in *M. smegmatis*, which is a major step in the 30S ribosomal subunit biogenesis [268]. The defect in the 30S ribosomal subunit can modulate the mRNA decoding efficiency of the ribosome and may result in a defective translation. Significance of RimP has been known in other bacterial genera as well, where a smaller number of polysomes were observed in rimP deletion mutant of *E. coli* as compared to the wild type leading to a translation deficient phenotype [269].

Although rimP gene has not been explored for virulence related studies, Chu et al. hypothesized rimP as a drug target in *M. tuberculosis* by studying rimP gene behavior in *M. smegmatis* [270] which is used as a model organism for studies related to tuberculosis virulence. Kolker et al. also suggested rimP gene involvement in other molecular processes including DNA unbinding in *Haemophilus influenza* [271].

Under stress conditions including acidic stress, translational variations occur in most pathogenic bacteria that are required for survival of the organism. RimP deletion mutant of *M. smegmatis* was unable to survive under nitrosative stress suggesting the requirement of rimP

under stress condition for protein synthesis [268]. Significance of ribosomal maturation factors under stress conditions has also been established in *E. coli* where delay in ribosomal assembly or defective ribosomal maturation leads to heat-sensitive [265], and cold-sensitive phenotype of *E. coli* [272], respectively. As rimP is involved in the maturation of the 30S ribosomal subunit [265], the mutation in rimP gene of *M. fortuitum* may lead to fewer polysomes formation under acidic stress conditions. Thus, reduction in the translation of proteins essential for survival under acidic stress might be the reason for an acid susceptible phenotype of MT727 due to rimP inactivation. However, the mutant did not show any appreciable deviation in its growth behavior under oxidative, nutrient starvation and heat stress conditions indicating a lack of essentiality of rimP gene for survival under these stress conditions in *M. fortuitum*.

Computational analysis of most potent ORF Mfsdr

The mutant MT726 showed high level of attenuation in animal infection model. The gene found to be mutated in mutant MT726 i.e. Mfsdr, was further characterized using computational approaches for identification of potential inhibitors of the corresponding protein MfSdr.

TMPRED program makes prediction of membrane-spanning regions and their orientation based on the statistical analysis of TMbase, a database of naturally occurring transmembrane proteins [273]. The presence of one transmembrane helix was observed in the MfSdr amino acid sequence. Hence, we can safely propose that MfSdr may be a membrane protein of *M. fortuitum*, an expected outcome concomitant with our objective to identify membrane proteins.

Short-chain dehydrogenases/reductases (SDRs) constitute a large family of NADP(H)-dependent oxidoreductases. SDR enzymes have critical roles in lipid, amino acid, carbohydrate, cofactor, hormone, and xenobiotic metabolism as well as in redox sensor mechanisms [274]. The structure of MfSdr was predicted using the Robetta server, which provides automated tools for prediction and analysis of protein structures. The predicted structure shows the presence of MfSdr in the form of a dimer, where each chain contains a Rossmann fold. Rossmann fold is a characteristic feature of short-chain dehydrogenase family which provides nucleotide binding site for completion of an enzymatic reaction. The presence

of Rossmann fold in MfSdr structure indicates the accuracy of the structure predicted by Robetta in our study.

To predict the probable function of *M. fortuitum* short-chain dehydrogenase (MfSdr) identified in the present study, a protein-protein functional interaction map was generated using STRING. *M. fortuitum* database is not available in STRING, hence, based on MfSdr amino acid sequence similarity with *M. tuberculosis* short-chain dehydrogenase Rv2509 in STRING, Rv2509 was used for prediction of the functional interaction map.

Rv2509 showed interaction predominantly with genes involved in the synthesis of mycolic acid. Mycolic acid is one of the important virulent factors of genus mycobacteria, which provides resistance towards various stress conditions, helps in host immune response evasion and provides resistance to mycobacteria against hydrophilic antibiotics [29]. Hence, the extrapolation of results to deduce the functional significance of MfSdr predicts it to be involved in the mycolic acid synthesis of *M. fortuitum*. In *Corynebacterium glutamicum*, a homolog of Rv2509 has been reported to function as mycolate reductase, which is required for the last step in mycolic acid synthesis [275]. Thus, we can propose that MfSdr may function as mycolate reductase in *M. fortuitum* which can be an important virulent factor for the bacilli.

Virtual screening has recently emerged as a powerful technique complementing traditional High Throughput Screening (HTS) technologies. Virtual screening can be broadly defined as the use of computational analyses of a database of chemical structures to identify possible drug candidates for a specific pharmaceutical target, often a particular enzyme or receptor [276]. The functional association of MfSdr with mycolic acid synthesis characterizes this protein as an important drug target against *M. fortuitum* infections, hence, MfSdr was subjected to virtual screening using molecular docking for identification of potential inhibitors for MfSdr. Virtual screening of predicted MfSdr structure led to the identification of Ergocalciferol, Tacrolimus, Paricalcitol, Doxercalciferol and Ursodeoxycholic acid as the top five potential inhibitors, based on most energetically favorable binding positions with MfSdr. The identified potential inhibitors can be exploited for *in vitro* and *in vivo* growth inhibition assays against *M. fortuitum* as well as other related mycobacterial species.

CONCLUSION AND FUTURE PROSPECTS

Animal infections studies, followed by genomic and computational analyses of a transposon mutant library led to the identification of four ORFs of *M. fortuitum* to be involved in its virulence, namely, short-chain dehydrogenase (MfSdr) in mutant MT726, anthranilate synthase component I (MfTrpE), and component II (MfTrpG) in mutant MT725, and ribosomal maturation factor (MfRimP) in mutant MT727. Sequences of the novel identified ORFs were submitted to GenBank.

In vitro stress studies were performed to get an insight into the underlying mechanism that may be responsible for the attenuated phenotype of the mutants. Short-chain dehydrogenase was required for growth under acidic stress, hypoxic stress, and nutrient starvation conditions. ORFs encoding components of Anthranilate synthase were essential for the endurance of *M. fortuitum* to acidic and hypoxic stress conditions, while RimP was found to be required for survival under acidic, detergent, and hypoxic stress. Molecular modeling and docking studies were carried out for the most potent ORF, MfSdr, considering it as a viable drug target.

Thus, the study identified four novel ORFs to be involved in *M. fortuitum* virulence, which may act as potential drug target(s) against the infection. Identification of corresponding homologs of the mutated ORFs in other members of the Mycobacterium family and other intracellular pathogens may lead to the identification and development of new drug targets against these pathogens, fueling the drug discovery efforts in this area.

The proposed inhibitors can be tested through *in vitro* and *in vivo* assays for development as potential lead molecules against *M. fortuitum* infections. The other identified ORFs can also be analyzed on similar lines through *in silico* approaches for prediction of three-dimensional protein structure and subsequent identification of potential inhibitors. The role of four ORFs in virulence of *M. fortuitum* has been suggested by our study, however further studies including gene complementation may be carried out to further validate their role. Furthermore, the prepared *M. fortuitum* transposon mutant library may be utilized to study other phenotypes of bacteria.

REFERENCES

- [1] R. S. Gupta, B. Lo, and J. Son, "Phylogenomics and comparative genomic studies robustly support division of the genus *Mycobacterium* into an emended genus *Mycobacterium* and four novel genera," *Frontiers in Microbiology*, vol. 9, p. 67, 2018.
- [2] T. S. Hermansen, P. Ravn, E. Svensson, and T. Lillebaek, "Nontuberculous mycobacteria in Denmark, incidence and clinical importance during the last quarter-century," *Scientific reports*, vol. 7, p. 6696, 2017.
- [3] A. Maurya, V. Nag, S. Kant, R. Kushwaha, M. Kumar, A. Singh, *et al.*, "Prevalence of nontuberculous mycobacteria among extrapulmonary tuberculosis cases in tertiary care centers in Northern India," *BioMed Research International*, vol. 2015, 2015.
- [4] S. Fatima and N. Aleemuddin, "Prevalence of nontuberculous Mycobacterial infection in Non-HIV subjects of clinically presumed tuberculosis at a tertiary care center, Hyderabad," *IP International Journal of Medical Microbiology and Tropical Diseases*, vol. 5, pp. 116-122, 2019.
- [5] W. Hoefsloot, J. Van Ingen, C. Andrejak, K. Ängeby, R. Bauriaud, P. Bemer, *et al.*, "The geographic diversity of nontuberculous mycobacteria isolated from pulmonary samples: an NTM-NET collaborative study," *European Respiratory Journal*, vol. 42, pp. 1604-1613, 2013.
- [6] R. Raveendran, J. K. Oberoi, and C. Wattal, "Multidrug-resistant pulmonary & extrapulmonary tuberculosis: A 13 years retrospective hospital-based analysis," *The Indian Journal of Medical Research*, vol. 142, p. 575, 2015.
- [7] J. Umrao, D. Singh, A. Zia, S. Saxena, S. Sarsaiya, S. Singh, *et al.*, "Prevalence and species spectrum of both pulmonary and extrapulmonary nontuberculous mycobacteria isolates at a tertiary care center," *International Journal of Mycobacteriology*, vol. 5, pp. 288-293, 2016.
- [8] S. Macente, C. Helbel, S. F. R. Souza, V. L. D. Siqueira, R. A. F. Padua, and R. F. Cardoso, "Disseminated folliculitis by *Mycobacterium fortuitum* in an immunocompetent woman," *Anais Brasileiros de Dermatologia*, vol. 88, pp. 102-104, 2013.
- [9] P. Chetchotisakd, P. Mootsikapun, S. Anunnatsiri, K. Jirattanapochai, C. Choonhakarn, A. Chaiprasert, *et al.*, "Disseminated infection due to rapidly growing

- mycobacteria in immunocompetent hosts presenting with chronic lymphadenopathy: a previously unrecognized clinical entity," *Clinical Infectious Diseases*, vol. 30, pp. 29-34, 2000.
- [10] S.-C. Tsai, L.-H. Chen, H.-H. Liao, C.-Y. Chiang, W.-L. Lin, S.-C. Chen, *et al.*, "Complicated skin and soft tissue infection with *Mycobacterium fortuitum* following excision of a sebaceous cyst in Taiwan," *The Journal of Infection in Developing Countries*, vol. 10, pp. 1357-1361, 2016.
- [11] K. Sharma, N. Gautam, M. Sharma, M. Dogra, P. Bajgai, B. Tigari, *et al.*, "Ocular mycobacteriosis—dual infection of *M. tuberculosis* complex with *M. fortuitum* and *M. bovis*," *Journal of Ophthalmic Inflammation and Infection*, vol. 7, p. 2, 2017.
- [12] T. R. M. da Silva, J. R. de Freitas, Q. C. Silva, C. P. Figueira, E. Roxo, S. C. Leao, *et al.*, "Virulent *Mycobacterium fortuitum* restricts NO production by a gamma interferon-activated J774 cell line and phagosome-lysosome fusion," *Infection and Immunity*, vol. 70, pp. 5628-5634, 2002.
- [13] O. H. Vandal, C. F. Nathan, and S. Ehrt, "Acid resistance in *Mycobacterium tuberculosis*," *Journal of Bacteriology*, vol. 191, pp. 4714-4721, 2009.
- [14] R. Parti, R. Shrivastava, S. Srivastava, A. Subramanian, R. Roy, B. S. Srivastava, *et al.*, "A transposon insertion mutant of *Mycobacterium fortuitum* attenuated in virulence and persistence in a murine infection model that is complemented by Rv3291c of *Mycobacterium tuberculosis*," *Microbial Pathogenesis*, vol. 45, pp. 370-376, 2008.
- [15] S. Sood, A. Yadav, and R. Shrivastava, "*Mycobacterium aurum* is Unable to Survive *Mycobacterium tuberculosis* latency associated stress conditions: Implications as non-suitable model organism," *Indian Journal of Microbiology*, vol. 56, pp. 198-204, 2016.
- [16] R. Koebnik, K. P. Locher, and P. Van Gelder, "Structure and function of bacterial outer membrane proteins: barrels in a nutshell," *Molecular Microbiology*, vol. 37, pp. 239-253, 2000.
- [17] R. K. Taylor, V. L. Miller, D. B. Furlong, and J. J. Mekalanos, "Use of *phoA* gene fusions to identify a pilus colonization factor coordinately regulated with cholera toxin," *Proceedings of the National Academy of Sciences*, vol. 84, pp. 2833-2837, 1987.

- [18] X. Wang, H. Wang, and J. Xie, "Genes and regulatory networks involved in persistence of *Mycobacterium tuberculosis*," *Science China Life Sciences*, vol. 54, pp. 300-310, 2011.
- [19] G. Majumdar, R. Mbau, V. Singh, D. F. Warner, M. S. Dragset, and R. Mukherjee, "Genome-wide transposon mutagenesis in *Mycobacterium tuberculosis* and *Mycobacterium smegmatis*," in *In Vitro Mutagenesis*, ed: Springer, 2017, pp. 321-335.
- [20] K. M. Ruley, J. H. Ansede, C. L. Pritchett, A. M. Talaat, R. Reimschuessel, and M. Trucksis, "Identification of *Mycobacterium marinum* virulence genes using signature-tagged mutagenesis and the goldfish model of mycobacterial pathogenesis," *FEMS Microbiology Letters*, vol. 232, pp. 75-81, 2004.
- [21] M. Jankute, J. A. Cox, J. Harrison, and G. S. Besra, "Assembly of the mycobacterial cell wall," *Annual Review of Microbiology*, vol. 69, pp. 405-423, 2015.
- [22] A. Bernardet and J. Bowman, "Bergey's manual of systematics of archaea and bacteria," ed: John Wiley & Sons, New York, 2015, pp. 1-75.
- [23] H. David, "Carotenoid pigments of the mycobacteria," *The Mycobacteria: A Source Book, Part A. Marcel Dekker. New York, NY*, pp. 537-545, 1984.
- [24] K. J. Kieser and E. J. Rubin, "How sisters grow apart: mycobacterial growth and division," *Nature Reviews Microbiology*, vol. 12, pp. 550-562, 2014.
- [25] E. C. Hett and E. J. Rubin, "Bacterial growth and cell division: a mycobacterial perspective," *Microbiology and Molecular Biology Reviews*, vol. 72, pp. 126-156, 2008.
- [26] V. Nataraj, C. Varela, A. Javid, A. Singh, G. S. Besra, and A. Bhatt, "Mycolic acids: deciphering and targeting the A chilles' heel of the tubercle bacillus," *Molecular Microbiology*, vol. 98, pp. 7-16, 2015.
- [27] S. Buckwalter, S. Olson, B. Connelly, B. Lucas, A. Rodning, R. Walchak, *et al.*, "Evaluation of matrix-assisted laser desorption ionization–time of flight mass spectrometry for identification of mycobacterium species, nocardia species, and other aerobic Actinomycetes," *Journal of Clinical Microbiology*, vol. 54, pp. 376-384, 2016.
- [28] L. Zhu, J. Zhong, X. Jia, G. Liu, Y. Kang, M. Dong, *et al.*, "Precision methylome characterization of *Mycobacterium tuberculosis* complex (MTBC) using PacBio single-molecule real-time (SMRT) technology," *Nucleic Acids Research*, vol. 44, pp. 730-743, 2015.

- [29] M. A. Forrellad, L. I. Klepp, A. Gioffré, J. Sabio y Garcia, H. R. Morbidoni, M. D. L. P. Santangelo, *et al.*, "Virulence factors of the Mycobacterium tuberculosis complex," *Virulence*, vol. 4, pp. 3-66, 2013.
- [30] S. Niemann, E. Richter, and S. Rüsç-Gerdes, "Differentiation among members of the Mycobacterium tuberculosis complex by molecular and biochemical features: evidence for two pyrazinamide-susceptible subtypes of M. bovis," *Journal of Clinical Microbiology*, vol. 38, pp. 152-157, 2000.
- [31] I. Smith, "Mycobacterium tuberculosis pathogenesis and molecular determinants of virulence," *Clinical Microbiology Reviews*, vol. 16, pp. 463-496, 2003.
- [32] P. Nguipdop-Djomo, E. Heldal, L. C. Rodrigues, I. Abubakar, and P. Mangtani, "Duration of BCG protection against tuberculosis and change in effectiveness with time since vaccination in Norway: a retrospective population-based cohort study," *The Lancet Infectious Diseases*, vol. 16, pp. 219-226, 2016.
- [33] K. Zaman, "Tuberculosis: a global health problem," *Journal Of Health, Population, and Nutrition*, vol. 28, p. 111, 2010.
- [34] <https://apps.who.int/iris/bitstream/handle/10665/329368/9789241565714-eng.pdf?ua=1/> (Last accessed: 29 December, 2019)
- [35] L. Nguyen and J. Pieters, "Mycobacterial subversion of chemotherapeutic reagents and host defense tactics: challenges in tuberculosis drug development," *Annual Review of Pharmacology and Toxicology*, vol. 49, pp. 427-453, 2009.
- [36] S. Pahari, G. Kaur, S. Negi, M. Aqdas, D. K. Das, H. Bashir, *et al.*, "Reinforcing the functionality of mononuclear phagocyte system to control tuberculosis," *Frontiers in Immunology*, vol. 9, p. 193, 2018.
- [37] B. Saviola, "Mycobacterium tuberculosis adaptation to survival in a human host," in *Tuberculosis-Current Issues in Diagnosis and Management*, ed: InTech, 2013.
- [38] G. Delogu, M. Sali, and G. Fadda, "The biology of Mycobacterium tuberculosis infection," *Mediterranean Journal Of Hematology and Infectious Diseases*, vol. 5, 2013.
- [39] J. O. Falkinham III, "Ecology of nontuberculous mycobacteria—where do human infections come from?," in *Seminars in Respiratory and Critical Care Medicine*, vol. 34, pp. 095-102, 2013.
- [40] M. S. Phillips and C. F. Von Reyn, "Nosocomial infections due to nontuberculous mycobacteria," *Clinical Infectious Diseases*, vol. 33, pp. 1363-1374, 2001.

- [41] A. H. Lewis and J. O. Falkinham III, "Microaerobic growth and anaerobic survival of *Mycobacterium avium*, *Mycobacterium intracellulare* and *Mycobacterium scrofulaceum*," *International Journal of Mycobacteriology*, vol. 4, pp. 25-30, 2015.
- [42] J. O. Falkinham III, "Challenges of NTM drug development," *Frontiers in Microbiology*, vol. 9, 2018.
- [43] R. J. Archuleta, P. Y. Hoppes, and T. P. Primm, "*Mycobacterium avium* enters a state of metabolic dormancy in response to starvation," *Tuberculosis*, vol. 85, pp. 147-158, 2005.
- [44] I. M. Orme and D. J. Ordway, "Host response to nontuberculous mycobacterial infections of current clinical importance," *Infection and Immunity*, vol. 82, pp. 3516-3522, 2014.
- [45] J. Honda, R. Viridi, and E. D. Chan, "Global environmental nontuberculous mycobacteria and their contemporaneous man-made and natural niches," *Frontiers in Microbiology*, vol. 9, 2018.
- [46] E. H. Runyon, "Anonymous mycobacteria in pulmonary disease," *Medical Clinics of North America*, vol. 43, pp. 273-290, 1959.
- [47] N. Gcebe, V. Rutten, N. C. Gey van Pittius, and A. Michel, "Prevalence and distribution of non-tuberculous mycobacteria (NTM) in cattle, african buffaloes (*syncerus caffer*) and their environments in South Africa," *Transboundary and Emerging Diseases*, vol. 60, pp. 74-84, 2013.
- [48] S. Malama, M. Munyeme, S. Mwanza, and J. B. Muma, "Isolation and characterization of non tuberculous mycobacteria from humans and animals in Namwala District of Zambia," *BMC Research Notes*, vol. 7, p. 622, 2014.
- [49] M. M. Johnson and J. A. Odell, "Nontuberculous mycobacterial pulmonary infections," *Journal of Thoracic Disease*, vol. 6, p. 210, 2014.
- [50] E. Henkle, K. Hedberg, S. D. Schafer, and K. L. Winthrop, "Surveillance of extrapulmonary nontuberculous mycobacteria infections, Oregon, USA, 2007–2012," *Emerging Infectious Diseases*, vol. 23, p. 1627, 2017.
- [51] R. Narang, P. Narang, and D. Mendiratta, "Isolation and identification of nontuberculous mycobacteria from water and soil in Central India," *Indian Journal of Medical Microbiology*, vol. 27, p. 247, 2009.

- [52] W. J. Kheir, H. Sheheitli, M. Abdul Fattah, and R. N. Hamam, "Nontuberculous mycobacterial ocular infections: a systematic review of the literature," *BioMed Research International*, vol. 2015, 2015.
- [53] C. S. Haworth, J. Banks, T. Capstick, A. J. Fisher, T. Gorsuch, I. F. Laurenson, *et al.*, "British Thoracic Society guidelines for the management of non-tuberculous mycobacterial pulmonary disease (NTM-PD)," *Thorax*, vol. 72, pp. ii1-ii64, 2017.
- [54] A. I. Gardner, E. McClenaghan, G. Saint, P. S. McNamara, M. Brodlie, and M. F. Thomas, "Epidemiology of nontuberculous mycobacteria infection in children and young people with cystic fibrosis: analysis of UK cystic fibrosis registry," *Clin Infect Dis*, vol. 68, pp. 731-737, 2018.
- [55] D. Weill, C. Benden, P. A. Corris, J. H. Dark, R. D. Davis, S. Keshavjee, *et al.*, "A consensus document for the selection of lung transplant candidates: 2014—an update from the Pulmonary Transplantation Council of the International Society for Heart and Lung Transplantation," *Journal of Heart and Lung Transplant*, vol. 34, pp. 1-15, 2015.
- [56] H. Nyamogoba, G. Mbuthia, S. Mining, G. Kikuvu, R. Kikuvu, S. Mpoke, *et al.*, "HIV co-infection with tuberculous and non-tuberculous mycobacteria in western Kenya: challenges in the diagnosis and management," *African Health Sciences*, vol. 12, pp. 305-311, 2012.
- [57] N. M. Shah, J. A. Davidson, L. F. Anderson, M. K. Lalor, J. Kim, H. L. Thomas, *et al.*, "Pulmonary *Mycobacterium avium-intracellulare* is the main driver of the rise in non-tuberculous mycobacteria incidence in England, Wales and Northern Ireland, 2007–2012," *BMC Infectious Diseases*, vol. 16, p. 195, 2016.
- [58] J. E. Stout, W.-J. Koh, and W. W. Yew, "Update on pulmonary disease due to non-tuberculous mycobacteria," *International Journal of Infectious Diseases*, vol. 45, pp. 123-134, 2016.
- [59] M. J. Van der Werf, C. Ködmön, V. Katalinić-Janković, T. Kummik, H. Soini, E. Richter, *et al.*, "Inventory study of non-tuberculous mycobacteria in the European Union," *BMC Infectious Diseases*, vol. 14, p. 62, 2014.
- [60] A.-L. Roux, E. Catherinot, F. Ripoll, N. Soismier, E. Macheras, S. Ravilly, *et al.*, "Multicenter study of prevalence of nontuberculous mycobacteria in patients with cystic fibrosis in France," *Journal of Clinical Microbiology*, vol. 47, pp. 4124-4128, 2009.

- [61] M. Panagiotou, A. I. Papaioannou, K. Kostikas, M. Paraskeua, E. Velentza, M. Kanellopoulou, *et al.*, "The epidemiology of pulmonary nontuberculous mycobacteria: data from a general hospital in Athens, Greece, 2007–2013," *Pulmonary Medicine*, vol. 2014, 2014.
- [62] H. S. P. Pedro, A. G. V. Coelho, I. M. Mansur, A. C. Chiou, M. I. F. Pereira, N. C. U. Belotti, *et al.*, "Epidemiological and laboratorial profile of patients with isolation of nontuberculous mycobacteria," *International Journal of Mycobacteriology*, vol. 6, p. 239, 2017.
- [63] D. Nunes-Costa, S. Alarico, M. P. Dalcolmo, M. Correia-Neves, and N. Empadinhas, "The looming tide of nontuberculous mycobacterial infections in Portugal and Brazil," *Tuberculosis*, vol. 96, pp. 107-119, 2016.
- [64] K. G. C. de Mello, F. C. Q. Mello, L. Borga, V. Rolla, R. S. Duarte, E. P. Sampaio, *et al.*, "Clinical and therapeutic features of pulmonary nontuberculous mycobacterial disease, Rio de Janeiro, Brazil," *Emerging Infectious Diseases*, vol. 19, p. 393, 2013.
- [65] G. V. Gole, R. Set, N. Khan, and J. Shastri, "Drug susceptibility testing of rapidly growing mycobacteria in extrapulmonary tuberculosis," *Indian Journal of Tuberculosis*, vol. 63, pp. 119-122, 2016.
- [66] R. M. Paulose, J. Joseph, R. Narayanan, and S. Sharma, "Clinical and microbiological profile of non-tuberculous mycobacterial endophthalmitis—experience in a tertiary eye care centre in Southern India," *Journal of Ophthalmic Inflammation and Infection*, vol. 6, p. 27, 2016.
- [67] A. Rao, B. Wallang, T. R. Padhy, R. Mittal, and S. Sharma, "Dual infection by streptococcus and atypical mycobacteria following Ahmed Glaucoma valve surgery," in *Seminars in Ophthalmology*, vol. 28, pp. 233-235, 2013.
- [68] T. Sengupta, P. Das, and T. Saha, "Epidemiology and drug resistance of non tuberculous mycobacteria in India: a mini review," *Biostatistics and Biometrics Open Access Journal*, vol. 1, p. 555568, 2017.
- [69] P. Sharma, D. Singh, K. Sharma, S. Verma, S. Mahajan, and A. Kanga, "are we neglecting nontuberculous mycobacteria just as laboratory contaminants? Time to Reevaluate Things," *Journal of Pathogens*, vol. 2018, 2018.
- [70] S. Jain, M. M. Sankar, N. Sharma, S. Singh, and T. Chugh, "High prevalence of non-tuberculous mycobacterial disease among non-HIV infected individuals in a TB

- endemic country—experience from a tertiary center in Delhi, India," *Pathogens and Global Health*, vol. 108, pp. 118-122, 2014.
- [71] M. Thomas, J. A. D'Silva, A. J. Borole, and R. M. Chilgar, "Periprosthetic atypical mycobacterial infection in breast implants: a new kid on the block!," *Journal of Plastic, Reconstructive & Aesthetic Surgery*, vol. 66, pp. e16-e19, 2013.
- [72] K. Lahiri, J. Jena, and K. Pannicker, "*Mycobacterium fortuitum* infections in surgical wounds," *Medical journal, Armed Forces India*, vol. 65, p. 91, 2009.
- [73] S. Shenai, C. Rodrigues, and A. Mehta, "Time to identify and define non-tuberculous mycobacteria in a tuberculosis-endemic region," *The International Journal of Tuberculosis and Lung Disease*, vol. 14, pp. 1001-1008, 2010.
- [74] A. K. Shah, R. Gambhir, N. Hazra, and R. Katoch, "Non tuberculous mycobacteria in surgical wounds—a rising cause of concern?," *Indian Journal of Surgery*, vol. 72, pp. 206-210, 2010.
- [75] A. D. Khosravi, M. Mirsaiedi, A. Farahani, M. R. Tabandeh, P. Mohajeri, S. Shoja, *et al.*, "Prevalence of nontuberculous mycobacteria and high efficacy of d-cycloserine and its synergistic effect with clarithromycin against *Mycobacterium fortuitum* and *Mycobacterium abscessus*," *Infection and Drug Resistance*, vol. 11, p. 2521, 2018.
- [76] M. J. Nasiri, M. M. Feizabadi, H. Dabiri, and A. A. Imani, "Prevalence of Nontuberculous Mycobacteria: A Single Center Study in Tehran, Iran," *Archives of Clinical Infectious Diseases*, vol. 13, 2018.
- [77] M. J. Nasiri, H. Dabiri, D. Darban-Sarokhalil, and A. H. Shahraki, "Prevalence of non-tuberculosis mycobacterial infections among tuberculosis suspects in Iran: systematic review and meta-analysis," *PloS One*, vol. 10, p. e0129073, 2015.
- [78] A. Y. Lim, S. H. Chotirmall, E. T. Fok, A. Verma, P. P. De, S. K. Goh, *et al.*, "Profiling non-tuberculous mycobacteria in an Asian setting: characteristics and clinical outcomes of hospitalized patients in Singapore," *BMC Pulmonary Medicine*, vol. 18, p. 85, 2018.
- [79] E. López-Varela, A. L. García-Basteiro, O. J. Augusto, O. Fraile, H. Bulo, T. Ira, *et al.*, "High rates of non-tuberculous mycobacteria isolation in Mozambican children with presumptive tuberculosis," *PloS One*, vol. 12, p. e0169757, 2017.
- [80] C. Okoi, S. T. Anderson, M. Antonio, S. N. Mulwa, F. Gehre, and I. M. Adetifa, "Non-tuberculous Mycobacteria isolated from pulmonary samples in sub-Saharan

- Africa-a systematic review and meta analyses," *Scientific Reports*, vol. 7, p. 12002, 2017.
- [81] M. M. Jones, K. L. Winthrop, S. D. Nelson, S. L. Duvall, O. V. Patterson, K. E. Nechodom, *et al.*, "Epidemiology of nontuberculous mycobacterial infections in the US Veterans Health Administration," *PloS One*, vol. 13, p. e0197976, 2018.
- [82] B. A. Forbes, G. S. Hall, M. B. Miller, S. M. Novak, M.-C. Rowlinson, M. Salfinger, *et al.*, "Practice guidelines for clinical microbiology laboratories: mycobacteria," *Clinical Microbiology Reviews*, vol. 31, pp. e00038-17, 2018.
- [83] M. J. Donohue, "Increasing nontuberculous mycobacteria reporting rates and species diversity identified in clinical laboratory reports," *BMC Infectious Diseases*, vol. 18, p. 163, 2018.
- [84] D. R. Prevots and T. K. Marras, "Epidemiology of human pulmonary infection with nontuberculous mycobacteria: a review," *Clinics in Chest Medicine*, vol. 36, pp. 13-34, 2015.
- [85] R. Thomson, L. Furuya-Kanamori, C. Coffey, S. Bell, L. Knibbs, and C. Lau, "Influence of Climate Variables on the Rising Incidence of Nontuberculous Mycobacterial (NTM) Infections in Queensland, Australia 2001-2016," in *A58. NTM: Epidemiology And Clinical Studies*, ed: American Thoracic Society, 2019, pp. A2043-A2043.
- [86] J. d. C. Cruz, "*Mycobacterium fortuitum*, un novo bacilo acido-resistente patogenico para o human," *Acta Med Ro de Janeiro*, vol. 1, p. 297, 1938.
- [87] E. J. Anaissie, S. R. Penzak, and M. C. Dignani, "The hospital water supply as a source of nosocomial infections: a plea for action," *Archives of Internal Medicine*, vol. 162, pp. 1483-1492, 2002.
- [88] M. D. Pinheiro, A. Ramos, T. Carvalho, and S. Costa, "*Mycobacterium fortuitum* spontaneous breast abscess: is there a laterality effect?," *JMM Case Reports*, vol. 3, 2016.
- [89] D. Lizaso, M. Garcia, A. Aguirre, and A. Esposto, "Breast implant infection by *Mycobacterium fortuitum* in a patient with systemic lupus erythematosus," *Revista Chilena de Infectologia: Organo Oficial de La Sociedad Chilena de Infectologia*, vol. 28, pp. 474-478, 2011.

- [90] G. J. Rosenmeier, J. H. Keeling, W. J. Grabski, M. L. McCollough, and G. A. Solivan, "Latent cutaneous *Mycobacterium fortuitum* infection in a healthy man," *Journal of the American Academy of Dermatology*, vol. 25, pp. 898-902, 1991.
- [91] D. S. Behroozan, M. M. Christian, and R. L. Moy, "*Mycobacterium fortuitum* infection following neck liposuction: A case report," *Dermatologic Surgery*, vol. 26, pp. 588-590, 2000.
- [92] J. Rose, T. G. Weiser, P. Hider, L. Wilson, R. L. Gruen, and S. W. Bickler, "Estimated need for surgery worldwide based on prevalence of diseases: a modelling strategy for the WHO Global Health Estimate," *The Lancet Global Health*, vol. 3, pp. S13-S20, 2015.
- [93] D. Z. Uslan, T. J. Kowalski, N. L. Wengenack, A. Virk, and J. W. Wilson, "Skin and soft tissue infections due to rapidly growing mycobacteria: comparison of clinical features, treatment, and susceptibility," *Archives of Dermatology*, vol. 142, pp. 1287-1292, 2006.
- [94] N. P. H. Lan, M.-E. Kolader, N. Van Dung, J. I. Campbell, N. thi Tham, N. V. V. Chau, *et al.*, "*Mycobacterium fortuitum* skin infections after subcutaneous injections with Vietnamese traditional medicine: a case report," *BMC Infectious Diseases*, vol. 14, p. 550, 2014.
- [95] S. Kumar, N. M. Joseph, J. M. Easow, and S. Umadevi, "Multifocal keloids associated with *Mycobacterium fortuitum* following intralesional steroid therapy," *Journal of Laboratory Physicians*, vol. 3, p. 127, 2011.
- [96] S. Okamori, T. Asakura, T. Nishimura, E. Tamizu, M. Ishii, M. Yoshida, *et al.*, "Natural history of *Mycobacterium fortuitum* pulmonary infection presenting with migratory infiltrates: a case report with microbiological analysis," *BMC Infectious Diseases*, vol. 18, p. 1, 2018.
- [97] R. Venter, C. Solomon, and M. Baartman, "*Mycobacterium fortuitum* as infectious agent in a septic total knee replacement: Case study and literature review," *SA Orthopaedic Journal*, vol. 14, pp. 52-56, 2015.
- [98] K. G. Luz, M. H. M. F. d. Britto, D. C. d. Farias, M. V. Almeida, and N. M. d. S. Figueirêdo, "*Mycobacterium fortuitum*-related lymphadenitis associated with the varicella-zoster virus," *Revista da Sociedade Brasileira de Medicina Tropical*, vol. 47, pp. 119-121, 2014.

- [99] K. C. Yeap, P. D. Sivagurunathan, P. Raman, and K. H. M. Khalid, "Non-tuberculous mycobacterial ocular infection masquerading as choroidal tumour—a diagnostic conundrum," *GMS Ophthalmology Cases*, vol. 9, 2019.
- [100] H. Inoue, N. Washida, K. Morimoto, K. Shinozuka, T. Kasai, K. Uchiyama, *et al.*, "Non-tuberculous mycobacterial infections related to peritoneal dialysis," *Peritoneal Dialysis International*, vol. 38, pp. 147-149, 2018.
- [101] M. A. Rodriguez-Coste, I. Chirca, L. L. Steed, and C. D. Salgado, "Epidemiology of rapidly growing mycobacteria bloodstream infections," *The American Journal of The Medical Sciences*, vol. 351, pp. 253-258, 2016.
- [102] J. Cong, C. Wang, L. Ma, S. Zhang, and J. Wang, "Septicemia and pneumonia due to *Mycobacterium fortuitum* infection in a patient with extranodal NK/T-cell lymphoma, nasal type: A case report," *Medicine*, vol. 96, 2017.
- [103] G. El Helou, G. M. Viola, R. Hachem, X. Y. Han, and I. I. Raad, "Rapidly growing mycobacterial bloodstream infections," *The Lancet Infectious Diseases*, vol. 13, pp. 166-174, 2013.
- [104] K. Longardner, A. Allen, and M. Ramgopal, "Spinal osteomyelitis due to *Mycobacterium fortuitum* in a former intravenous drug user," *BMJ Case Reports*, vol. 2013, p. bcr2013010326, 2013.
- [105] J. Natsag, Z. Min, Y. Hamad, B. Alkhalil, A. Rahman, and R. Williams, "A mysterious gram-positive rods," *Case Reports in Infectious Diseases*, vol. 2012, 2012.
- [106] L. Lazzarini, S. Amina, J. Wang, J. Calhoun, and J. Mader, "*Mycobacterium tuberculosis* and *Mycobacterium fortuitum* osteomyelitis of the foot and septic arthritis of the ankle in an immunocompetent patient," *European Journal of Clinical Microbiology and Infectious Diseases*, vol. 21, pp. 468-470, 2002.
- [107] K. Kwan and S. Ho, "*Mycobacterium chelonae* and *Mycobacterium fortuitum* infection following open fracture: a case report and review of the literature," *Indian Journal of Medical Microbiology*, vol. 28, p. 248, 2010.
- [108] C. Sanghvi, "*Mycobacterium fortuitum* keratitis," *Indian Journal of Medical Microbiology*, vol. 25, p. 422, 2007.
- [109] J. B. Sack, "Disseminated infection due to *Mycobacterium fortuitum* in a patient with AIDS," *Reviews of Infectious Diseases*, pp. 961-963, 1990.

- [110] C. Kell, K. Hunfeld, S. Wagner, C. Nern, V. Seifert, H. Brodt, *et al.*, "Chronic meningoencephalomyelitis due to *Mycobacterium fortuitum* in an immunocompetent patient," *Journal of Neurology*, vol. 255, p. 1847, 2008.
- [111] S. Park, G. Y. Suh, M. P. Chung, H. Kim, O. J. Kwon, K. S. Lee, *et al.*, "Clinical significance of *Mycobacterium fortuitum* isolated from respiratory specimens," *Respiratory Medicine*, vol. 102, pp. 437-442, 2008.
- [112] R. Bouchentouf, "*Mycobacterium fortuitum* infection associated with achalasia," *La Tunisie Medicale*, vol. 96, pp. 311-313, 2018.
- [113] <https://www.contagionlive.com/news/fda-grants-qidp-designation-to-spr720-for-ntm-infections> (Last accessed: 29 December, 2019)
- [114] R. Weinstein and W. Stamm, "Pseudoepidemics in hospital," *The Lancet*, vol. 310, pp. 862-864, 1977.
- [115] H. Nguyen, C. Le, and H. Nguyen, "An unusual case of a cervical mass due to nontuberculous *Mycobacterium fortuitum* infection," *The Permanente Journal*, vol. 12, p. 49, 2008.
- [116] E. Tortoli, "Epidemiology of cervico-facial pediatric lymphadenitis as a result of nontuberculous mycobacteria," *International Journal of Mycobacteriology*, vol. 1, pp. 165-169, 2012.
- [117] J. Olalla, M. Pombo, J. Aguado, E. Rodríguez, E. Palenque, J. Costa, *et al.*, "*Mycobacterium fortuitum* complex endocarditis—case report and literature review," *Clinical Microbiology and Infection*, vol. 8, pp. 125-129, 2002.
- [118] D. Vuković, V. Parezanović, B. Savić, I. Dakić, S. Laban-Nestorović, S. Ilić, *et al.*, "*Mycobacterium fortuitum* endocarditis associated with cardiac surgery, Serbia," *Emerging Infectious Diseases*, vol. 19, pp. 517-519, 2013.
- [119] V. K. Phadke, D. S. Hirsh, and N. D. Goswami, "Patient report and review of rapidly growing mycobacterial infection after cardiac device implantation," *Emerging Infectious Diseases*, vol. 22, p. 389, 2016.
- [120] J. Zhu, Q. Yang, J. Pan, H. Shi, B. Jin, and Q. Chen, "Cardiac resynchronization therapy-defibrillator pocket infection caused by *Mycobacterium fortuitum*: a case report and review of the literature," *BMC Cardiovascular Disorders*, vol. 19, p. 53, 2019.
- [121] A. C. Helguera-Repetto, R. Chacon-Salinas, J. F. Cerna-Cortes, S. Rivera-Gutierrez, V. Ortiz-Navarrete, I. Estrada-Garcia, *et al.*, "Differential macrophage response to

- slow-and fast-growing pathogenic mycobacteria," *BioMed Research International*, vol. 2014, 2014.
- [122] M. C. Núñez, M. C. Menéndez, M. J. Rebollo, and M. J. García, "Transcriptional analysis of *Mycobacterium fortuitum* cultures upon hydrogen peroxide treatment using the novel standard rrn A-P1," *BMC Microbiology*, vol. 8, p. 100, 2008.
- [123] A. M. Gupta and S. Mandal, "Distribution of Sigma factors delineates segregation of virulent and avirulent Mycobacterium," *bioRxiv*, p. 235986, 2017.
- [124] R. Saavedra, E. Segura, R. Leyva, L. A. Esparza, and L. M. López-Marín, "Mycobacterial di-O-acyl-trehalose inhibits mitogen-and antigen-induced proliferation of murine T cells *in vitro*," *Clinical and Diagnostic Laboratory Immunology*, vol. 8, pp. 1081-1088, 2001.
- [125] S. Sharbati, K. Schramm, S. Rempel, H. Wang, R. Andrich, V. Tykiel, *et al.*, "Characterisation of porin genes from *Mycobacterium fortuitum* and their impact on growth," *BMC Microbiology*, vol. 9, p. 31, 2009.
- [126] D. K. Parandhaman and S. Narayanan, "Cell death paradigms in the pathogenesis of *Mycobacterium tuberculosis* infection," *Frontiers in Cellular and Infection Microbiology*, vol. 4, p. 31, 2014.
- [127] D. Datta, P. Khatri, C. Banerjee, A. Singh, R. Meena, D. R. Saha, *et al.*, "Calcium and superoxide-mediated pathways converge to induce nitric oxide-dependent apoptosis in *Mycobacterium fortuitum*-infected fish macrophages," *PloS One*, vol. 11, p. e0146554, 2016.
- [128] S. Ramón-García, I. Otal, C. Martín, R. Gómez-Lus, and J. A. Aínsa, "Novel streptomycin resistance gene from *Mycobacterium fortuitum*," *Antimicrobial Agents And Chemotherapy*, vol. 50, pp. 3920-3922, 2006.
- [129] K. A. Nash, Y. Zhang, B. A. Brown-Elliott, and R. J. Wallace Jr, "Molecular basis of intrinsic macrolide resistance in clinical isolates of *Mycobacterium fortuitum*," *Journal of Antimicrobial Chemotherapy*, vol. 55, pp. 170-177, 2005.
- [130] C. Martin, J. Timm, J. Rauzier, R. Gomez-Lus, J. Davies, and B. Gicquel, "Transposition of an antibiotic resistance element in mycobacteria," *Nature*, vol. 345, p. 739, 1990.
- [131] J. van Ingen, M. J. Boeree, D. van Soolingen, and J. W. Mouton, "Resistance mechanisms and drug susceptibility testing of nontuberculous mycobacteria," *Drug Resistance Updates*, vol. 15, pp. 149-161, 2012.

- [132] J. Jacobs, C. Stine, A. Baya, and M. Kent, "A review of mycobacteriosis in marine fish," *Journal of Fish Diseases*, vol. 32, pp. 119-130, 2009.
- [133] A. M. Talaat, M. Trucksis, A. S. Kane, and R. Reimschuessel, "Pathogenicity of *Mycobacterium fortuitum* and *Mycobacterium smegmatis* to goldfish, *Carassius auratus*," *Veterinary Microbiology*, vol. 66, pp. 151-164, 1999.
- [134] R. Francis-Floyd, "Mycobacterial infections of fish," *Southern Regional Aquaculture Center*, 2011.
- [135] A. Uma and B. Ronald, "Drug Resistance in *Mycobacterium fortuitum* isolated from gold fish, *Carassius auratus*," *International Journal of Science, Environmental and Technology*, vol. 5, pp. 4411-4417, 2016.
- [136] H. Saito and H. Tasaka, "Comparison of the pathogenicity for mice of *Mycobacterium fortuitum* and *Mycobacterium abscessus*," *Journal of Bacteriology*, vol. 99, pp. 851-855, 1969.
- [137] R. P. Parti, S. Srivastava, R. Gachhui, K. K. Srivastava, and R. Srivastava, "Murine infection model for *Mycobacterium fortuitum*," *Microbes and Infection*, vol. 7, pp. 349-355, 2005.
- [138] T. R. M. d. Silva, A. L. d. O. A. Petersen, T. d. A. Santos, T. F. d. Almeida, L. A. R. d. Freitas, and P. S. T. Veras, "Control of *Mycobacterium fortuitum* and *Mycobacterium intracellulare* infections with respect to distinct granuloma formations in livers of BALB/c mice," *Memórias do Instituto Oswaldo Cruz*, vol. 105, pp. 642-648, 2010.
- [139] C. Nicod, A. Banaei-Esfahani, and B. C. Collins, "Elucidation of host–pathogen protein–protein interactions to uncover mechanisms of host cell rewiring," *Current Opinion in Microbiology*, vol. 39, pp. 7-15, 2017.
- [140] C. J. Queval, R. Brosch, and R. Simeone, "The macrophage: a disputed fortress in the battle against *Mycobacterium tuberculosis*," *Frontiers in Microbiology*, vol. 8, p. 2284, 2017.
- [141] A. MacNeil, P. Glaziou, C. Sismanidis, S. Maloney, and K. Floyd, "Global epidemiology of tuberculosis and progress toward achieving global targets—2017," *Morbidity and Mortality Weekly Report*, vol. 68, p. 263, 2019.
- [142] J. A. Awuh and T. H. Flo, "Molecular basis of mycobacterial survival in macrophages," *Cellular and Molecular Life Sciences*, vol. 74, pp. 1625-1648, 2017.
- [143] R. W. Stokes, I. D. Haidl, W. A. Jefferies, and D. P. Speert, "Mycobacteria-macrophage interactions. Macrophage phenotype determines the nonopsonic binding

- of *Mycobacterium tuberculosis* to murine macrophages," *The Journal of Immunology*, vol. 151, pp. 7067-7076, 1993.
- [144] J. Pieters, "Mycobacterium tuberculosis and the macrophage: maintaining a balance," *Cell Host & Microbe*, vol. 3, pp. 399-407, 2008.
- [145] H. Chen, S. A. Nyantakyi, M. Li, P. Gopal, D. B. Aziz, T. Yang, *et al.*, "The mycobacterial membrane: a novel target space for anti-tubercular drugs," *Frontiers in Microbiology*, vol. 9, 2018.
- [146] M. Ocampo, M. A. Patarroyo, M. Vanegas, M. P. Alba, and M. E. Patarroyo, "Functional, biochemical and 3D studies of *Mycobacterium tuberculosis* protein peptides for an effective anti-tuberculosis vaccine," *Critical Reviews in Microbiology*, vol. 40, pp. 117-145, 2014.
- [147] D. C. Rodríguez, M. Ocampo, C. Reyes, G. Arévalo-Pinzón, M. Muñoz, M. A. Patarroyo, *et al.*, "Cell-peptide specific interaction can inhibit *Mycobacterium tuberculosis* h37rv infection," *Journal of Cellular Biochemistry*, vol. 117, pp. 946-958, 2016.
- [148] D. C. Rodríguez, M. Ocampo, Y. Varela, H. Curtidor, M. A. Patarroyo, and M. E. Patarroyo, "Mce4F *Mycobacterium tuberculosis* protein peptides can inhibit invasion of human cell lines," *Pathogens and Disease*, vol. 73, 2015.
- [149] J. J. Athman, Y. Wang, D. J. McDonald, W. H. Boom, C. V. Harding, and P. A. Wearsch, "Bacterial membrane vesicles mediate the release of *Mycobacterium tuberculosis* lipoglycans and lipoproteins from infected macrophages," *The Journal of Immunology*, vol. 195, pp. 1044-1053, 2015.
- [150] E. Russell-Goldman, J. Xu, X. Wang, J. Chan, and J. M. Tufariello, "A *Mycobacterium tuberculosis* Rpf double-knockout strain exhibits profound defects in reactivation from chronic tuberculosis and innate immunity phenotypes," *Infection and Immunity*, vol. 76, pp. 4269-4281, 2008.
- [151] J. Humann and L. L. Lenz, "Bacterial peptidoglycan-degrading enzymes and their impact on host muropeptide detection," *Journal of Innate Immunity*, vol. 1, pp. 88-97, 2009.
- [152] L. S. Schlesinger, S. R. Hull, and T. M. Kaufman, "Binding of the terminal mannosyl units of lipoarabinomannan from a virulent strain of *Mycobacterium tuberculosis* to human macrophages," *The Journal of Immunology*, vol. 152, pp. 4070-4079, 1994.

- [153] R. Van Crevel, T. H. Ottenhoff, and J. W. van der Meer, "Innate immunity to *Mycobacterium tuberculosis*," *Clinical Microbiology Reviews*, vol. 15, pp. 294-309, 2002.
- [154] T. Fukuda, T. Matsumura, M. Ato, M. Hamasaki, Y. Nishiuchi, Y. Murakami, *et al.*, "Critical roles for lipomannan and lipoarabinomannan in cell wall integrity of mycobacteria and pathogenesis of tuberculosis," *MBio*, vol. 4, pp. e00472-12, 2013.
- [155] D. Dao, L. Kremer, Y. Guérardel, A. Molano, W. Jacobs, S. A. Porcelli, *et al.*, "*Mycobacterium tuberculosis* lipomannan induces apoptosis and interleukin-12 production in macrophages," *Infection and Immunity*, vol. 72, pp. 2067-2074, 2004.
- [156] A. Queiroz and L. W. Riley, "Bacterial immunostat: *Mycobacterium tuberculosis* lipids and their role in the host immune response," *Revista da Sociedade Brasileira de Medicina Tropical*, vol. 50, pp. 9-18, 2017.
- [157] H. Målen, G. A. De Souza, S. Pathak, T. Søfteland, and H. G. Wiker, "Comparison of membrane proteins of *Mycobacterium tuberculosis* H37Rv and H37Ra strains," *BMC Microbiology*, vol. 11, p. 18, 2011.
- [158] O. Danilchanka, J. Sun, M. Pavlenok, C. Maueröder, A. Speer, A. Siroy, *et al.*, "An outer membrane channel protein of *Mycobacterium tuberculosis* with exotoxin activity," *Proceedings of the National Academy of Sciences*, vol. 111, pp. 6750-6755, 2014.
- [159] T. Tan, W. L. Lee, D. C. Alexander, S. Grinstein, and J. Liu, "The ESAT-6/CFP-10 secretion system of *Mycobacterium marinum* modulates phagosome maturation," *Cellular Microbiology*, vol. 8, pp. 1417-1429, 2006.
- [160] R. Gao, T. R. Mack, and A. M. Stock, "Bacterial response regulators: versatile regulatory strategies from common domains," *Trends in Biochemical Sciences*, vol. 32, pp. 225-234, 2007.
- [161] V. Peddireddy, S. N. Doddam, and N. Ahmed, "Mycobacterial dormancy systems and host responses in tuberculosis," *Frontiers in Immunology*, vol. 8, p. 84, 2017.
- [162] J.-M. Zhang and J. An, "Cytokines, inflammation and pain," *International Anesthesiology Clinics*, vol. 45, p. 27, 2007.
- [163] J.-M. Cavaillon and M. Adib-Conquy, "The pro-inflammatory cytokine cascade," in *Immune Response in the Critically Ill*, ed: Springer, 2002, pp. 37-66.
- [164] S. M. Opal and V. A. DePalo, "Anti-inflammatory cytokines," *Chest Journal*, vol. 117, pp. 1162-1172, 2000.

- [165] S. H. Kaufmann, "Tuberculosis: back on the immunologists' agenda," *Immunity*, vol. 24, pp. 351-357, 2006.
- [166] F. McNab, K. Mayer-Barber, A. Sher, A. Wack, and A. O'Garra, "Type I interferons in infectious disease," *Nature Reviews Immunology*, vol. 15, pp. 87-103, 2015.
- [167] B. M. Saunders and A. M. Cooper, "Restraining mycobacteria: role of granulomas in mycobacterial infections," *Immunology and Cell Biology*, vol. 78, pp. 334-341, 2000.
- [168] Y. V. N. Cavalcanti, M. C. A. Brelaz, J. K. d. A. L. Neves, J. C. Ferraz, and V. R. A. Pereira, "Role of TNF-alpha, IFN-gamma, and IL-10 in the development of pulmonary tuberculosis," *Pulmonary Medicine*, vol. 2012, 2012.
- [169] A. Harari, V. Rozot, F. B. Enders, M. Perreau, J. M. Stalder, L. P. Nicod, *et al.*, "Dominant TNF-[alpha]+ *Mycobacterium tuberculosis*-specific CD4+ T cell responses discriminate between latent infection and active disease," *Nature Medicine*, vol. 17, pp. 372-376, 2011.
- [170] N. Caccamo, G. Guggino, S. A. Joosten, G. Gelsomino, P. Di Carlo, L. Titone, *et al.*, "Multifunctional CD4+ T cells correlate with active *Mycobacterium tuberculosis* infection," *European Journal of Immunology*, vol. 40, pp. 2211-2220, 2010.
- [171] J. L. Flynn and J. Chan, "What's good for the host is good for the bug," *Trends in Microbiology*, vol. 13, pp. 98-102, 2005.
- [172] A. Mootoo, E. Stylianou, M. A. Arias, and R. Reljic, "TNF- α in Tuberculosis: A Cytokine with a Split Personality," *Inflammation & Allergy-Drug Targets*, vol. 8, pp. 53-62, 2009.
- [173] C. Cambier, S. Falkow, and L. Ramakrishnan, "Host evasion and exploitation schemes of *Mycobacterium tuberculosis*," *Cell*, vol. 159, pp. 1497-1509, 2014.
- [174] A. Cooper, A. Roberts, E. Rhoades, J. Callahan, D. Getzy, and I. Orme, "The role of interleukin-12 in acquired immunity to *Mycobacterium tuberculosis* infection," *Immunology*, vol. 84, p. 423, 1995.
- [175] C. Fieschi and J. L. Casanova, "Mini-review The role of interleukin-12 in human infectious diseases: only a faint signature," *European Journal of Immunology*, vol. 33, pp. 1461-1464, 2003.
- [176] J. Estaquier, T. Idziorek, W. Zou, D. Emilie, C.-M. Farber, J.-M. Bourez, *et al.*, "T helper type 1/T helper type 2 cytokines and T cell death: preventive effect of interleukin 12 on activation-induced and CD95 (FAS/APO-1)-mediated apoptosis of

- CD4⁺ T cells from human immunodeficiency virus-infected persons," *The Journal of Experimental Medicine*, vol. 182, pp. 1759-1767, 1995.
- [177] S. F. Wolf, D. Sieburth, and J. Sypek, "Interleukin 12: a key modulator of immune function," *Stem Cells*, vol. 12, pp. 154-168, 1994.
- [178] T. Fukao, S. Matsuda, and S. Koyasu, "Synergistic effects of IL-4 and IL-18 on IL-12-dependent IFN- γ production by dendritic cells," *The Journal of Immunology*, vol. 164, pp. 64-71, 2000.
- [179] C. J. Hertz, S. M. Kiertscher, P. J. Godowski, D. A. Bouis, M. V. Norgard, M. D. Roth, *et al.*, "Microbial lipopeptides stimulate dendritic cell maturation via Toll-like receptor 2," *The Journal of Immunology*, vol. 166, pp. 2444-2450, 2001.
- [180] N. P. Kumar, K. Moideen, V. V. Banurekha, D. Nair, R. Sridhar, T. B. Nutman, *et al.*, "IL-27 and TGF β mediated expansion of Th1 and adaptive regulatory T cells expressing IL-10 correlates with bacterial burden and disease severity in pulmonary tuberculosis," *Immunity, Inflammation and Disease*, vol. 3, pp. 289-299, 2015.
- [181] S. P. Hickman, J. Chan, and P. Salgame, "*Mycobacterium tuberculosis* induces differential cytokine production from dendritic cells and macrophages with divergent effects on naive T cell polarization," *The Journal of Immunology*, vol. 168, pp. 4636-4642, 2002.
- [182] Z.-m. Chen, M. J. O'Shaughnessy, I. Gramaglia, A. Panoskaltsis-Mortari, W. J. Murphy, S. Narula, *et al.*, "IL-10 and TGF- β induce alloreactive CD4⁺ CD25⁻T cells to acquire regulatory cell function," *Blood*, vol. 101, pp. 5076-5083, 2003.
- [183] C. S. Hirsch, T. Yoneda, L. Averill, J. J. Ellner, and Z. Toossi, "enhancement of intracellular growth of *Mycobacterium tuberculosis* in human monocytes by transforming growth factor- β 1," *Journal of Infectious Diseases*, vol. 170, pp. 1229-1237, 1994.
- [184] J. Turner, J. Cyktor, B. Carruthers, R. Kominsky, P. Stromberg, and G. Beamer, "Deficiency in interleukin 10 reverses the susceptibility phenotype of CBA/J mice during infection with *Mycobacterium tuberculosis*," *The Journal of Immunology*, vol. 188, p. 43.23, 2012.
- [185] P. Redford, P. Murray, and A. O'garra, "The role of IL-10 in immune regulation during *M. tuberculosis* infection," *Mucosal Immunology*, vol. 4, p. 261, 2011.

- [186] A. E. Abdalla, N. Lambert, X. Duan, and J. Xie, "Interleukin-10 Family and Tuberculosis: An Old Story Renewed," *International Journal of Biological Sciences*, vol. 12, p. 710, 2016.
- [187] N. A. Cilfone, C. R. Perry, D. E. Kirschner, and J. J. Linderman, "Multi-scale modeling predicts a balance of tumor necrosis factor- α and interleukin-10 controls the granuloma environment during *Mycobacterium tuberculosis* infection," *Plos One*, vol. 8, p. e68680, 2013.
- [188] C. Hölscher, A. Hölscher, D. Rückerl, T. Yoshimoto, H. Yoshida, T. Mak, *et al.*, "The IL-27 receptor chain WSX-1 differentially regulates antibacterial immunity and survival during experimental tuberculosis," *The Journal of Immunology*, vol. 174, pp. 3534-3544, 2005.
- [189] E. Torrado, J. J. Fountain, M. Liao, M. Tighe, W. W. Reiley, R. P. Lai, *et al.*, "Interleukin 27R regulates CD4+ T cell phenotype and impacts protective immunity during *Mycobacterium tuberculosis* infection," *Journal of Experimental Medicine*, vol. 212, pp. 1449-1463, 2015.
- [190] S. Bakour, S. A. Sankar, J. Rathored, P. Biagini, D. Raoult, and P.-E. Fournier, "Identification of virulence factors and antibiotic resistance markers using bacterial genomics," *Future Microbiology*, vol. 11, pp. 455-466, 2016.
- [191] P. Wah Tang, P. San Chua, S. Kee Chong, M. Saberi Mohamad, Y. Wen Choon, S. Deris, *et al.*, "A review of gene knockout strategies for microbial cells," *Recent Patents on Biotechnology*, vol. 9, pp. 176-197, 2015.
- [192] P. Kaur, S. Datta, R. K. Shandil, N. Kumar, N. Robert, U. K. Sokhi, *et al.*, "Unravelling the secrets of mycobacterial cidality through the lens of antisense," *PloS One*, vol. 11, p. e0154513, 2016.
- [193] A. Chandolia, N. Rathor, M. Sharma, N. K. Saini, R. Sinha, P. Malhotra, *et al.*, "Functional analysis of mce4A gene of *Mycobacterium tuberculosis* H37Rv using antisense approach," *Microbiological Research*, vol. 169, pp. 780-787, 2014.
- [194] F. Movahedzadeh, R. Frita, and H. J. Gutka, "A two-step strategy for the complementation of *M. tuberculosis* mutants," *Genetics and Molecular Biology*, vol. 34, pp. 286-289, 2011.
- [195] M. H. Lee, L. Pascopella, W. R. Jacobs, and G. F. Hatfull, "Site-specific integration of mycobacteriophage L5: integration-proficient vectors for *Mycobacterium smegmatis*,

- Mycobacterium tuberculosis*, and bacille Calmette-Guerin," *Proceedings of the National Academy of Sciences*, vol. 88, pp. 3111-3115, 1991.
- [196] T. Parish, G. Roberts, F. Laval, M. Schaeffer, M. Daffé, and K. Duncan, "Functional complementation of the essential gene *fabG1* of *Mycobacterium tuberculosis* by *Mycobacterium smegmatis* *fabG* but not *Escherichia coli* *fabG*," *Journal of Bacteriology*, vol. 189, pp. 3721-3728, 2007.
- [197] S. Sakthi and S. Narayanan, "The *lpqS* knockout mutant of *Mycobacterium tuberculosis* is attenuated in macrophages," *Microbiological research*, vol. 168, pp. 407-414, 2013.
- [198] S. Ravindran, "Barbara McClintock and the discovery of jumping genes," *Proceedings of the National Academy of Sciences*, vol. 109, pp. 20198-20199, 2012.
- [199] Y.-C. Wong, M. Abd El Ghany, R. Naeem, K.-W. Lee, Y.-C. Tan, A. Pain, *et al.*, "Candidate essential genes in *Burkholderia cenocepacia* J2315 identified by genome-wide TraDIS," *Frontiers in Microbiology*, vol. 7, p. 1288, 2016.
- [200] A. J. McCarthy, R. A. Stabler, and P. W. Taylor, "Genome-wide identification by transposon insertion sequencing of *Escherichia coli* K1 genes essential for *in vitro* growth, gastrointestinal colonizing capacity, and survival in serum," *Journal of Bacteriology*, vol. 200, pp. e00698-17, 2018.
- [201] R. C. Shields, L. Zeng, D. J. Culp, and R. A. Burne, "Genome wide identification of essential genes and fitness determinants of *Streptococcus mutans* UA159," *MSphere*, vol. 3, pp. e00031-18, 2018.
- [202] M. A. DeJesus, E. R. Gerrick, W. Xu, S. W. Park, J. E. Long, C. C. Boutte, *et al.*, "Comprehensive essentiality analysis of the *Mycobacterium tuberculosis* genome via saturating transposon mutagenesis," *MBio*, vol. 8, pp. e02133-16, 2017.
- [203] W. S. Reznikoff, "Transposon Tn 5," *Annual review of genetics*, vol. 42, pp. 269-286, 2008.
- [204] A. Loureiro and G. J. da Silva, "Crispr-cas: Converting a bacterial defence mechanism into a state-of-the-art genetic manipulation tool," *Antibiotics*, vol. 8, p. 18, 2019.
- [205] L. S. Qi, M. H. Larson, L. A. Gilbert, J. A. Doudna, J. S. Weissman, A. P. Arkin, *et al.*, "Repurposing CRISPR as an RNA-guided platform for sequence-specific control of gene expression," *Cell*, vol. 152, pp. 1173-1183, 2013.
- [206] E. Choudhary, P. Thakur, M. Pareek, and N. Agarwal, "Gene silencing by CRISPR interference in mycobacteria," *Nature communications*, vol. 6, pp. 1-11, 2015.

- [207] M. B. McNeil and G. M. Cook, "Utilization of CRISPR interference to validate MmpL3 as a drug target in *Mycobacterium tuberculosis*," *Antimicrobial agents and chemotherapy*, vol. 63, pp. e00629-19, 2019.
- [208] A. S. Meijers, R. Troost, R. Ummels, J. Maaskant, A. Speer, S. Nejentsev, *et al.*, "Efficient genome editing in pathogenic mycobacteria using *Streptococcus thermophilus* CRISPR1-Cas9," *Tuberculosis*, vol. 124, p. 101983, 2020.
- [209] S. Ehrt and D. Schnappinger, "Controlling gene expression in mycobacteria," *Future Microbiology*, vol. 1, pp. 177-184, 2006.
- [210] S. D. Riggs-Shute, J. O. Falkinham, and Z. Yang, "Construction and use of transposon mycotetop2 for isolation of conditional mycobacteria mutants," *Frontiers in Microbiology*, vol. 10, 2019.
- [211] Q. Deng, J. Meng, Y. Guan, Y. Liu, and C. Xiao, "Plasmid to generate Mycobacteria mutants," *AMB Express*, vol. 8, pp. 1-7, 2018.
- [212] M. Liu, "Plasmid-Based Reporter Genes," in *E. coli Plasmid Vectors*, ed: Springer, 2003, pp. 289-296.
- [213] O. A. Dellagostin, G. Esposito, L.-J. Eales, J. W. Dale, and J. McFadden, "Activity of mycobacterial promoters during intracellular and extracellular growth," *Microbiology*, vol. 141, pp. 1785-1792, 1995.
- [214] P. Carroll, L. J. Schreuder, J. Muwanguzi-Karugaba, S. Wiles, B. D. Robertson, J. Ripoll, *et al.*, "Sensitive detection of gene expression in mycobacteria under replicating and non-replicating conditions using optimized far-red reporters," *PloS one*, vol. 5, p. e9823, 2010.
- [215] R. Srivastava, D. Kumar, P. Subramaniam, and B. S. Srivastava, " β -Galactosidase reporter system in mycobacteria and its application in rapid antimycobacterial drug screening," *Biochemical and Biophysical Research Communications*, vol. 235, pp. 602-605, 1997.
- [216] S. Jain, D. Kaushal, S. K. Dasgupta, and A. K. Tyagi, "Construction of shuttle vectors for genetic manipulation and molecular analysis of mycobacteria," *Gene*, vol. 190, pp. 37-44, 1997.
- [217] S. Michaelis, H. Inouye, D. Oliver, and J. Beckwith, "Mutations that alter the signal sequence of alkaline phosphatase in *Escherichia coli*," *Journal of Bacteriology*, vol. 154, pp. 366-374, 1983.

- [218] E. M. Lim, J. Rauzier, J. Timm, G. Torrea, A. Murray, B. Gicquel, *et al.*, "Identification of *Mycobacterium tuberculosis* DNA sequences encoding exported proteins by using *phoA* gene fusions," *Journal of Bacteriology*, vol. 177, pp. 59-65, 1995.
- [219] C. Manoil and J. Beckwith, "TnphoA: a transposon probe for protein export signals," *Proceedings of the National Academy of Sciences*, vol. 82, pp. 8129-8133, 1985.
- [220] S. Sood, S. Kaur, and R. Shrivastava, "A *lacZ* reporter-based strategy for rapid expression analysis and target validation of *Mycobacterium tuberculosis* latent infection genes," *Current Microbiology*, vol. 72, pp. 213-219, 2016.
- [221] M. R. Kaufman and R. K. Taylor, "Identification of bacterial cell-surface virulence determinants with TnphoA," in *Methods in enzymology*. vol. 235, ed: Elsevier, 1994, pp. 426-448.
- [222] C. Job and C. Chacko, "A modification of Fite's stain for demonstration of *M. leprae* in tissue sections," *Indian Journal of Leprosy*, vol. 58, p. 17, 1986.
- [223] J. Sambrook, E. F. Fritsch, and T. Maniatis, *Molecular cloning: a laboratory manual*, Cold spring harbor laboratory press, 1989.
- [224] D. Hanahan, "Studies on transformation of *Escherichia coli* with plasmids," *Journal of Molecular Biology*, vol. 166, pp. 557-580, 1983.
- [225] D. E. Geiman, T. R. Raghunand, N. Agarwal, and W. R. Bishai, "Differential gene expression in response to exposure to antimycobacterial agents and other stress conditions among seven *Mycobacterium tuberculosis* *whiB*-like genes," *Antimicrobial Agents and Chemotherapy*, vol. 50, pp. 2836-2841, 2006.
- [226] S. Kawaji, L. Zhong, and R. J. Whittington, "Partial proteome of *Mycobacterium avium* subsp. paratuberculosis under oxidative and nitrosative stress," *Veterinary Microbiology*, vol. 145, pp. 252-264, 2010.
- [227] G. Xie, N. O. Keyhani, C. A. Bonner, and R. A. Jensen, "Ancient origin of the tryptophan operon and the dynamics of evolutionary change," *Microbiology and Molecular Biology Reviews*, vol. 67, pp. 303-342, 2003.
- [228] S. Sethi, S. Arora, V. Gupta, and S. Kumar, "Cutaneous *Mycobacterium fortuitum* infection: successfully treated with amikacin and ofloxacin combination," *Indian Journal of Dermatology*, vol. 59, p. 383, 2014.

- [229] J. Fowler and S. D. Mahlen, "Localized cutaneous infections in immunocompetent individuals due to rapidly growing mycobacteria," *Archives of Pathology and Laboratory Medicine*, vol. 138, pp. 1106-1109, 2014.
- [230] S. Sarma and R. Thakur, "Cutaneous infection with *Mycobacterium fortuitum*: An unusual presentation," *Indian Journal of Medical Microbiology*, vol. 26, p. 388, 2008.
- [231] K. Gopinath and S. Singh, "Non-tuberculous mycobacteria in TB-endemic countries: are we neglecting the danger?," *PLoS Neglected Tropical Diseases*, vol. 4, p. e615, 2010.
- [232] D. Datta, P. Khatri, A. Singh, D. R. Saha, G. Verma, R. Raman, *et al.*, "*Mycobacterium fortuitum*-induced ER-Mitochondrial calcium dynamics promotes calpain/caspase-12/caspase-9 mediated apoptosis in fish macrophages," *Cell Death Discovery*, vol. 4, p. 30, 2018.
- [233] C. L. Stallings and M. S. Glickman, "Is *Mycobacterium tuberculosis* stressed out? A critical assessment of the genetic evidence," *Microbes and Infection*, vol. 12, pp. 1091-1101, 2010.
- [234] S. Dam, J.-M. Pagès, and M. Masi, "Stress responses, outer membrane permeability control and antimicrobial resistance in Enterobacteriaceae," *Microbiology*, 2018.
- [235] Y. Guo, Y. Li, W. Zhan, T. K. Wood, and X. Wang, "Resistance to oxidative stress by inner membrane protein ElaB is regulated by OxyR and RpoS," *Microbial Biotechnology*, vol. 12, pp. 392-404, 2019.
- [236] V. Rosas-Magallanes, G. Stadthagen-Gomez, J. Rauzier, L. B. Barreiro, L. Tailleux, F. Boudou, *et al.*, "Signature-tagged transposon mutagenesis identifies novel *Mycobacterium tuberculosis* genes involved in the parasitism of human macrophages," *Infection and Immunity*, vol. 75, pp. 504-507, 2007.
- [237] M. Hensel, J. E. Shea, C. Gleeson, M. D. Jones, E. Dalton, and D. W. Holden, "Simultaneous identification of bacterial virulence genes by negative selection," *Science*, vol. 269, pp. 400-403, 1995.
- [238] D. H. Shah, X. Zhou, H.-Y. Kim, D. R. Call, and J. Guard, "Transposon mutagenesis of *Salmonella enterica* serovar Enteritidis identifies genes that contribute to invasiveness in human and chicken cells and survival in egg albumen," *Infection and Immunity*, vol. 80, pp. 4203-4215, 2012.

- [239] J. M. Mei, F. Nourbakhsh, C. W. Ford, and D. W. Holden, "Identification of *Staphylococcus aureus* virulence genes in a murine model of bacteraemia using signature-tagged mutagenesis," *Molecular Microbiology*, vol. 26, pp. 399-407, 1997.
- [240] W. Wang, J. Chen, G. Chen, X. Du, P. Cui, J. Wu, *et al.*, "Transposon mutagenesis identifies novel genes associated with *Staphylococcus aureus* persister formation," *Frontiers in Microbiology*, vol. 6, p. 1437, 2015.
- [241] S. L. Chiang and J. J. Mekalanos, "Use of signature-tagged transposon mutagenesis to identify *Vibrio cholerae* genes critical for colonization," *Molecular Microbiology*, vol. 27, pp. 797-805, 1998.
- [242] D. E. Cameron, J. M. Urbach, and J. J. Mekalanos, "A defined transposon mutant library and its use in identifying motility genes in *Vibrio cholerae*," *Proceedings of the National Academy of Sciences*, vol. 105, pp. 8736-8741, 2008.
- [243] A. Polissi, A. Pontiggia, G. Feger, M. Altieri, H. Mottl, L. Ferrari, *et al.*, "Large-Scale Identification of Virulence Genes from *Streptococcus pneumoniae*," *Infection and Immunity*, vol. 66, pp. 5620-5629, 1998.
- [244] T. van Opijnen and A. Camilli, "A fine scale phenotype–genotype virulence map of a bacterial pathogen," *Genome Research*, vol. 22, pp. 2541-2551, 2012.
- [245] R. Domingo-Gonzalez, O. Prince, A. Cooper, and S. Khader, "Cytokines and chemokines in *Mycobacterium tuberculosis* infection," *Microbiology Spectrum* 2016.
- [246] Y. Hu, B. Henderson, P. A. Lund, P. Tormay, M. T. Ahmed, S. S. Gurcha, *et al.*, "A *Mycobacterium tuberculosis* mutant lacking the groEL homologue cpn60. 1 is viable but fails to induce an inflammatory response in animal models of infection," *Infection and Immunity*, vol. 76, pp. 1535-1546, 2008.
- [247] R. H. Pando, L. D. Aguilar, I. Smith, and R. Manganelli, "Immunogenicity and protection induced by a *Mycobacterium tuberculosis* sigE mutant in a BALB/c mouse model of progressive pulmonary tuberculosis," *Infection and Immunity*, vol. 78, pp. 3168-3176, 2010.
- [248] W. R. Pearson, "An introduction to sequence similarity ("homology") searching," *Current Protocols In Bioinformatics*, vol. 42, pp. 3.1. 1-3.1. 8, 2013.
- [249] D. Wheeler and M. Bhagwat, "BLAST QuickStart," in *Comparative Genomics*, ed: Springer, 2007, pp. 149-175.

- [250] P. Pumirat, M. Vanaporn, P. Pinweha, S. Tandhavanant, S. Korbsrisate, and N. Chantratita, "The role of short-chain dehydrogenase/oxidoreductase, induced by salt stress, on host interaction of *B. pseudomallei*," *BMC Microbiology*, vol. 14, p. 1, 2014.
- [251] C. M. Sasseti and E. J. Rubin, "Genetic requirements for mycobacterial survival during infection," *Proceedings of the National Academy of Sciences*, vol. 100, pp. 12989-12994, 2003.
- [252] A. R. Flores, L. M. Parsons, and M. S. Pavelka, "Characterization of novel *Mycobacterium tuberculosis* and *Mycobacterium smegmatis* mutants hypersusceptible to β -lactam antibiotics," *Journal of Bacteriology*, vol. 187, pp. 1892-1900, 2005.
- [253] P. Bijtenhoorn, H. Mayerhofer, J. Müller-Dieckmann, C. Utpatel, C. Schipper, C. Hornung, *et al.*, "A novel metagenomic short-chain dehydrogenase/reductase attenuates *Pseudomonas aeruginosa* biofilm formation and virulence on *Caenorhabditis elegans*," *PLoS One*, vol. 6, p. e26278, 2011.
- [254] C. Carminatti, I. Oliveira, D. Recouvreux, R. Antônio, and L. Porto, "Anthranilate synthase subunit organization in *Chromobacterium violaceum*," *Genetics and Molecular Research*, vol. 7, pp. 830-838, 2008.
- [255] H. Zalkin and D. Ebole, "Organization and regulation of genes encoding biosynthetic enzymes in *Bacillus subtilis*," *Journal of Biological Chemistry*, vol. 263, pp. 1595-1598, 1988.
- [256] A. J. Olive and C. M. Sasseti, "Metabolic crosstalk between host and pathogen: sensing, adapting and competing," *Nature Reviews Microbiology*, vol. 14, p. 221, 2016.
- [257] S. K. Schmidt, S. Ebel, E. Keil, C. Woite, J. F. Ernst, A. E. Benzin, *et al.*, "Regulation of IDO activity by oxygen supply: inhibitory effects on antimicrobial and immunoregulatory functions," *PloS One*, vol. 8, p. e63301, 2013.
- [258] L. Alibaud, T. Köhler, A. Coudray, C. Prigent-Combaret, E. Bergeret, J. Perrin, *et al.*, "*Pseudomonas aeruginosa* virulence genes identified in a *Dictyostelium* host model," *Cellular Microbiology*, vol. 10, pp. 729-740, 2008.
- [259] Y. J. Zhang, M. C. Reddy, T. R. Ioerger, A. C. Rothchild, V. Dartois, B. M. Schuster, *et al.*, "Tryptophan biosynthesis protects mycobacteria from CD4 T-cell-mediated killing," *Cell*, vol. 155, pp. 1296-1308, 2013.

- [260] D. A. Smith, T. Parish, N. G. Stoker, and G. J. Bancroft, "Characterization of auxotrophic mutants of *Mycobacterium tuberculosis* and their potential as vaccine candidates," *Infection and Immunity*, vol. 69, pp. 1142-1150, 2001.
- [261] M. A. Bachman, P. Breen, V. Deornellas, Q. Mu, L. Zhao, W. Wu, *et al.*, "Genome-wide identification of *Klebsiella pneumoniae* fitness genes during lung infection," *MBio*, vol. 6, pp. e00775-15, 2015.
- [262] A. Cossu, L. A. Sechi, S. Zanetti, and V. Rosu, "Gene expression profiling of *Mycobacterium avium* subsp. *paratuberculosis* in simulated multi-stress conditions and within THP-1 cells reveals a new kind of interactive intramacrophage behaviour," *BMC Microbiology*, vol. 12, p. 87, 2012.
- [263] J. L. Gallant, A. J. Viljoen, P. D. Van Helden, and I. J. Wiid, "Glutamate dehydrogenase is required by *Mycobacterium bovis* BCG for resistance to cellular stress," *PloS One*, vol. 11, p. e0147706, 2016.
- [264] C. Yanofsky, "RNA-based regulation of genes of tryptophan synthesis and degradation, in bacteria," *Rna*, vol. 13, pp. 1141-1154, 2007.
- [265] O. René and J.-H. Alix, "Late steps of ribosome assembly in *E. coli* are sensitive to a severe heat stress but are assisted by the HSP70 chaperone machine," *Nucleic Acids Research*, vol. 39, pp. 1855-1867, 2010.
- [266] A. E. Bunner, S. Nord, P. M. Wikström, and J. R. Williamson, "The effect of ribosome assembly cofactors on *in vitro* 30S subunit reconstitution," *Journal of Molecular Biology*, vol. 398, pp. 1-7, 2010.
- [267] G. O. Bylund, J. M. Lövgren, and P. M. Wikström, "Characterization of mutations in themety-nusa-infb operon that suppress the slow growth of a Δ rimM mutant," *Journal of Bacteriology*, vol. 183, pp. 6095-6106, 2001.
- [268] X. Weng, "Functional characterization of ribosome maturation factor RimP in *Mycobacterium smegmatis*," Dissertation, City University of Hong Kong, 2016.
- [269] S. Nord, G. O. Bylund, J. M. Lövgren, and P. M. Wikström, "The RimP protein is important for maturation of the 30S ribosomal subunit," *Journal of Molecular Biology*, vol. 386, pp. 742-753, 2009.
- [270] T. Chu, X. Weng, C. O. K. Law, H.-K. Kong, J. Lau, S. Li, *et al.*, "The ribosomal maturation factor P from *Mycobacterium smegmatis* facilitates the ribosomal biogenesis by binding to the small ribosomal protein S12," *Journal of Biological Chemistry*, vol. 294, pp. 372-378, 2019.

- [271] E. Kolker, K. S. Makarova, S. Shabalina, A. F. Picone, S. Purvine, T. Holzman, *et al.*, "Identification and functional analysis of 'hypothetical' genes expressed in *Haemophilus influenzae*," *Nucleic Acids Research*, vol. 32, pp. 2353-2361, 2004.
- [272] R. E. Bryant and P. S. Sypherd, "Genetic analysis of cold-sensitive ribosome maturation mutants of *Escherichia coli*," *Journal of Bacteriology*, vol. 117, pp. 1082-1092, 1974.
- [273] K. Hofmann, "TMbase-A database of membrane spanning proteins segments," *Biological Chemistry Hoppe-Seyler*, vol. 374, p. 166, 1993.
- [274] K. Kavanagh, H. Jörnvall, B. Persson, and U. Oppermann, "Medium- and short-chain dehydrogenase/reductase gene and protein families," *Cellular and Molecular Life Sciences*, vol. 65, p. 3895, 2008.
- [275] D. J. Lea-Smith, J. S. Pyke, D. Tull, M. J. McConville, R. L. Coppel, and P. K. Crellin, "The reductase that catalyzes mycolic motif synthesis is required for efficient attachment of mycolic acids to arabinogalactan," *Journal of Biological Chemistry*, vol. 282, pp. 11000-11008, 2007.
- [276] D.-L. Ma, D. S.-H. Chan, and C.-H. Leung, "Molecular docking for virtual screening of natural product databases," *Chemical Science*, vol. 2, pp. 1656-1665, 2011.

APPENDIX

7.1 General Media

All the media were prepared in Milli RO grade water and autoclaved at 15 pounds per square inch for 15 min unless otherwise indicated.

I. Nutrient Broth

Peptone	5 g
Yeast extract	1.5 g
Beef extract	1.5g
NaCl	10 g

The components were dissolved in Milli RO water according to manufacturer's guidelines.

II. LB Broth (Luria Bertani Broth)

Tryptone	10 g
Yeast extract	5 g
NaCl	10 g

The components were dissolved in Milli RO water according to manufacturer's guidelines. Agar at a concentration of 1.5 % was added whenever solid medium was required.

III. LB broth with Glycerol and Tween-80

5 mL of glycerol and 2 mL of Tween-80 was added to 1L LB broth and sterilized.

IV. Nutrient Agar Tween-80 (NAT)

Nutrient Broth	13 g
Tween-80	2 ml

The components were dissolved in Milli RO water according to manufacturer's guidelines. Agar at a concentration of 1.5 % was added whenever solid medium was required.

V. Middle brook (MB) 7H9 broth

MB7H9 broth base	4.7 g
Tween-80	2 ml

Glycerol	5 ml
Milli RO water	900 ml

The components were dissolved in Milli RO water according to manufacturer's guidelines.

7.2 Reagents for Acid Fast Staining

I. Carbol fuchsin (Primary stain)

Basic fuchsin	3 g
Phenol	5 %
Ethanol (96 %)	10 ml

Mixed 10 ml of Basic fuchsin to 90 ml of phenol and the solution was filtered through Whatman filter paper No. 1.

II. Acid alcohol (Decolorizer)

HCl (conc.)	3 ml
Ethanol (96 %)	97 ml

III. Malachite green solution (Counter stain)

Malachite green	0.25 g in Milli RO water
-----------------	--------------------------

7.3 Antibiotics and Substrates

All antibiotics were filter sterilized by a 0.22 μm filter (Millipore) and stock solutions were stored at -20°C for long term use.

Antibiotic/Substrate	Stock Solution	Working Solution
Ampicillin	20 mg/mL	50 $\mu\text{g/mL}$
Kanamycin	10 mg/mL	30 $\mu\text{g/mL}$
X-Gal	40 mg/mL	40 $\mu\text{g/mL}$
p-nitrophenyl phosphate	1M	2mM
X-P	40 mg/mL	80 $\mu\text{g/mL}$

7.4 Reagents and Buffers

All the reagents and buffers for DNA and protein work were prepared in Milli Q grade water and sterilized by autoclaving for 15 minutes at 15-psi pressure unless otherwise indicated.

7.4.1 Commonly used Buffers

I. Phosphate Buffer

KH ₂ PO ₄	2.31 g
K ₂ HPO ₄	12.54 g
Milli RO water	90 ml

The pH of the solution was adjusted to 7.5 and the volume made up to 100 ml and sterilized.

II. Phosphate Buffered Saline (PBS), per liter

KH ₂ PO ₄	0.34 g
K ₂ HPO ₄	1.21 g
NaCl	8.0 g
pH	7.3

III. Tris HCl buffer

Tris-HCl buffer of desired strength was prepared by dissolving appropriate amount of Tris in distilled water and adjusting the pH with concentrated HCl. For bacteriological work 10 mM Tris-HCl (pH 8.0) was used.

IV. Ethylene diamine tetra acetic acid (EDTA)

0.5 M solution of disodium salt of EDTA was prepared in Milli Q, pH adjusted to 8.0 with NaOH pellets and stored at 4°C.

V. Normal Saline

NaCl	8.50 g
Milli RO water	1000 ml (final volume)

VI. Tween Normal Saline

0.02 % Tween -80 was added to normal saline.

7.4.2 Reagents for Genomic DNA Isolation from Mycobacterium

I. TE Buffer

Tris-HCl (pH 8.0)	10 mM
EDTA	1 mM

II. Tris EDTA Saline (TES) Buffer

Tris-HCl (pH 8.0)	10 mM
EDTA	1 mM
NaCl	150 mM

III. Lysozyme

Lysozyme	50 mg/ml in Milli Q (Store at -20°C)
----------	--------------------------------------

IV. Proteinase K

Proteinase K	20 mg/ml in Milli Q (Store at -20°C)
--------------	--------------------------------------

V. Buffered Phenol

Molten phenol containing 0.1 % 8-hydroxyquinoline was equilibrated with 1M Tris-HCl (pH 8.0) and twice with 0.1M Tris-HCl (pH 8.0) till the pH > 7.8 and then it is stored submerged in 10 mM Tris-HCl (pH 8.0) in dark bottle at 4°C away from direct light.

VI. Chloroform: Isoamyl alcohol

Solution contains 24 parts chloroform and 1 part isoamyl alcohol. The solution is stored in dark bottles at 4°C.

7.4.3 Buffers for Plasmid Isolation from *E. coli*

I. Alkaline Lysis Solution I

Tris-HCl (pH 8.0)	25 mM
EDTA (pH 8.0)	10 mM
Glucose	50 mM

II. Alkaline Lysis Solution II

NaOH	0.2 N
SDS	1.0 %

III. Alkaline Lysis Solution III

Solution contains 3 volumes of 3 M sodium acetate and 4 volumes of 7.5 M ammonium acetate.

7.4.4 Buffers for Electrophoresis

I. TAE Buffer (50X)

Tris Base	242 g
Glacial Acetic Acid	57.1 ml
0.5 M EDTA (pH 8.0)	100 ml
Final Volume	1000 ml
RNase free water	880 ml

7.4.5 Buffers for Transformation

I. Transformation Buffer I (TFB I)

MOPS Buffer (pH 7.0)	10 mM
RbCl	10 mM

II. Transformation Buffer II (TFB II)

MOPS Buffer (pH 6.5)	100 mM
RbCl	10 mM
CaCl ₂	50 mM

7.4.6 Buffers for Gel Loading

I. 6X dye for agarose gel electrophoresis

Bromophenol Blue	0.25 %
Sucrose	40 %

7.4.7 Buffer for Histopathology Studies

Formal saline	10% Formaldehyde in Normal Saline
---------------	-----------------------------------

LIST OF PUBLICATIONS

Journal Publications:

1. **Poonam**, R. M. Yennamalli, G. S. Bisht, and R. Shrivastava, "Ribosomal maturation factor (RimP) is essential for survival of nontuberculous mycobacteria *Mycobacterium fortuitum* under in vitro acidic stress conditions," *3 Biotech*, vol. 9, pp. 127, 2019. (Scopus, SCI, Impact factor 1.78). doi: 10.1007/s13205-019-1659-y.
2. **P. Katoch**, K. Gupta, R. M. Yennamalli, J. Vashist, G. S. Bisht, and R. Shrivastava, "Random insertion transposon mutagenesis of *Mycobacterium fortuitum* identified mutant defective in biofilm formation," *Biochemical and Biophysical Research Communications*, vol. 521, pp. 991-996, 2020. (Scopus, SCI, Impact factor 2.7). doi: 10.1016/j.bbrc.2019.11.021
3. **P. Katoch**, G. S. Bisht and R. Shrivastava, "In vivo infection and in vitro stress survival studies of acid susceptible mutant of *Mycobacterium fortuitum*," *International Journal of Mycobacteriology*, vol. 8, pp. 390-396, 2019. (Scopus, SCI). doi: 10.4103/ijmy.ijmy_166_19
4. D. Sharma, **Poonam**, R. Shrivastava, and G. S. Bisht, "In Vitro Efficacy of Lipid Conjugated Peptidomimetics Against *Mycobacterium smegmatis*," *International Journal of Peptide Research and Therapeutics*, vol. 26, pp. 1-7, 2019. (Scopus, SCI, Impact factor 1.219). doi: 10.1007/s10989-019-09859-7

Journal Publications (*Manuscript under preparation*):

5. Identification and *in silico* characterization of transcription termination/antitermination protein NusA of *Mycobacterium fortuitum*. *International Journal of Data Mining and Bioinformatics* (Under Review).
6. Computational analysis of *Mycobacterium fortuitum* anthranilate synthase complex: Drug discovery and evolutionary implications. *Journal of Molecular Structure and Dynamics* (Under Review)

Book Chapter Publication:

1. **Poonam**, R. Ghildiyal, G. S. Bisht, and R. Shrivastava, "Engineering Yeast as Cellular Factory," in *Metabolic Engineering for Bioactive Compounds*, ed: Springer, pp. 173-208, 2017. (Scopus)

Conference Publications:

1. **Poonam**, J. Vashistt, G.S. Bisht, and R. Shrivastava, "Ribosomal maturation factor RimP as potential drug target for *M. fortuitum*," in *Proceedings of the International Conference on Advances in Plant and Microbial Biotechnology*, Jaypee Institute of Information Technology, Noida, India, February 2017.
2. **Poonam**, P. K. Agrawal, and R. Shrivastava, "Antimycobacterial activity of leaf extracts of medicinal plants against *M. smegmatis*," in *Proceedings of the Recent Advances in Green Technology*, Bahara University, Shimla, India, September 2016.
3. **Poonam**, M. Pradhan, K. Sharma, and R. Shrivastava, "Identification of *Mycobacterium fortuitum* virulence factors using transposon mutagenesis," in *Proceedings of the 56th Annual Conference of Association of Microbiologists of India (AMI-2015) & International Symposium on Emerging Discoveries in Microbiology*, JNU, New Delhi, India, December 2015.

GenBank Submissions:

1. **Poonam**, R. M. Yennamalli and R. Shrivastava, [*Mycobacterium fortuitum* ATCC 6841] Short Chain Dehydrogenase Sequence of *Mycobacterium fortuitum* (ATCC 6841). [BankIt1962983 Seq KY250516]
2. **Poonam**, R. M. Yennamalli, and R. Shrivastava, [*Mycobacterium fortuitum* ATCC 6841] Peptidase S9, prolyl oligopeptidase Protein. [BankIt1971929 Seq KY250519]
3. **Poonam**, S. Sood, and R. Shrivastava [*Mycobacterium fortuitum* ATCC 6841] Probable Anthranilate Synthase Subunit I of *Mycobacterium fortuitum*. [BankIt1971940 Seq KY250521]
4. **Poonam**, S. Sood, and R. Shrivastava, [*Mycobacterium fortuitum* ATCC 6841] Probable X-Pro dipeptidase. [BankIt1971887 Seq KY250518]

5. **Poonam**, S. Sood, and R. Shrivastava, [*Mycobacterium fortuitum* ATCC 6841] Probable Replication Initiation and Membrane Attachment Protein DnaB. [BankIt1971879 Seq KY250517]
6. **Poonam**, S. Sood, and R. Shrivastava, [*Mycobacterium fortuitum* ATCC 6841] Tentative Anthranilate Synthase Subunit II of *Mycobacterium fortuitum* ATCC 6841. [BankIt1971935 Seq1 KY250520]
7. **Poonam**, S. Sood, and R. Shrivastava, [*Mycobacterium fortuitum* ATCC 6841] Tentative Anthranilate Phosphoribosyltransferase of *Mycobacterium fortuitum* ATCC 6841 [BankIt1971941 Seq1 KY250522]
8. **Poonam**, and R. Shrivastava, [*Mycobacterium fortuitum* ATCC 6841] Probable Ribosomal maturation factor RimP of *Mycobacterium fortuitum* [BankIt2094302 Seq1 MH052677].
9. **Poonam**, and R. Shrivastava, [*Mycobacterium fortuitum* ATCC 6841] Putative transcription termination/antitermination factor NusA of *Mycobacterium fortuitum* [BankIt2198443 Seq MK574079]